Erica Monaco, née Sjöholm

Tailored Doses by Means of Semi-Solid Extrusion-Based 3D Printing

A Study in Pharmaceutical Sciences

Åbo Akademi University

Erica Monaco, née Sjöholm

Born 1991 in Kimito, Finland

Previous degrees

MBA in Pharmaceutical and Healthcare Business, St. Joseph's University, 2023

M.Sc. in Bioscience (Pharmacy), Åbo Akademi University, 2016

B.Sc. in Pharmacy, Åbo Akademi University, 2014

Tailored Doses by Means of Semi-Solid Extrusion-Based 3D Printing

A Study in Pharmaceutical Sciences

Erica Monaco, née Sjöholm

Pharmaceutical Sciences Laboratory
Faculty of Sciences and Engineering
Åbo Akademi University
Åbo, Finland, 2023

Supervisors

Main supervisor

Prof. Dr. Niklas Sandler
Formerly at Pharmaceutical Sciences Laboratory
Åbo Akademi University, Finland

and currently at
CurifyLabs Oy, Helsingfors, Finland

Official assistant supervisor

Dr. Xiaoju Wang
Pharmaceutical Sciences Laboratory
Åbo Akademi University, Finland

Reviewers

Assoc. Prof. Dr. Karin Kogermann
Institute of Pharmacy
University of Tartu, Estonia

Asst. Prof. Dr. Julian Quodbach
Utrecht Institute for Pharmaceutical Sciences
Utrecht University, Netherlands

Opponent

Assoc. Prof. Dr. Karin Kogermann
Institute of Pharmacy
University of Tartu, Estonia

Preface

This thesis is based on research conducted at the Åbo Akademi University, Finland, in the Drug-Delivery and Pharmaceutical Technology Research Group, Pharmaceutical Sciences Laboratory (PSL), Faculty of Science and Engineering in 2017-2023. Additionally, research was conducted during the six-month external research stay at the Department of Pharmaceutics, School of Pharmacy, Virginia Commonwealth University, USA, in 2019.

Abstract (in English)

The field of pharmaceutical sciences recognizes the need for tailored doses to address dosing challenges in specific patient populations, particularly pediatric and veterinary patients. Conventional manufacturing methods lack the flexibility required to produce personalized dosage forms, and compounding in pharmacies is labor-intensive and prone to errors. Three-dimensional printing (3DP) offers a transformative approach to the production of tailored dosage forms. Of particular interest is the application of semi-solid extrusion (SSE) 3DP, which enables printing at ambient conditions, making it suitable for a wide range of drugs, including thermolabile active pharmaceutical ingredients (API). The utilization of disposable pre-filled syringes in SSE 3DP ensures compliance with critical quality requirements set by regulatory agencies. This technology has been investigated specifically for the production of orodispersible and chewable dosage forms, which cater to patient populations with swallowing difficulties.

This thesis investigates the suitability of SSE 3DP for the production of tailored solid oral dosage forms for pediatric and veterinary patients, addressing the limitations in dose customization and dosage form flexibility. In this thesis, individual customization of five drugs is investigated through the preparation of tailored doses, sizes, and types of solid oral dosage forms. These five drugs were formulated into semi-solid drug inks adapted for SSE 3DP.

In the first study, thin and flexible orodispersible films (ODFs) in various sizes containing therapeutic doses were successfully printed. Low standard deviation in drug content indicates the suitability of this method for drugs with narrow therapeutic indexes. In the second study, SSE 3DP and inkjet printing (IJP) were evaluated and compared to oral dose sachets (OPS) prepared at the hospital pharmacy using a standard operating procedure for the preparation of personalized doses. SSE 3DP demonstrated superior characteristics compared to the two other methods in producing tailored ODFs. The third study assesses different SSE printers' capability to produce tailored doses for veterinary care, achieving a strong correlation between designed size and drug amount for the best performing printer. The fourth study explores the production of hard ChewTs for veterinary care, achieving excellent content uniformity. The fifth study investigates the loading of a different drug using the same ink base as in the fourth study, showcasing the feasibility of manufacturing pet-friendly ChewTs utilizing a standard ink base. In the sixth study, oral thin films containing therapeutic doses of nanoformed particles were successfully printed using SSE 3DP, highlighting the potential for personalized medicine of poorly soluble drugs.

This thesis contributes to the advancement of personalized medicine by exploring the application of SSE 3DP as a novel approach for on-demand manufacturing of tailored drug-loaded solid oral dosage forms close to the point-of-care. The findings of this research demonstrate the potential of SSE 3DP in

addressing dosing challenges, improving treatment outcomes, and enhancing patient adherence and comfort, particularly in the fields of pediatric and veterinary care. By harnessing the capabilities of SSE 3DP, the healthcare industry can unlock new possibilities for personalized medicine, optimizing treatment outcomes, and enhancing patient experiences. The ability to create customized dosage forms with specific properties showcases the potential of SSE 3DP to shape the future of pharmaceutical manufacturing and healthcare delivery. This thesis highlights the importance of SSE 3DP in advancing personalized medicines and provides insights that can contribute to the development of innovative solutions in the field of pharmaceutical sciences.

Abstrakt (in Swedish)

Forskningsområdet inom farmaceutiska vetenskaper erkänner behovet av skräddarsydda doser för att möta doseringsutmaningar hos specifika patientgrupper, särskilt hos barn och djur. Konventionella tillverkningsmetoder saknar den flexibilitet som krävs för att producera individanpassade dosformer och framställning av läkemedel på apotek är arbetsintensivt och kan leda till fel. Tredimensionell utskrift (3DP) erbjuder ett revolutionerande tillvägagångssätt för tillverkning av skräddarsydda dosformer. Av särskilt intresse är tillämpningen av halvfast extrudering (SSE), vilket möjliggör utskrift utan användning av värme och passar således för ett brett spektrum av läkemedel, inklusive värmeömtåliga aktiva substanser. Användningen av förfyllda engångssprutor i SSE 3DP säkerställer att de kritiska kvalitetskrav som ställs av regleringsmyndigheter uppfylls. Denna teknik har specifikt undersökts för framställning av munsönderfallande och tuggbara dosformer som riktar sig till patientgrupper med svårigheter att svälja.

Denna avhandling undersöker lämpligheten av SSE 3DP för framställning av skräddarsydda fasta orala läkemedel för barn och djur. I denna avhandling undersöks individanpassning av fem läkemedel genom framställning av skräddarsydda doser, storlek och typ av fasta orala dosformer. Dessa fem läkemedel var formulerade till halvfasta läkemedelsbläck anpassade för SSE 3DP.

I den första studien utskrevs framgångsrikt tunna och flexibla munsönder-fallande filmer (ODF) av olika storlekar som innehöll terapeutiska läkemedelsdoser. Låg standardavvikelse i läkemedelsinnehåll indikerar lämplighet för läkemedel med smalt terapeutiskt fönster. I den andra studien utvärderas och jämförs SSE 3DP med bläckstråleutskrift (IJP) och orala pulver i endospåsar (OPS) framställda på sjukhusapoteket enligt standardiserat förfarande för beredning av individanpassade doser. SSE 3DP uppvisade superioritet jämfört med de två andra metoderna för framställning av skräddarsydda ODF. I den tredje studien bedöms olika SSE-skrivares förmåga att producera skräddarsydda doser för veterinärvård. Den overlag bäst presterande skrivaren visade en stark korrelation mellan modellerad storlek och läkemedelsmängd. Den fjärde studien utforskar tillverkningen av hårda tuggtabletter för veterinärvård, med utmärkt enhetlig innehållsmängd. Den femte studien undersöker möjligheten att använda samma bläckbas som i den fjärde studien men med ett annat läkemedel. Studien visar att det är möjligt att framställa tuggtabletter som är anpassade för djur med hjälp av en standardiserad bläckbas. Den sjätte studien framställer framgångsrikt oral tunnfilm med terapeutiska doser av nanopartiklar med hjälp av SSE 3DP, vilket betonar potentialen för skräddarsydd medicin för dåligt lösliga läkemedel.

Denna avhandling bidrar till framsteg inom individanpassad medicinering genom att utforska tillämpningen av SSE 3DP som ett nytt tillvägagångssätt för

att tillverka skräddarsydda läkemedelsinnehållande fasta orala dosformer vid behov i närheten av vårdplatsen. Resultaten av denna forskning visar potentialen för SSE 3DP för att möta doseringsutmaningar, förbättra behandlingsresultat och öka patienternas följsamhet och upplevelse, särskilt inom pediatrisk och veterinär vård. Genom att utnyttja möjligheterna som SSE 3DP erbjuder kan hälso- och sjukvårdsbranschen öppna nya möjligheter för individanpassad medicinering, optimera behandlingsresultat och förbättra patientupplevelsen. Möjligheten att tillverka individanpassade dosformer med specifika egenskaper visar potentialen hos SSE 3DP att forma framtidens läkemedelsframställning och hälso- och sjukvård. Denna avhandling lyfter fram betydelsen av SSE 3DP för att främja individanpassad medicinering och ger insikter som kan bidra till utvecklingen av innovativa lösningar inom farmaceutisk vetenskap.

List of original publications

The thesis is based on the following publications, which in the text is referred to by Roman numerals (I-VI).

I.   **Sjöholm, E.**, Sandler, N., 2019. Additive manufacturing of personalized orodispersible warfarin films. *International Journal of Pharmaceutics* 564, 117-123.
https://doi.org/10.1016/j.ijpharm.2019.04.018

II.   Öblom, H., **Sjöholm, E.**, Rautamo, M., Sandler, N., 2019. Towards printed pediatric medicines in hospital pharmacies: Comparison of 2D and 3D printed orodispersible warfarin films with conventional oral powders in unit dose sachets. *Pharmaceutics 11*, 334.
https://doi.org/10.3390/pharmaceutics11070334

III. **Sjöholm, E.**, Mathiyalagan, R., Rajan Prakash, D., Lindfors, L., Wang, Q., Wang, X., Ojala, S., Sandler, N., 2020. 3D-Printed Veterinary Dosage Forms — a Comparative Study of Three Semi-Solid Extrusion 3D Printers. *Pharmaceutics* 12(12), 1239.
https://doi.org/10.3390/pharmaceutics12121239

IV.   **Sjöholm, E.**, Mathiyalagan, R., Lindfors, L., Wang, X., Ojala, S., Sandler, N., 2022. Semi-Solid Extrusion 3D Printing of Tailored ChewTs for Veterinary Use - A Focus on Spectrophotometric Quantification of Gabapentin. *European Journal of Pharmaceutical Sciences*, 174, 106190.
https://doi.org/10.1016/j.ejps.2022.106190

V.   **Sjöholm, E.**, Mathiyalagan, R., Wang, X., Sandler, N., 2022. Compounding Tailored Veterinary Chewable Tablets Close to the Point-of-Care by Means of 3D Printing. *Pharmaceutics*, 14(7), 1339.
https://doi.org/10.3390/pharmaceutics14071339

VI.   Mathiyalagan, R., **Sjöholm, E.,** Manandhar, S., Lakio, S., Rosenholm, J. M., Kaasalainen, M., Wang, X., & Sandler, N. (2023). Personalizing oral delivery of nanoformed piroxicam by semi-solid extrusion 3D printing. *European Journal of Pharmaceutical Sciences*, 188, 106497.
https://doi.org/10.1016/J.EJPS.2023.106497

Contribution of **Erica Monaco, née Sjöholm** to the original publications:

I. Designing most of the study, performing all the experiments, performing all the data analysis, and writing the paper.

II. Participation in the study design, performing half of the experiments, performing half of the data analysis, and reviewing the paper.

III. Designing the study, performing most of the experiments, performing most of the data analysis, and writing the paper.

IV. Designing most of the study, performing many of the experiments, data analysis, and writing the paper.

V. Designing the study, performing many of the experiments, data analysis, and writing the paper.

VI. Participation in the study design, performing some of the experiments, data analysis, and participation in writing the paper.

List of supporting publication

The author has moreover contributed to the following publication that is not included in the thesis:

VII. Tian, Y., Orlu, M., Woerdenbag, H.J., Scarpa, M., Kiefer, O., Kottke, D., **Sjöholm, E.**, Öblom, H., Sandler, N., Hinrichs, W.L.J., Frijlink, H.W., Breitkreutz, J., Visser, J.C., 2019. Oromucosal films: from patient centricity to production by printing techniques. Expert Opin. Drug Deliv. 16, 981–993.
https://doi.org/10.1080/17425247.2019.1652595

Abbreviations

3D	Three-dimensional
3DP	Three-dimensional printing
API	Active pharmaceutical ingredient
ASTM	American Society for Testing and Materials
ATR-FTIR	Attenuated total reflectance Fourier transform infrared
AV	Acceptance value
BCS	Biopharmaceutical Classification System
BJ	Binder jetting
CAD	Computer-aided design
ChewT	Chewable tablets
CIJ	Continuous inkjet printing
CU	Content uniformity
DIS	Disintegration
DLS	Dynamic light scattering
DoD	Drop-on-demand
DPE	Direct powder extrusion
DQSA	The Drug Quality and Security Act
DSC	Differential scanning calorimetry
EAHP	The European Association of Hospital Pharmacists
EMA	The European Medicine Agency
EtOH	Ethanol
ETT	Emerging Technology Team
FD	Freeze-dried
FDA	The U.S. Food and Drug Association
FDM	Fused deposition modeling
FTIR	Fourier transform infrared
GBP	Gabapentin
GMP	Good Manufacturing Practice
GRAS	Generally Recognized As Safe
HME	Hot melt extrusion
HPC	Hydroxypropyl cellulose
HPLC	High-performance liquid chromatography
HPMC	Hydroxypropyl methylcellulose
HUS	Helsinki University Hospital
IJP	Inkjet printing
IND	Investigational new drug
LP	Liver powder
MA	Marketing authorization

MED	Melt Extrusion Deposition
MW	Molecular weight
nanoPRX	Nanoformed piroxicam
NIR	Near-infrared
ODF	Orodispersible film
ODT	Orodispersible tablets
OPS	Oral powders in unit dose sachet
PAM	Pressure-assisted microsyringe
PAT	Process analytical technology
PDI	Polydispersity index
PEG	Polyethylene glycol
PG	Propylene glycol
Ph. Eur.	The European Pharmacopoeia
PIJ	Piezoelectric inkjet
PRE	Prednisolone
PRX	Piroxicam
PSI	Pounds per square inch
PVA	Poly(vinyl alcohol)
QR	Quick Response
RTD	Room-temperature dried
SEM	Scanning electron microscopy
SLA	Stereolithography
SLS	Selective laser sintering
SSE	Semi-solid extrusion
TEM	Transmission electron microscopy
TIJ	Thermal inkjet
TPH	Theophylline
UC	Uniformity of content
USP	The United States Pharmacopeia
UV	Ultraviolet
UV-Vis	Ultraviolet–visible
WS	Warfarin sodium
XRPD	X-ray powder diffraction
Z-average	Hydrodynamic diameter

Table of contents

1. Introduction

There is a growing acknowledgement of the pressing need for tailored doses to address the challenges of appropriate dosing in specific patient populations, including pediatric and veterinary patients. The scarcity of appropriate doses and dosage forms on the market has underscored the significance of personalized medicines. Conventional manufacturing methods, such as tableting and encapsulating, are well-established and regulated but lack the flexibility required to produce personalized dosage forms. Tablets, being the most commonly used solid oral dosage form, suffer from limitations in dose adjustments, often resulting in manual division practices that lead to uneven weight distribution and inconsistent delivery of the active pharmaceutical ingredient (API). This issue is particularly critical for drugs with narrow therapeutic indices or patients requiring precise dosing. Compounding in pharmacies has played a vital role in answering to this unmet need. However, it is a labor-intensive process prone to human error. To address the challenges of appropriate dosing and personalized medicines, three-dimensional (3D) printing (3DP), also known as additive manufacturing, offers a transformative approach to the production of tailored dosage forms. With its flexibility and high accuracy, 3DP technology has demonstrated significant potential in fabricating customized dosage forms and enabling precise dose adjustments. It facilitates an automated and easily adaptable production process suitable for small-scale drug manufacturing, rapid modifications, and personalized treatments. Of particular interest is the application of semi-solid extrusion (SSE) 3DP, which caters to patient populations with swallowing difficulties, such as geriatric, pediatric, and veterinary patients, by producing tailored orodispersible films (ODFs) and chewable dosage forms. SSE 3DP has emerged as a promising solution to meet the specific needs of these populations, providing improved drug delivery options, and enhancing patient adherence and comfort.

Regulatory guidelines and considerations are crucial for successfully implementing 3DP in pharmaceutical manufacturing. The U.S. Food and Drug Administration (FDA), a leading regulatory authority, recognizes the potential of 3DP technology and has issued guidance focusing on the advancement of emerging technology applications for pharmaceutical innovation and modernization. Although the FDA has provided technical guidance for medical devices and prosthetics manufactured using additive manufacturing, specific considerations and regulations for 3D-printed products with drug delivery functions are still evolving. Efforts by regulatory bodies like the European Medicines Agency (EMA) aim to support scientific and technological progress in medicine development, including precision medicine, as well as to transform the regulatory framework for veterinary medicines and facilitate the implementation of novel manufacturing technologies. The recently established Quality Innovation Group (QIG) by the EMA seeks to provide regulatory guidance

and define expectations for innovative manufacturing technologies, including decentralized manufacturing, with the primary objective of facilitating the introduction of these advanced products into the market.

The commercialization of 3D-printed dosage forms is still in its early stages. However, notable progress has been made, with the FDA-approval of Spritam® by Aprecia as the first printed dosage form in 2015. Triastek's Melt Extrusion Deposition (MED®) has also gained regulatory approval for clinical trials in various indications. Numerous companies, including start-ups and pharmaceutical giants, are exploring the potential of 3DP in drug delivery, aiming to meet the personalized drug requirements of patients across different age groups and disease states.

This thesis investigates the suitability of 3DP, specifically SSE 3DP, for on-demand production of tailored solid oral dosage forms suitable for pediatric and veterinary patients, contributing to the advancement of personalized medicines and addressing the current limitations in dose customization and dosage form flexibility.

2. Literature overview

2.1 Personalized medicines

The current medical treatment model, often characterized by a "one-size-fits-all" approach, has inherent limitations. Administering the same drug and dose to every patient can lead to divergent responses, including adverse drug reactions or inadequate therapeutic effects. Recognizing these challenges, personalized medicine has emerged as a solution to tailor medicines based on individual patient characteristics, such as genetics, physiology, or pathology. The primary objective of personalized medicines is to identify the most appropriate drug, dose, dosage form, and timing for a specific patient's condition. By considering individual variations, personalized medicines aim to deliver more precise, safe, and effective medicines. This approach has the potential to enhance patient compliance, minimize adverse effects, and optimize treatment outcomes, ultimately contributing to improved healthcare cost-effectiveness (Vaz & Kumar, 2021). This approach considers interpatient variability and leverages advancements in human genome research and pharmacogenomics to understand the impact of genetic characteristics on drug responses. EMA defines personalized medicine as tailoring therapeutic strategies based on individual phenotypes and genotypes, including molecular profiling, medical imaging, and lifestyle data. It aims to provide the right treatment approach for the right patient at the right time and to enhance disease prevention through personalized and targeted interventions (2015/C 421/03 Council Conclusions on Personalised Medicine for Patients, 2015). The concept of personalized medicine is also recognized by the FDA, who defines it as precision medicine, which is an innovative approach that customizes disease prevention and treatment by considering variations in individuals' genes, environments, and lifestyles. The primary objective of precision medicines is to deliver the most suitable treatments to patients based on their unique characteristics, at the optimal time for maximum effectiveness (The U.S. Food & Drug Administration, 2018). A cornerstone of personalized medicine is precision dosing.

Despite advancements in drug delivery, the oral route remains the most preferred by consumers globally due to its convenience (Alhnan et al., 2016). Tablets are the most commonly used solid oral dosage form, making up 70% of all production (Roulon et al., 2021). However, dose adjustments are a common need, and manually dividing tablets using hands, knives, or splitters is a typical practice that often leads to uneven weight distribution, causing variations in the amount of API delivered to the patient. This variability in dosing can be particularly problematic for drugs with a narrow therapeutic index or for patients with conditions that require precise dosing. Furthermore, such manipulation of solid oral dosage forms is not accurate and may lead to day-to-day variability of the administered dose and thus result in undesired over- or under-dosing, potentially compromising the effectiveness of the medicine and increasing the risk of adverse effects (Habib et al., 2014; Helmy, 2015; Marriott

& Nation, 2002; McDevitt et al., 1998). In addition, manipulating solid oral dosage forms can have detrimental effects on the properties of the medicine, including hazardous outcomes such as dose dumping of sustained-release dosage forms or the breakdown of pH-sensitive coatings. These can result in the release of the API at an incorrect site in the gastrointestinal tract, potentially causing drug degradation and reduced therapeutic efficacy (Habib et al., 2014; Marriott & Nation, 2002; McDevitt et al., 1998). Alternative approaches include the use of oral liquids or compounding of oral dose powders or hard capsules in hospital pharmacies (Brion et al., 2010). Although oral liquids offer greater dosing flexibility compared to solid dosage forms, their usage comes with some challenges. For instance, potentially requiring the administration of large volumes, a limited selection of suitable solvents and excipients (especially for pediatric use), and a shorter shelf life compared to solid dosage forms (Batchelor & Marriott, 2015). Compounding in pharmacies plays a vital role in facilitating personalized medicine by enabling the production of customized dosages and dosage forms to meet individual patient needs. However, compounding oral dose powders or capsules is highly labor intensive, and human error is prevalent. 3DP, on the other hand, offers a solution to these issues by enabling an automated approach to the production of personalized medicines and moving away from mass production and the "one-size-fits-all" approach.

2.2   Veterinary medicines

Administering veterinary drugs can be challenging due to the variations in animals' size and body mass and differences in pharmacokinetics between species. In addition, the limited availability of approved veterinary drugs has led to the need for compounding tailored doses to fill the therapeutic gaps for non-human species and provide dosage forms that are easier for pets to tolerate and owners to administer (I. Ahmed & Kasraian, 2002; Davidson, 2017). FDA estimates that 75,000 pharmacies fill 6,350,000 compounded animal prescriptions annually (U.S. Food and Drug Association, 2015). Despite the lack of available data on compounded animal preparations in other countries, it is reasonable to assume that the worldwide prevalence is significant, given the many roles that animals play in our lives. But the development of veterinary formulations requires consideration of differences between humans and animals, including toxicity of excipients, anatomical differences, and animal preferences (I. Ahmed & Kasraian, 2002; Davidson, 2017). Chewable tablets (ChewTs) and oral solutions are common dosage forms for veterinary medicines, as they are easier to administer. Overall, veterinary pharmaceuticals play an important role in preserving and restoring animal health. Hence, developing animal-appropriate medicines with a wide range of doses and dosage forms is necessary to meet animals' needs.

2.3 Compounding

Preparing medicines tailored to individual patients' specific needs has always been integral to pharmacy practice, however, with the rise of industrialization and drug manufacturing in the early 1900s, prescriptions gradually shifted towards proprietary medicines. While proprietary medicines have their value, they are manufactured in limited forms, including specific dosage forms and strengths, and are designed to meet the needs of the majority of patients. However, there are always individuals with unique health conditions that require a personalized approach to treatment. In such cases, the pharmaceutical industry may not be able to provide cost-effective solutions to meet their specific needs. The growing emphasis on personalized patient care has led to the recognition of the flexibility and customization offered by compounded medicines (Watson et al., 2021).

The global community uses varied terminology to describe the extemporaneous preparation of medicines, such as pharmacy preparation, extemporaneous manufacturing/preparation/compounding, magistral compounding, or simply compounding. In this thesis, the practice will be referred to as "compounding." Compounding is typically employed when commercially available products cannot meet the specific requirements of a patient's therapy. The practice of compounding involves several activities, such as mixing multiple approved drug products into a single dosage form, altering the dosage form, or adding patient-preferred flavoring to an approved drug product. In the absence of an approved drug product, compounding can also involve starting with bulk API and other excipients. Pharmaceutical compounding remains vital for catering to those with challenges related to medicine ingestion, allergies to standard product components, or specific age-related needs, especially in pediatric and elderly patients. Furthermore, pharmacists play a unique role in providing pharmaceutical care not only to human patients but also to animals. This positions pharmacists to collaborate with veterinarians in developing high-quality compounded formulations that are safe and effective for animal patients (Davidson, 2017).

However, the practice of compounding is not without its set of intricate challenges. A prime one being the formulation of poorly soluble drugs. Such drugs, predominantly from class II and IV under the Biopharmaceutical Classification System (BCS), often have limited absorption in the body, resulting in reduced therapeutic effects. Addressing this limitation in compounding requires advanced formulation strategies, which enhance drug solubility and promise more effective treatment outcomes. While techniques like nanonization, which reduces particle size to potentially increase surface area and improve solubility, offer hope, they also introduce complexities. These can include concerns over altered drug stability or difficulties ensuring uniform drug distribution (Singh et al., 2011). Beyond the formulation issues with poorly soluble drugs, compounding faces several concerns. There are inherent risks of

contamination and inconsistent drug quality, as compounded drugs might not be created using validated processes or equipment. The source of ingredients and the expertise of the compounding personnel remain areas of concern. Unlike FDA-approved drugs, compounded medicines lack a standardized testing regimen, casting doubts over their potency, purity, and quality. Sterile compounding exacerbates these concerns (Gudeman et al., 2013).

Hence, compounding poses significant risks to patients attributed to preparation errors, contamination, chemical and physical instability, and lack of bioavailability in the targeted patient. For instance, the Missouri Board of Pharmacy annually evaluates, and reports compounded drug preparations from licensed pharmacies in Missouri, and the results from 2006-2022 are gathered in Table 1. Analysis of the results shows that, on average, one in every five compounded dosage forms fails to meet the targeted strength criteria. The potency ranges from zero API to as much as 450.4% of the expected potency (Missouri Board of Pharmacy, 2023). This indicates the need for a robust technology in combination with quality assurance measures for compounded doses to ensure the quality of manufactured drug doses.

Table 1. *Results of the potency ranges of extemporaneously manufactured drug products prepared between 2006–2022. Modified and reproduced from (III), with permission from MDPI.*

Year	Tests Performed	Unsatisfactory Percentage (%)	Potency Range (%)
2022	46	13.0	82.5–111.1
2021	61	26.2	0.0–124.8
2020	57	19.3	21.2–130.7
2019	55	36.4	53.7–193.9
2018	72	23.6	64.4–175.3
2017	80	27.5	66.0–235.2
2016	83	22.9	37.6–155.8
2015	58	22.4	13.4–258.0
2014	70	18.6	64.6–156.7
2013	56	12.5	3.3–226.6
2012	63	11.1	3.3–226.6
2011	158	17.1	8.3–196.1
2010	225	15.1	28.0–197.2
2009	242	11.6	0.0–145.2
2008	186	24.7	21.3–373.7
2007	213	23.9	21.2–450.4
2006	274	25.2	0.0–259.0

Hospital pharmacies across Europe have established national rules tailored to pharmacy compounding to ensure proper procedures, quality, and safety of preparations. Compounding is crucial in closing the treatment gap for patients with extraordinary medical conditions or needs and is widely adopted across Europe. Adequate staffing levels and continuous professional development are necessary to ensure this important area of practice is carried out effectively. The European Association of Hospital Pharmacists (EAHP) supports the European-wide application of the European Statements of Hospital Pharmacy and the Council of Europe Resolution on quality and safety assurance requirements for medicinal products prepared in pharmacies. EAHP calls for an environment that enables hospital pharmacists to provide compounding services, including adequate facilities and equipment. Compounding has also become increasingly important in addressing medicine shortages and facilitating patient access to rational, proven treatment (European Association of Hospital Pharmacists, 2020).

2.3.1 Regulations

European pharmaceutical laws require a marketing authorization (MA) before a medicinal product can be placed on the market. However, this requirement does not apply to products prepared in a pharmacy, which fall under the exceptions of formula magistralis and formula officinalis in European law. The European Pharmacopoeia (Ph. Eur.) Monograph permits complementary pharmacy compounding to supply unlicensed products for the special needs of individual patients. The Convention's Committee of Ministers Resolution CM/Res(2016)1 emphasizes that pharmacy preparations are only advisable if a suitable pharmaceutical equivalent with an MA is not available. It is important to note that compounding is intended to complement authorized medicinal products, not replace them (Meulenbelt & Betts, 2019).

The regulations of compounding are similar in the US. Compounded drugs are not FDA-approved as the FDA does not review their safety, effectiveness, or quality before they reach the patient. As a result, the FDA has investigated cases of serious patient injury and linked them to poor-quality compounded drugs. The Drug Quality and Security Act (DQSA) was passed in response to the event in 2012 where compounded drugs led to more than 750 cases of infection and more than 60 deaths of patients in 20 states, leading to important updates to the Federal Food, Drug and Cosmetic Act regarding human drug compounding. The DQSA established a new, voluntary category of compounders known as outsourcing facilities, which are subject to good manufacturing practice (GMP) requirements and must meet certain conditions, such as reporting adverse events and providing information to the FDA. The FDA inspects outsourcing facilities on a risk-based schedule (US Food and Drug Administration, 2020).

2.4 Pharmaceutical printing

2.4.1 Perspectives of printed medicines

Printing technologies offer a promising approach to achieving personalized drug treatments through pharmacoprinting, which utilizes printing technologies to manufacture pharmaceutical products. Printing technologies' precise and highly flexible nature allows for easy manipulation of the printed solid dosage form (Sandler & Preis, 2016). The versatility of 3DP technology allows for the customization of medicines by adjusting technical parameters, including size, shape, and fill rate (Singhvi et al., 2018). Specifically, 3DP can be used to produce low-dose personalized medicines suitable for pediatric patients, improving their taste and appearance to increase compliance (Scoutaris et al., 2018; Tabriz et al., 2021). For elderly patients who have difficulty swallowing, 3DP can be used to prepare suitable preparations to aid in drug intake. Additionally, 3DP can be utilized to combine different drugs into a single tablet to increase compliance by reducing the number of daily tablets (Khaled et al., 2015a).

The pharmaceutical industry is characterized by large production capacities and equipment, which lack the flexibility to quickly make changes in the drug production process. In contrast, 3DP technology provides a compact, automated, and easily customizable production process suitable for small-scale drug production, frequent design modifications, and rapid responses to changes in treatment regimens, bringing the production closer to the patient and allowing for the production of small, unique batches based on the specific needs of individual patients at any given time (Sandler & Preis, 2016; Seoane-Viaño et al., 2021a). Specifically, SSE 3DP technology enables the direct replacement of syringes containing different drug varieties, thus eliminating the need for extensive cleaning, and thus reduces downtime.

A case study revealed that pediatric healthcare professionals expressed a favorable attitude toward 3D-printed solid oral dosage forms (Rautamo et al., 2020). They identified several attractive features, such as personalization of dosage forms, more precise dosing, age-appropriate forms, and the ability to produce combination products. Additionally, they found short delivery times for on-demand printed dosage forms at hospitals valuable and considered the identification possibilities an added benefit. However, the safety of the dosage form and dose verification remained a concern. In a case study conducted by Beer et al., stakeholders were interviewed to assess the feasibility of implementing 3DP in the European pharmaceutical system. Factors such as specialized knowledge, logistics, safety, liability, legislation, and economic feasibility were considered when discussing potential printing locations. While pharmacies were viewed as suitable due to their compounding activities, some respondents suggested limiting printing to large hospital pharmacies and compounding facilities. Cost was a significant concern, with expectations of high expenses for 3D printers and pre-filled cartridges. Turnover, patient volume, and

printing hours were identified as factors influencing cost-effectiveness. Training and competency of community pharmacists in 3DP raised concerns, and the need for safeguards like traceable barcodes and error detection mechanisms was emphasized. Limited space in pharmacies and the risk of cross-contamination were also discussed, prompting suggestions for disposable parts. Liability issues related to the complex nature of 3DP technology were raised, with the importance of establishing a clear responsible entity. Large hospital pharmacies were seen as more inclined to adopt 3DP compared to small hospital pharmacies, in general hospital pharmacists were considered better equipped for this technology compared to community pharmacists. 3DP in compounding facilities was deemed viable due to existing production capacities. Although viewed as futuristic, the potential for 3DP in patients' homes was acknowledged, emphasizing the need for safety, regulatory compliance, and reliable control mechanisms. Remote printer control by professionals was proposed as a potential solution (Beer et al., 2021).

Currently, Uppsala University researchers are working on the development of 3D-printed medicines specifically designed for critically ill children. The aim is to establish a testing facility at Uppsala University Hospital by 2025, enabling patients' families to eventually take the 3D printer home and independently produce the necessary medicines. To ensure proper control and safety, guardians will be required to log in to the 3D printer using their bank ID, and the printing of medicine will be registered simultaneously with the doctor and pharmacy (Karlsson, 2022).

In another case study by Beer et al., where they interviewed different stakeholders regarding how 3DP could be integrated as a compounding practice. The respondents identified various advantages with utilizing 3DP for compounding, including dosage strength adjustments, excipient customization, and the ability to create polypills. Other benefits mentioned were improving administration through smaller tablet sizes or orally disintegrating tablets, and the ability to print tablets with different release profiles. Respondents acknowledged the need for regulatory guidance and validation processes to ensure the safety and quality of 3D-printed medicines, including raw materials, software, printer validation, cleaning procedures, and quality attributes of the final product. Safeguards such as traceable barcodes on prefilled cartridges were suggested to enhance safety and minimize errors in implementation (Beer et al., 2023).

Quality control of 3D-printed dosage forms is an important consideration that requires attention. As 3D-printed oral medicines lack a regulatory framework, they currently need to meet the same quality standards as conventional dosage forms. However, this can be challenging as 3DP techniques follow a different process than conventional tableting, which involves mixing, blending, milling, and compression into tablets. Furthermore, in contrast to traditional mass production, 3DP allows for small-scale production on-site at clinics or

pharmacies. This could potentially eliminate intermediate steps involved in conventional manufacturing, significantly changing quality standards for 3D-printed dosage forms. As a result, it is essential to establish appropriate quality control measures that account for the unique properties of 3D-printed medicines (Karalia et al., 2021).

2.4.2   Printing methods

3DP, also known as additive manufacturing, is a technique that allows the creation of customized objects by building them up layer by layer (Singhvi et al., 2018). There are several different 3DP technologies, which can be grouped into seven categories according to American Society for Testing and Materials (ASTM) standards: vat polymerization, material jetting, binder jetting, material extrusion, powder bed fusion, directed energy deposition, and sheet lamination (International Organization for Standardization, 2015). In the production of pharmaceutical oral dosage forms, a few specific printing technologies are commonly investigated, namely, material extrusion (including SSE, fused deposition modeling (FDM), and direct powder extrusion (DPE)), binder jetting (BJ), selective laser sintering (SLS) (a subcategory of powder bed fusion), and stereolithography (SLA) (a subcategory of vat polymerization) (Karalia et al., 2021). Moreover, the two-dimensional printing technique, inkjet printing (IJP), has also been extensively investigated for producing solid oral dosage forms (Daly et al., 2015).

The process of 3DP involves three fundamental steps, regardless of the specific technique employed. Firstly, the object is designed using a computer-aided design (CAD) software. Secondly, the CAD design is converted into a rapid prototyping stereolithography (.stl) format, where the 3D model is divided into layers. Finally, the resulting file can be exported to the 3D printer in machine-specific code (.gcode) that the printer can read and utilize to fabricate the object layer by layer. This allows for the creation of personalized objects of any desired shape and size (Zema et al., 2017). Compared to conventional manufacturing processes, one major advantage of 3DP is the reduction in production time, cost, and manual labor due to the computer-controlled procedure used throughout the entire process (Norman et al., 2017). Furthermore, mathematical algorithm can be utilized to automate the digital design to obtain the recommended dose which in turn can minimize the need for distributing specialized workforce at the manufacturing site (Eleftheriadis et al., 2021).

Below are schematic illustrations (Figure 1) and descriptions of the current printing methods being investigated for preparing personalized medicines, with a focus on SSE 3DP.
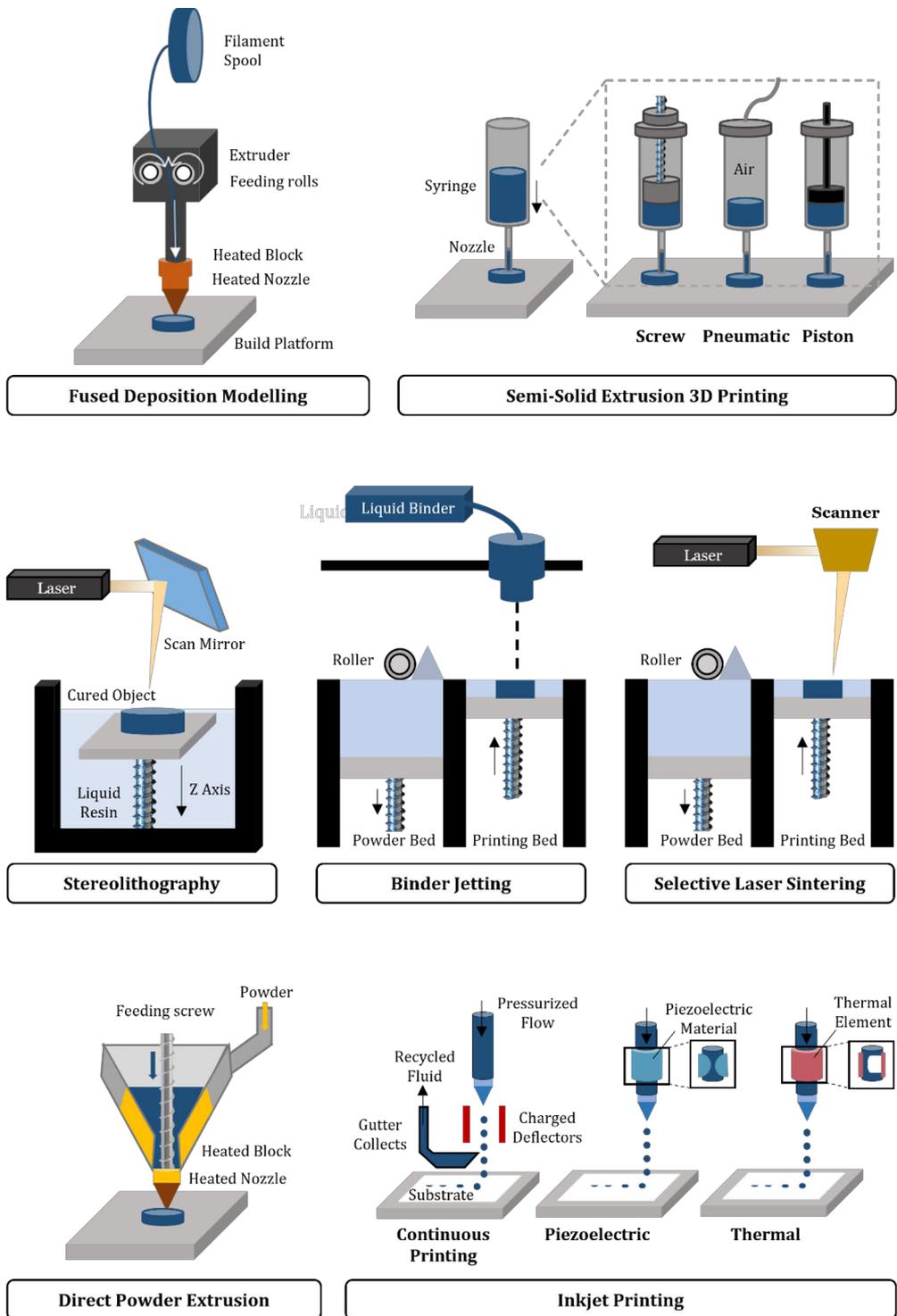
Figure 1. *Schematic overview of the different printing technologies used for the production of solid oral dosage forms.*

2.4.2.1   Semi-solid extrusion (SSE) 3D printing

SSE is a 3DP technique that involves the deposition of a gel or paste in sequential layers to create an object. This differs from other material extrusion techniques like FDM or DPE, where the printing material is in the form of a solid filament or powder, respectively. SSE 3DP is also known as bioprinting, pressure-assisted microsyringe (PAM) printing, robocasting or robotic material extrusion, cold extrusion-based printing, hydrogel-forming extrusion, melting extrusion, thermal extrusion, soft-material extrusion, a melting solidification printing process, direct ink writing, hot-melt ram extrusion, hot-melt pneumatic extrusion, and micro-extrusion (Seoane-Viaño et al., 2021a). SSE 3DP's unique attributes have prompted the exploration of utilization in drug development to produce novel dosage forms. SSE 3DP enables printing at ambient conditions, making it suitable for a wide range of drugs, including thermolabile APIs. Furthermore, using disposable pre-filled syringes employed in SSE 3DP ensures meeting critical quality requirements demanded by regulatory agencies (Park et al., 2019). SSE's single-step printing process allows for the rapid production of 3D-printed oral dosage forms and other devices, making it a perfect candidate for clinical and research settings. In fact, SSE 3DP was used in the first clinical study that prepared on-demand, personalized ChewTs in a hospital setting, which were administered to children with a rare metabolic disease (Goyanes et al., 2019b). Recently, a study successfully demonstrated the feasibility of developing and manufacturing a 3D-printed tablet at the point-of-care that meets quality standards for clinical use, including conducting bioequivalence studies in healthy adults (Lyousoufi et al., 2023). An extensive list of investigated SSE 3D-printed oral dosage forms can be found in Table 2.

There are different methods for extruding material through the syringe (Figure 1). Pneumatic systems use pressurized air to compress and extrude the material and offer precision and rapid response time, making them suitable for printing highly viscous materials. Mechanical-based systems apply mechanical force directly to the syringe either through a piston-based or screw-based system. The piston-based system can obtain greater flow over the extrusion, while the screw-based system allows for more spatial control (Hospodiuk et al., 2018). The mechanical systems are simpler and more affordable than pneumatic systems, as there is no need for an air compressor; however, uneven printing has been observed with the mechanical-based system, specifically the screw-based system (Sjöholm et al., 2020).

The SSE 3DP process entails placing a disposable syringe loaded with a viscous gel or paste into the printer. The material is then extruded through a nozzle that is attached to the syringe onto the build platform. Several critical parameters play a vital role in determining the printing precision and quality of the final product, including dose accuracy. Firstly, the nozzle diameter plays a vital role in the process (Firth et al., 2018; Zidan et al., 2019), and smaller diameters are preferred for higher resolution and smooth surface objects, but it increases the

printing time. Conversely, a larger nozzle diameter is suitable for greater structural stability and prevents blockages, a common issue with smaller diameter nozzles (Z. Liu & Zhang, 2019). Additionally, the nozzle travel speed and extrusion rate also contribute to the printing precision, where high travel speed results in less material deposition and smaller diameter strands, while a high extrusion rate produces larger extruded filament diameters, and vice versa (Khalil & Sun, 2007). Furthermore, some feedstock material is dependent on heating, making the printing temperature another important parameter, as it directly influences the material extrusion. If the printing temperature is too high, over-extrusion can occur, while too low temperature leads to nozzle clogging (Seoane-Viaño et al., 2021b; Vithani et al., 2019a). The distance between the nozzle and the build plate is also critical and should be calibrated according to the material viscosity. A too large distance can cause material adhesion issues, while positioning the nozzle too close to the build plate may result in insufficient and inconsistent material flow (Firth et al., 2018; Zidan et al., 2019). Therefore, accurately calibrating the distance between the nozzle and the build plate is essential.

To obtain the final printed object, the object has to solidify, and there are various solidification strategies, but two of the most common are heat-induced and solvent-induced solidification. In the first approach, heat is used to extrude the material, and solidification occurs during the cooling process. The second approach involves using a solvent or a combination of solvents, and solidification occurs as the solvent is removed through evaporation (Khaled et al., 2015a; Vithani et al., 2019a). Other less common strategies include photopolymerization (Holländer et al., 2018; Sydney Gladman et al., 2016), ionic crosslinking (Wu et al., 2020), and chemical reactions (Croitoru-Sadger et al., 2019).

SSE 3DP is a highly promising and suitable technology for producing personalized medicine due to its simplicity, versatility, and ability to create a wide variety of dosage forms in various shapes and flavors. This technology enables the direct mixing of drugs with excipients, which can then be filled into disposable syringes, thereby facilitating compliance with GMP guidelines. SSE 3DP is particularly advantageous in creating chewable formulations for patients with swallowing difficulties and for use in preclinical studies. However, certain issues such as material viscosity, drying time, resolution, and long-term storage need to be addressed before implementation in healthcare. Nonetheless, SSE 3DP has the potential to revolutionize adherence and accuracy, paving the way for personalized treatment approaches.

Table 2. *A comprehensive list of examples of dosage forms produced by semi-solid extrusion (SSE) 3D printing.*

Formulation details/Properties	Drug	Ref.
Polypills		
Combination of five different drugs with dual-release mechanisms	Pravastatin, atenolol, ramipril, aspirin, and hydrochlorothiazide	(Khaled et al., 2015a)
Combination of three drugs with osmotic pump and sustained-release mechanisms	Captopril, nifedipine, and glipizide	(Khaled et al., 2015b)
Three different drugs with programmed release profiles	Glyburide, metformin hydrochloride, and acarbose	(Haring et al., 2018)
Controlled-release fixed dose combination comprising of three anti-HIV-1 drugs	Efavirenz, tenofovir disoproxil fumarate, and emtricitabine	(Siyawamwaya et al., 2019)
Immediate-release tablets		
High drug loading immediate-release tablets	Paracetamol	(Khaled et al., 2018)
Immediate-release tablets	Levetiracetam	(Cui et al., 2019, 2020; El Aita et al., 2019, 2020)
Immediate-release tablets with cyclodextrin	Carbamazepine	(Conceição et al., 2019)
Subdivided tablets as an alternative to the splitting of conventional tablets	Spironolactone, hydrochlorothiazide	(Zheng et al., 2020)
Rapid-release tablets	Puerarin	(P. Li et al., 2020)
Immediate release formulations using thermosensitive gelatin pastes	Ibuprofen	(Y. Yang et al., 2020)
Temperature and solvent-facilitated extrusion	Theophylline	(Dores et al., 2020)
3D-printed tablets for pediatric use	Furosemide, sildenafil	(Lafeber et al., 2021)

Orodispersible printed tablets	Hydrochloro-thiazide	(Eduardo et al., 2021; Suárez-González et al., 2021)
Child-friendly cereal-based dosage forms	Paracetamol, ibuprofen	(Karavasili et al., 2022)
Nanocrystal-based solvent-free 3D-printed tablets	Albendazole nanocrystals	(Lopez-Vidal et al., 2022)
Orally disintegrating tablets	Loratadine	(Yi et al., 2023)
GMP-produced tablets used in clinical trial	Sildenafil	(Lyousoufi et al., 2023)
Modified-release tablets		
Gastro-floating tablets	Dipyridamole	(Q. Li et al., 2018)
Tablets with different dissolution profiles	Naftodipil	(Tagami et al., 2019)
Sustained-release tablets fabricated with two-component cross-linkable gels	Prednisone and bovine serum albumin	(Croitoru-Sadger et al., 2019)
Tablets with complex structures	Glipizide	(M. Cui, Yang, et al., 2019)
Sustained-release tablets	Theophylline	(Cheng et al., 2020)
Floating sustained-release systems	Ricobendazole	(Real et al., 2020)
Printable formulations after several days of storage	Levetiracetam	(El Aita et al., 2020)
Sustained-release formulations using thermosensitive pastes	Diclofenac	(Y. Yang et al., 2020)
Multi-compartment self-nanoemulsifying tablet	Rosuvastatin, glimepiride	(T. A. Ahmed et al., 2021)
Floating drug delivery system by coaxial extrusion	Propranolol hydrochloride	(Falcone et al., 2021)
Core-shell gastric floating system	Clarithromycin	(Chen et al., 2021)
Self-nanoemulsifying drug delivery system	Glimepiride	(T. A. Ahmed et al., 2022)

3D-printed gastro-retentive dosage form	Ricobendazole	(Falcone et al., 2022)
Redispersible oral solid forms containing drug-loaded polymeric nanocapsules	Resveratrol, curcumin	(de Oliveira et al., 2022)
Oral macromolecule administration	Octreotide	(Chatzitaki et al., 2023)
Orodispersible mini-tablets	Carbamazepine	(Hu et al., 2023)
pH-responsive dosage form	Bovine serum albumin	(F. Wang et al., 2023)
3D-printed gastro-retentive tablets	Niclosamide nanocrystals	(Real et al., 2023)
3D printed pill-in-pill colon-targeted tablets	Budesonide	(Ou et al., 2023)
Gastro-floating tablets	Famotidine	(H. S. Yang & Kim, 2023)
Combined-release tablets		
Bilayer tablet with immediate- and sustained-release	Guaifenesin	(Khaled et al., 2014)
SSE and FDM combination printing	Tranexamic acid, indomethacin	(Zhang et al., 2022)
Chewable tablets		
Printed tablets prepared for a clinical study	Isoleucine	(Goyanes et al., 2019b)
Lego™-like chewable bricks	Paracetamol, ibuprofen	(Rycerz et al., 2019)
Chewable chocolate-based dosage form	Paracetamol, ibuprofen	(Karavasili et al., 2020)
Printed oral gummy dosages	Ranitidine hydrochloride	(Herrada-Manchón et al., 2020)
Printed oral gummy dosages	Lamotrigine	(Tagami et al., 2021)
Starch-based soft dosage forms	Isoniazid	(Chatzitaki et al., 2021)
ChewaTs for veterinary use	Gabapentin	(Sjöholm et al., 2022a)

Chocolate-based dosage forms comparison to mold-casting	Paracetamol	(Chachlioutaki et al., 2022)
ChewTs for veterinary use	Theophylline	(Sjöholm et al., 2022b)
Oral films		
ODFs prepared by hot melt ram extrusion	Paracetamol	(Musazzi et al., 2018)
ODFs of different sizes	Warfarin	(Öblom et al., 2019a; Sjöholm & Sandler, 2019)
ODFs for veterinary use	Prednisolone	(Sjöholm et al., 2020)
Printed ODFs of three sizes	Levocetirizine dihydrochloride	(Yan et al., 2020)
Multi-layered ODFs fabricated with in-process drying	Benzydamine hydrochloride	(Elbl et al., 2020)
3D-printed oral films with nanocrystallized drug	Indomethacin nanocrystals	(Germini & Peltonen, 2021)
Prolonged-release buccal films	Propranolol hydrochloride	(Jovanović et al., 2021)
In vivo rat studies on 3D-printed mucoadhesive film	Apigenin	(Takashima et al., 2022)
Printed ODFs compared to casted ODFs	Mirtazapin	(Chaiwarit et al., 2022)
Multi-layer ionic liquid oral films	Ibuprofen, lidocaine	(Tagami et al., 2022)
Oral solid films for neonates	Caffeine	(Roche et al., 2023)
Oral films of nanosized drug	Nanoformed piroxicam	(Mathiyalagan et al., 2023)
Additional solid oral dosage forms		
Solid self-microemulsifying tablets in various geometries	Fenofibrate and cinnarizine	(Vithani et al., 2019a)
Solid lipid tablets	Fenofibrate	(Johannesson et al., 2021)
Effervescent tablets	Xianganfang	(Dong et al., 2022)
Lipid-rich solid tablets	Fenofibrate	(Johannesson et al., 2023)

2.4.2.2   Fused deposition modeling (FDM)

FDM technology is one of the most studied and commonly investigated 3DP approaches in the pharmaceutical field due to its simplicity, low cost, high product strength, and ability to produce complex structures (Cailleaux et al., 2021). The manufacturing process involves extruding a thermoplastic polymer filament to a printhead with a heated nozzle that melts the filament (Figure 1). The molten material is then deposited layer by layer according to a predetermined design and hardens upon cooling. There are three primary ways to prepare 3D-printed tablets using FDM technology. In the dipping-melting method, a pre-made filament is loaded with API by dipping it into a drug-loaded solution or dispersion prior to FDM printing. The hot melt extrusion (HME)-FDM method, which is the most common, involves mixing the drug with excipients such as polymers, which are then transferred to a conveyor. The powder blend is molten and mixed before being extruded at a certain temperature, pressure, and speed through a nozzle to obtain the desired diameter. Upon cooling, it solidifies into drug-loaded filaments ready for FDM printing. In the filling method, an empty shell is first printed, the API is filled in, and the shell is continued to be printed, enclosing the API within the dosage form. The printing and filling processes can be carried out simultaneously or sequentially (Cailleaux et al., 2021; Melocchi et al., 2020; Quodbach et al., 2022).

The FDM technology has significant potential in the pharmaceutical field. However, to optimize its use, it is important to consider the limitations and challenges associated with the different preparation methods and FDM in general. The physicochemical properties of the filament significantly affect the printability of the material, including mechanical, thermal, and rheological properties. The prepared filament should have a homogeneous diameter and drug loading to ensure accurate and precise dosing (P. Wang et al., 2019). Therefore, selecting suitable thermoplastic polymers with specific characteristics, such as appropriate glass transition and melting temperatures, is critical. Although FDM technology can produce complex geometries with excellent hardness and low friability, each preparation method has limitations. For instance, the dipping method is limited by a low drug-loading capacity of up to only 3%, making it unsuitable for drugs with low potency (Cerda et al., 2020). In contrast, while the HME-FDM method offers high drug-loading capacity, it significantly restricts the choice of API and excipients due to subjecting the materials twice to highly elevated temperatures, which can cause thermal degradation, a common concern with FDM in general (Kollamaram et al., 2018; P. Wang et al., 2019).

FDM technology has been widely used to prepare various types of preparations due to its unique properties. It allows for the creation of 3D-printed preparations of different shapes and sizes (Goyanes et al., 2017), with different infill levels, resulting in various release profiles (Öblom et al., 2019b). FDM technology also enables the incorporation of multiple drugs into a single dosage form

(Ghanizadeh Tabriz et al., 2021). In addition, it has been explored as a method to produce orodispersible dosage forms (Jamróz et al., 2017) and intravaginal rings (Tiboni et al., 2021). These applications demonstrate the versatility and potential of FDM technology for pharmaceutical development.

2.4.2.3   Direct powder extrusion (DPE)

DPE has recently gained attention in the pharmaceutical field. It is similar to FDM, but instead of using filaments produced by HME as feedstock, it directly extrudes powders or pellets using a single screw extruder (Figure 1). Unlike FDM, DPE does not require the preparation of filaments, making the manufacturing process a one-step approach saving time and cost during manufacturing. This simplification enables the extrusion of mixtures that conventional FDM cannot print due to inadequate mechanical characteristics of the prepared filaments, such as brittleness or lack of flexibility (Goyanes et al., 2019a). Moreover, the one-step approach reduces the risk of drug degradation, as the drug is not exposed twice for long durations to elevated temperatures. However, DPE still requires high temperatures to melt the material at the nozzle to enable extrusion, potentially still making it unsuitable for highly thermal-labile compounds. Good powder or pellets flow properties are crucial to obtain even extrusion and printing. DPE has been investigated for the production of immediate-release tablets with different infills (Fanous et al., 2020), modified-release tablets (Ong et al., 2020), and dosage forms consisting of low melting carriers (P. Li et al., 2020).

2.4.2.4   Binder jetting (BJ)

BJ is a 3DP technique that utilizes IJP to precisely apply a liquid binder solution (described in detail in section 2.4.2.7) to a powder substrate, building up the object layer by layer (Scoutaris et al., 2016). A typical BJ system includes a binder solution reservoir, a powder reservoir, and a build platform. The process involves discharging powder from the powder reservoir onto the build platform, spreading it with a roller, and jetting the binder solution based on the desired object geometry (Figure 1). The process repeats until the final 3D object is created (Yu et al., 2009). In BJ, the printing ink typically contains only the binder, while the API is in the powder bed with other excipients. However, the API can also be sprayed into the powder bed in the form of a solution or a suspension of nanoparticles (Ameeduzzafar et al., 2019). Developed at the Massachusetts Institute of Technology in the late 1980s and later commercialized by Z corporation (Choong, 2022), BJ has been extensively used in rapid prototyping, plastic surgery, bone scaffolds, and the cosmetic industry (Sen et al., 2021). In 2015, the first 3D-printed tablet was approved by the FDA, which was fabricated using BJ, and since then, various studies have been conducted to develop different types of solid dosage forms using this printing process (Trenfield et al., 2018; Vaz & Kumar, 2021). These include rapid-release preparations (Kreft et al., 2022; Z. Wang et al., 2021), controlled-release dosage forms (C.-C. Wang et al., 2006), and multi-drug dosage forms (Hong et al., 2021).

BJ is a highly versatile and promising technique for personalized medicine, as it allows for the fabrication of tailored, patient-specific dosages with precise control over drug release kinetics (Trenfield et al., 2018). It has several advantages for the production of pharmaceutical dosage forms, including its ability to operate at ambient conditions, which prevents the degradation of APIs through oxidation or thermal degradation (Mostafaei et al., 2021). Additionally, BJ is compatible with a wide range of materials and can produce highly porous tablets with high drug loadings, making it suitable for the preparation of immediate-release, fast-dissolving, and orodispersible dosage forms. However, BJ is a multi-step process that requires post-processing steps, which can lead to increased complexity and reduced efficiency (Vithani et al., 2019b). Furthermore, producing tablets with adequate mechanical properties is particularly challenging due to the high porosity of the final object. To address this issue, excipients such as fillers with high water solubility, humectants with high water content, and binders with high viscosity in solution can be used to increase the hardness and binding strength of the dosage form, thereby prolonging their disintegration (Vaz & Kumar, 2021). Despite these challenges, BJ has demonstrated significant potential for the development of novel, personalized dosage forms and continues to be a subject of intense research in the pharmaceutical industry.

2.4.2.5 Selective laser sintering (SLS)

SLS is a highly promising 3DP technique that offers unique advantages in the production of pharmaceutical dosage forms. Similar to BJ, SLS uses a powder bed as a starting material. However, the main difference is that SLS uses a laser beam to heat and fuse the powder particles together rather than a liquid binder solution (Figure 1). There are several advantages of SLS. Firstly, it is a one-step process, which eliminates the need for prior preparation of filaments as in FDM or post-processing steps such as drying, which is necessary for SSE 3DP and BJ. Secondly, it is a solvent-free process and offers high-resolution printing due to high laser precision. However, there are concerns about the high energy input of the laser and its potential to cause drug degradation, limiting its application. Despite these concerns, SLS-printed formulations offer the advantage of controllable porosity and reproducibility by modifying the printing parameters, such as laser scanning speed (Karalia et al., 2021). Although the laser scanning speed significantly affects the final formulation's mechanical properties, a low-speed results in higher contact time, resulting in harder and denser dosage forms and vice versa (Charoo et al., 2020). Due to the ability to produce highly porous products, SLS has been mainly used for the production of orodispersible (Allahham et al., 2020) and immediate-release tablets (Gueche et al., 2021). However, SLS has also been used to prepare sustained-release products (Y. Yang et al., 2021).

2.4.2.6 Stereolithography (SLA)

Similarly to SLS, SLA technology utilizes a ultraviolet (UV) laser beam to cure liquid photosensitive polymer resin into 3D-printed objects, layer by layer (Dabbagh et al., 2021). The process of SLA (Figure 1) involves exposing a liquid resin to UV light which triggers a chemical reaction, leading to the formation of solid layers. The degree of curing depends on light intensity and exposure time, and the viscosity of the resin affects the SLA process. When the printing is complete, excess resin and support structure is removed. In addition, post-curing with a UV oven can increase the object's mechanical properties (Melchels et al., 2010). SLA offers several advantages, such as high precision, making it suitable for the fabrication of microneedles, scaffolds, and other medical devices, and low local heating, which is ideal for thermo-labile drugs. However, the limited availability of photocrosslinkable polymers that are considered safe for pharmaceutical applications has hindered the widespread use of SLA in the pharmaceutical industry (Curti et al., 2021). Hence, it has not been widely investigated for pharmaceutical purposes. Nonetheless, some studies have demonstrated its potential in the fabrication of extended-release tablets of thermo-labile drugs with reduced drug degradation compared to FDM-printed tablets (J. Wang et al., 2016).

2.4.2.7 Inkjet printing (IJP)

IJP is the deposition or jetting of small liquid droplets onto a substrate according to a predetermined design (Figure 1). In the pharmaceutical industry, drug and excipient mixtures are deposited as small drops on a suitable substrate. Two main IJP platforms are utilized: continuous inkjet printing (CIJ) and drop-on-demand (DoD) (Goole & Amighi, 2016). CIJ printers eject a stream of liquid droplets continuously, while DoD printers eject drops only when necessary. DoD inkjet printers are further classified into thermal inkjet (TIJ) and piezoelectric inkjet (PIJ) printers based on the trigger mechanism used to discharge droplets. TIJ printers use resistors embedded in the printheads that produce heat to create bubbles, which then eject a small volume of fluid out of the nozzle forming a droplet. In contrast, PIJ printers use a piezoelectric element or actuator that generates pressure to eject fluid out of the nozzle. CIJ is advantageous due to its high-speed continuous droplet generation, which prevents nozzle clogging. However, it suffers from low-resolution printing and requires expensive maintenance. DoD printing is relatively simple and offers high precision at a lower cost than CIJ. It has the potential to deposit small drops of controllable sizes with good placement accuracy, which minimizes drug wastage. As a result, it is preferred over CIJ printing for pharmaceutical applications. The main limitation of TIJ printing is the high temperature (200–300°C) of the resistor, which may degrade thermo-labile APIs. On the other hand, PIJ printing operates at room temperature using less volatile and more biocompatible fluids, making it advantageous for pharmaceutical printing. One of IJP's advantages is the capacity to produce very low and highly precise doses, rendering it particularly well-suited for potent drugs (Vaz & Kumar, 2021). However, it's crucial to

acknowledge that the limited amount of ink deposition imposes a constraint on the achievable drug dose. This constraint is influenced by both the substrate's capacity for ink deposition and the drug's solubility within the printing ink.

In addition to CIJ and DoD, there are a few other IJP technologies worth mentioning. One such alternative is valve jet or electromagnetic printing, which relies on miniature solenoid valves. Glass inkjet tools have also been developed for pharmaceutical applications, allowing high-frequency droplet ejection due to their inertness. Moreover, inkjet technology can be combined with UV photo-initiation for rapid material hardening upon demand (Vaz & Kumar, 2021).

IJP has been used in various pharmaceutical applications. The main application is ODF formulations (Öblom et al., 2020; Vakili et al., 2017), where the drug is jetted onto edible substrates. These films are designed to rapidly release drugs in the mouth without the need for chewing or water consumption (Musazzi et al., 2020).

2.4.3 Current state of commercialization and regulatory landscape of pharmaceutical printing

Despite the potential of 3DP technology in the pharmaceutical field, its adoption is still facing several challenges. The first 3DP company was founded in 1996 but was unsuccessful. However, in 2003, Aprecia re-licensed their technology, and in 2015, Spritam®, the world's first and only 3D-printed preparation, gained FDA approval (US Food and Drug Administration, 2015). The FDA's Emerging Technology Team (ETT) actively supported the development of this product. In January 2017, the FDA released a review discussing the emergence of 3D-printed drug products as a new chapter in pharmaceutical manufacturing, highlighting 3DP as a technology of the future. The FDA issued industry guidance in July of the same year, focusing on the advancement of emerging technology applications for pharmaceutical innovation and modernization. The guidance specifically highlighted the importance of 3DP technology and continuous manufacturing as key strategic directions (US Food and Drug Administration, 2017). While the FDA has issued technical guidance on medical devices and prosthetics manufactured using additive manufacturing, no technical considerations or regulations have been issued for 3D-printed products with drug delivery functions.

EMA too is lacking guidelines and regulations when it comes to 3DP, especially in terms of the production of medicinal products. However, guidelines exist for 3D printers and 3DP of medical devices. In the EU, 3D printers are considered "harmonised products" and are regulated by specific product harmonization legislation. They are classified as machinery under the Machinery Directive 2006/42/EC, requiring manufacturers to comply with health and safety requirements, to prepare a technical file, and to affix the CE marking before market entry. Additionally, 3D-printed products used for medical devices fall under the scope of EU product legislation, such as the Medical Devices Directive

93/42/EEC. Manufacturers must ensure compliance with relevant EU regulations for these medical devices (European Commission, 2020). In the Final Programming Document 2023-2025 by EMA, they highlight key strategic goals. These include supporting the integration of scientific and technological progress in medicine development, with a focus on precision medicine, transforming the regulatory framework for veterinary medicines to foster innovation and effective regulation, and facilitating the implementation of novel manufacturing technologies (European Medicines Agency, 2023a). The recently established Quality Innovation Group (QIG) by the EMA seeks to provide regulatory guidance and define expectations for innovative manufacturing technologies, including decentralized manufacturing with the primary objective to facilitate the introduction of these advanced products into the market (European Medicines Agency, 2023b).

Currently, there are several 3DP drug companies, mainly in Europe, the US, and China. Aprecia forged two strategic partnerships in the recent years. In 2020, Aprecia partnered with Battelle to accelerate and expand their pharmaceutical 3DP manufacturing capabilities focusing on increasing throughput and efficiency (Aprecia, 2020) and in 2021 Glatt Pharmaceutical Services and Aprecia partnered to combine Glatt's multiparticulate technologies with Aprecia's 3DP manufacturing. The collaboration aims to overcome design challenges in oral pharmaceuticals and focus on modified release extensions and new chemical entities, utilizing Aprecia's ZipDose™ technology for patient-focused dosage forms and accelerated clinical development (Aprecia, 2021a). They also started a collaboration with Nanoform in 2021 to explore synergies between their respective technologies, investigating nanoparticle-enabled 3D-printed dosage forms (Aprecia, 2021b). In addition to Aprecia, Triastek is also focusing on large-scale 3DP and launched their MED® 3DP technology in 2018, which was approved by the ETT in 2020, and three of their products have obtained clinical trial approval on their investigational new drug (IND) applications, namely T19 for rheumatoid arthritis, T20 for clotting disorders, and T21 for ulcerative colitis (Triastek, n.d.). Furthermore, in 2022, they entered into partnerships with Siemens to accelerate digital transformation of the pharmaceutical industry (Triastek, 2022a) and Eli Lilly to improve oral delivery of drugs (Triastek, 2022b), and in 2023 they announced a collaboration with Boehringer Ingelheim China to accelerate new drug development (Triastek, 2023).

In addition to large-scale production, 3DP is highly suitable for personalized drug delivery, and several companies are investigating this avenue. 3DP drug technology is an ideal solution, particularly in hospital pharmacies to meet the personalized drug requirements of patients of different ages and disease states. FabRx, a UK-based company founded in 2014, is one of the most active companies in this area. They have conducted extensive research on various 3DP technologies, including FDM, SLS, SLA, SSE, and DPE (FabRx, n.d.-b, n.d.-a). In 2020, the company launched M3DIMAKER™, a breakthrough 3D printer that

enables fast and flexible preparation of various 3D-printed drugs (FabRx, 2020). In 2021, they started a collaboration with the French Cancer Centre Gustave Roussy to develop personalized multi-drug dosage forms for the treatment of early-stage breast cancer (FabRx, 2021). In 2023, they announced a new clinical study to begin in Spain to assess personalized 3D-printed medicines for children (FabRx, 2023). In San Francisco, Multiply Labs was founded in 2016. They focus on developing robotic manufacturing platforms that help pharmaceutical companies produce biological medicines, but they also produce personalized medicines through a two-step approach of FDM printing and drug-filling (Carlota, 2019). Doser is a Dutch startup that together with strategic partners are bringing personalized 3D-printed medicines to pharmacies in the Netherlands. Other companies worth mentioning are Craft Health in Singapore, CurifyLabs in Finland, DiHeSys in Germany, MB Therapeutics in France, and Vitae Industries in USA (Craft Health, n.d.; CurifyLabs, n.d.; DiHeSys, n.d.; MB Therapeutics, n.d.; Vitae Industries, n.d.). Furthermore, Merck is presently exploring 3DP technology to decrease preparation development time and API usage for clinical trials. The company believes that 3DP can expedite pharmaceutical development by rapidly producing prototypes for clinical trials and printing small drug batches, thereby reducing costs and saving time in setting up large-scale manufacturing lines (Merck, 2022).

2.4.4 Implementing pharmaceutical printing near the point-of-care

Although 3DP has shown great potential for personalized drug delivery, its implementation in healthcare still requires new regulatory agreements and standardization of 3D printers to meet regulatory and quality control requirements. One proposed approach is the conventional processing of drugs and excipients at licensed manufacturing facilities under GMP to create intermediate materials called pharma-inks. These pharma-inks would undergo quality control measures before being distributed to decentralized manufacturing sites for the production of administrable dosage forms (Beer et al., 2023). Subsequently, the printed dosage forms must undergo validation to ensure patient safety and therapeutic effectiveness (Quodbach et al., 2022). To address this issue, Process Analytical Technology (PAT) and non-destructive in-line analytical techniques such as near-infrared (NIR) and Raman spectroscopy have been proposed for real-time quality control measures (Khairuzzaman, 2018). In addition, Quick Response (QR) codes and data matrices on dosage forms have been suggested and investigated as track-and-trace measures (Edinger et al., 2018; Öblom et al., 2020; Öblom et al., 2019a). While various 3D printers have been used for printing dosage forms and medical devices in research, they are not suitable for pharmaceutical production since they do not meet GMP regulations (Khairuzzaman, 2018). Currently, the M3DIMAKER by FabRx, the MED 3D printer by Triastek, the Z-Form Flex machine by Aprecia, and the Doser MedPrint by Doser are specifically designed and fully validated according to GMP regulations for the production of personalized medicines (Doser, 2021). In addition, Craft Health's 3D printer CraftMake™, CurifyLabs'

MiniLab, DiHeSys' FlexDose™ printer, and Vitae Industries' AutoCompounder are designed for GMP manufacturing (Craft Health, n.d.; CurifyLabs, n.d.; Pflieger et al., 2022; Vitae Industries, n.d.). Certain 3DP technologies, such as SSE 3DP, might be the most appropriate and have more potential than others to be used for medicine production due to the use of disposable syringes that can meet GMP requirements and as most of the excipients used to prepare the formulations are pharmaceutical, food-grade excipients or listed as Generally Recognized As Safe (GRAS) (Elder et al., 2016).

Standardization of 3D printers, adoption of quality control measures, and development of suitable 3DP technologies are necessary to ensure that the produced products close to the point-of-care meet the required quality standards and regulatory compliance.

2.5   Solid oral dosage forms

Dosage forms are the physical forms in which drugs are formulated and delivered to the body to achieve their desired therapeutic effect. The selection of a particular dosage form is dependent on the method of administration, which can vary depending on factors such as the patient's condition, the drug's physicochemical properties, and the desired pharmacokinetic profile. Solid oral dosage forms can be used to achieve a localized therapeutic effect in the mouth, throat, or digestive tract, or to produce a systemic effect in the body after oral or gastrointestinal absorption (Sohail Arshad et al., 2021). Solid oral dosage forms, such as tablets and capsules, are commonly used due to their several advantages. The oral route of administration is minimally invasive and is typically preferred by patients, which increases compliance. Additionally, patients can self-administer the medicine at home, making it a convenient option. Manufacturers prefer solid oral dosage forms as they are relatively inexpensive to produce and use well-established and reliable manufacturing techniques. These forms are usually stable and have a long shelf-life, making them easy to store and transport. Moreover, manufacturers can modify the appearance of solid oral dosage forms to promote brand recognition, which can be important for marketing purposes (Davies, 2009).

Tablets and capsules are two of the most widely used solid oral dosage forms due to their versatility in terms of drug delivery. Different types of tablets and capsules are designed to meet specific therapeutic needs, with each having unique characteristics. Immediate-release tablets are designed to release the drug substance immediately after ingestion, providing rapid symptom relief. On the other hand, modified-release tablets are formulated to modify the rate, place, or time at which the drug is released. Depending on the drug release characteristics, modified-release tablets can be either prolonged-release, delayed-release, or pulsatile-release tablets. ChewTs provide a satisfying mouthfeel and are intended to be chewed before being swallowed. Solid oromucosal preparations, such as pastilles and lozenges, are designed to be

slowly dissolved or disintegrated in the mouth for the delivery of active substances. They are typically intended for local effects in the oral cavity and throat and are single-dose preparations that contain one or more active substances in a sweetened and flavored base. Pastilles are soft and flexible while lozenges are hard preparations. Sublingual tablets and buccal tablets are designed to deliver active substances for a systemic effect by being applied under the tongue or to the buccal cavity, respectively. Effervescent tablets are intended to be dissolved or dispersed in water before administration and react rapidly in the presence of water, releasing carbon dioxide. Capsules, like tablets, can also exhibit immediate release and modified release. Hard gelatin capsules have two-piece shells that can be filled with powders, pellets, semisolids, or liquids. Soft gelatin capsules have a one-piece shell and contain a liquid or semisolid fill, making them easier to swallow for patients who have difficulty swallowing solid oral dosage forms (European Pharmacopoeia Commission, 2022a, 2022b, 2022c).

In recent times, there has been a significant surge of interest in the development of innovative oral solid dosage forms, for the purpose of enhancing product performance and addressing the unmet medical needs of specific patient populations. This evolution in pharmaceutical formulation approaches aims to cater to the diverse needs of patients by providing tailored solutions that align with their unique therapeutic requirements and challenges. Matrix tablets, for instance, are composed of either inert or water-soluble matrices that release the drug substance in a time-controlled manner. Another emerging dosage form is tablet-in-tablets, also known as compressed-coated tablets. This system consists of an inner drug core and an outer coating shell that regulates drug release and formulation stability. The tablet-in-capsule system is another innovative approach that involves filling and sealing one or multiple tablets in a capsule for site-specific drug delivery or controlled release rate. This system can enclose multiple tablets with different coatings, resulting in pulsatile drug release, which simulates periodic dose administration. Multilayered tablets are another type of solid oral dosage form that consists of two to five layers that incorporate different drugs with incompatible or varying release profiles in each layer. They can also deliver fixed-dose combinations of various APIs while controlling their administration rate. Furthermore, they allow for the separation of incompatible therapeutic components by loading them in distinct layers, thus ensuring their stability and efficacy (Sohail Arshad et al., 2021). Orodispersible tablets (ODTs) are a suitable dosage form for specific patient populations that exhibit difficulties swallowing. In addition to ODTs, ODFs are also gaining popularity as solid oral dosage forms that disintegrate rapidly in the mouth, making them extremely convenient to administer without water. They can be used to deliver a wide range of drugs, and their convenience makes them an attractive option for pediatric and geriatric populations (Davies, 2009).

2.5.1   Printed solid oral dosage forms

The conventional tablet manufacturing process poses limitations in terms of customization, as it results in fixed drug dosages that cannot be easily tailored to individual patient needs. However, the advent 3DP technology has revolutionized this situation, offering promising prospects for personalized medicine. 3DP offers several advantages over traditional manufacturing processes, including its simplicity, the ability to quickly make adjustments, and the flexibility to create oral solid dosage forms with customized dosages (Singhvi et al., 2018). The layer-by-layer printing method, in particular, has proven valuable for preparing polypills and dosage forms with complex internal structures and various geometric shapes (Khaled et al., 2015a). Furthermore, 3DP can improve drug solubility and precisely modify drug release by selecting appropriate formulations and designing printing structures thoughtfully (Singhvi et al., 2018). Figure 2 gives an overview of various solid oral dosage forms prepared by the means of 3DP.
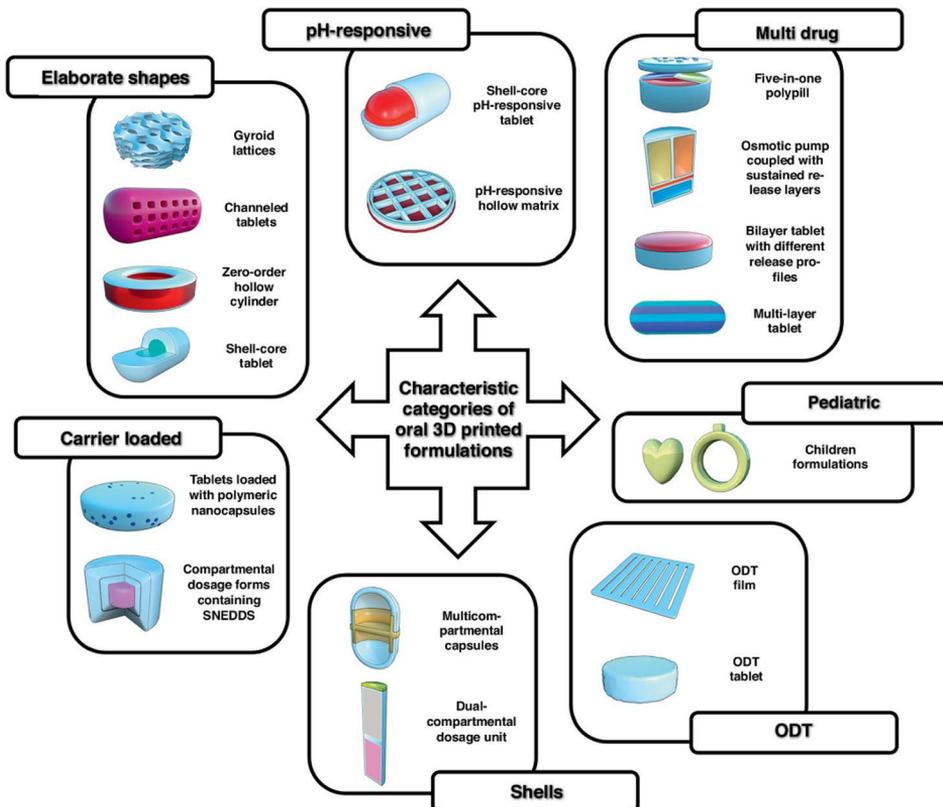

Figure 2. *Overview of characteristic categories of oral 3D-printed dosage forms. Reproduced from Gioumouxouzis et al. (2019), with permission from Elsevier.*

Studies have demonstrated the application of 3DP in producing various types of solid oral dosage forms (Figure 2), with various release profiles such as immediate-release (Fanous et al., 2020), controlled-release (Khaled et al., 2014), delayed-release (Okwuosa et al., 2017), and sustained-release (Qian et al., 2022). However, despite its potential, 3DP oral solid dosage forms still face challenges, including the lack of standardization in formulation selection, analysis, and quality assurance. Therefore, the development of standardized guidelines for the production of 3D-printed dosage forms is crucial to ensure consistency and reliability across different manufacturing facilities. Nevertheless, the potential of 3DP to revolutionize the production of personalized medicines is enormous, with the technology paving the way for tailored dosage forms that can optimize drug efficacy, minimize side effects, and improve patient outcomes.

Moreover, it is important to recognize that dysphagia, a condition characterized by difficulty in swallowing, affects individuals of all ages, particularly children and the elderly. Additionally, animals can also face challenges in swallowing solid oral dosage forms. To address these challenges, there has been growing interest in the development of patient-friendly dosage forms such as ODFs and ChewTs. These dosage forms will be further explored in the following sections, as they offer potential solutions for individuals with difficulty swallowing.

2.5.1.1   Orodispersible films (ODFs)

ODFs, also known as orally disintegrating films, are thin, stamp-sized, solid oral dosage forms that are designed to disintegrate and disperse rapidly in the oral cavity (Gupta et al., 2021). Ph. Eur. defines ODFs as "solid oromucosal preparations intended for administration in the mouth, where they disperse rapidly to deliver active substances. They consist of single- or multilayer sheets of suitable materials" (European Pharmacopoeia Commission, 2022b), while the United States Pharmacopoeia (USP) uses the definition oral films and defines it as "Thin sheets that are placed in the oral cavity. They contain one or more layers. A layer might or might not contain API" (United States Pharmacopeial Convention, 2017). Unlike chewable dosage forms, which require masticatory activity to break down, ODFs disintegrate within a matter of seconds after application. The disintegration in saliva leads to the release of the API, which can then dissolve or disperse in the oral cavity and be absorbed via the oral mucosa for local or systemic therapy. Alternatively, the API can be swallowed and subsequently absorbed through the gastrointestinal tract. Thus, ODFs offer a convenient and versatile delivery option for patients who have difficulty swallowing conventional tablets or capsules (Krämer et al., 2019).

The traditional method of manufacturing ODFs is through the solvent casting method, where a solution or a dispersion containing film-forming polymers and the drug is cast into a thin film and cut into the desired size (Hoffmann et al., 2011). However, newer methods such as HME (Cilurzo et al., 2008), semi-solid casting, rolling, electrospinning (Ravasi et al., 2023), and various printing technologies including IJP, flexographic printing, FDM, and SSE 3DP, have been

employed (Gupta et al., 2021). Printing technologies, in particular, offer the potential for producing personalized and precise doses of ODFs.

2.5.1.2 Chewable tablets (ChewTs)

Chewable dosage forms are used to deliver pharmaceutical, nutraceutical, and veterinary active substances. They are intended for oral administration and require active chewing to break down the dosage form. Chewable products are initially absorbed through the mucosal lining. However, it is important to note that drug absorption is not restricted solely to the oral cavity, as the rate and extent of absorption also depend on peroral transit to the gastrointestinal tract and drug dissolution rate, both of which are influenced by physiological factors and the drug product itself. Examples of chewable dosage forms include chewing gums, ChewTs, lozenges, and soft gel capsules (Krämer et al., 2019). ChewTs are defined by the Ph. Eur. as tablets that "are intended to be chewed before being swallowed (European Pharmacopoeia Commission, 2022c). ChewTs offer the same benefits as conventional tablets, such as dosing accuracy, portability, and long-term stability, but with the added benefit of being more easily swallowed, making it a patient-friendlier dosage form. They are especially useful in patient-centric formulations for specific populations, such as pediatrics, geriatrics, and animals, for whom swallowing conventional tablets can be challenging (Nyamweya & Kimani, 2020).

ChewTs, like conventional tablets, are typically produced using compaction, molding, or extrusion techniques. The specific manufacturing process used typically distinguishes ChewTs into two categories: hard and soft ChewTs. Hard ChewTs are produced through compaction, while soft ChewTs are typically made through molding or extrusion processes (Krämer et al., 2019). However, in recent years, there has been growing interest in 3DP technologies, particularly SSE 3DP, for the production of ChewTs with personalized doses for both pediatric and veterinary use (Rycerz et al., 2019; Sjöholm et al., 2022b; Tagami et al., 2021). Children have been found to prefer ChewTs over other oral dosage forms prepared using different 3DP technologies such as SLS, FDM, and SSE 3DP (Januskaite et al., 2020). Animals too have been found to prefer chewable dosage forms, but in contrast to children who like soft ChewTs, cats and dogs prefer hard ChewTs with a protein-based taste and scent enhancer from animal origin (Aleo et al., 2018; Nyamweya & Kimani, 2020). It is worth noting that the use of 3DP in the production of ChewTs offers several advantages, including the ability to produce complex shapes, customized doses, and personalized formulations with improved dosing accuracy, consistency, and safety. In addition, the use of 3DP technologies in the production of ChewTs offers the potential for on-demand production, reducing waste and increasing efficiency. Overall, 3DP technologies show great promise in the development and manufacturing of ChewTs for various patient populations.

2.5.1.3 Characterization of printed solid oral dosage forms

Ensuring the consistent quality, efficacy, and safety of printed solid oral dosage forms demands a comprehensive understanding of their distinct attributes and the methods used to evaluate them. While many conventional characterization approaches are relevant, printed ChewTs and ODFs present specific challenges due to their unique properties and roles. Several printing techniques have been identified as potential modifiers of the drug molecules' physical state, facilitating new interactions amongst the dosage form constituents, and subsequently impacting their stability, solubility, and dissolution rates. Thus, rigorous physicochemical characterization becomes imperative during preformulation, development, and quality control stages. This is essential to understand the variables influencing the behavior of the printed pharmaceutical entities and to ensure the integrity of the end product (Deon et al., 2022). Figure 3 outlines the primary characterization methods.
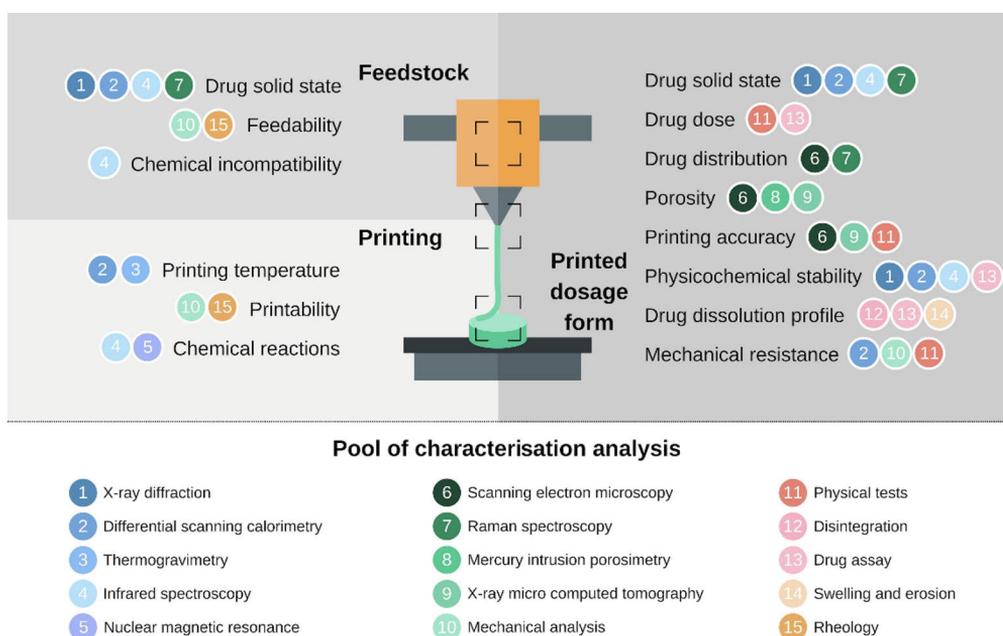
Figure 3. Pool of characterization tools applied for the evaluation of attributes in different points: feedstock, 3D printing process and final 3D printed drug dosage form. Reproduced from Deon et al. (2022), with permission from Elsevier.

a) Physical properties

The physical uniformity of ODFs is fundamental to their function. The thickness of these films, typically evaluated using micrometers, should remain consistent across the entirety of the film to ensure a uniform dose delivery, as thickness variations can significantly impact the drug dose accuracy. Delving deeper into the film's microstructure, the uniform distribution of ingredients and the

potential formation of pores or crystals can be determined using scanning electron microscopy (SEM) (Salawi, 2022). Both ODFs and ChewTs should exhibit a weight uniformity to ensure accurate dosing as the drug directly correlates to the amount of ink extruded.

Within this framework of ensuring uniformity and improving drug efficacy, the practice of nanonization emerges as significant. Deployed primarily to enhance the bioavailability of poorly soluble drugs, nanonization addresses particle size, a pivotal factor influencing surface area and thereby, bioavailability (Rizvi & Saleh, 2018). The precision in particle size, and its direct relation to increased surface area, can be accurately gauged using dynamic light scattering (DLS). This technique captures the hydrodynamic diameter (Z-average) and polydispersity index (PDI) (Clayton et al., 2016). As the particle size decreases, the surface area increases (Anderson et al., 2013), increasing drug solubility and consequently, its bioavailability (Rizvi & Saleh, 2018). The PDI represents the distribution range of particle size in a sample, with values spanning from 0.0 (perfectly homogenized) to 1.0 (highly polydisperse). Notably, a sample with a PDI value under 0.05 is considered highly monodispersed (Danaei et al., 2018), though values up to 0.2 are typically acceptable in polymer-based nanoparticle materials. Further enhancing our comprehension of particle size, transmission electron microscopy (TEM) offers an intricate view of nanoparticle dimensions.

b) Mechanical properties
Mechanical properties of ODFs are another essential characteristic. Sufficient mechanical strength is required in ensuring the structural integrity and resilience of ODFs throughout their lifecycle, from processing and packaging to transit and eventual administration (Visser et al., 2015). Parameters such as tensile strength, which offers insights into the film's fragility, and elongation at break, indicating the film's inherent flexibility, play a pivotal role in the product's durability and the patient's experience. Furthermore, the Young's Modulus provides an understanding of the film's stiffness, where a softer film might translate to better patient comfort (Mishra & Amin, 2011). A puncture test can be performed to test the strength of the films and elongation at break. Folding endurance, however, delves into the robustness of the film, assessing its resilience to repeated mechanical stressors like bending or folding. In order to demonstrate good flexibility and pass the folding endurance test, the film should be capable of withstanding more than 300 folds (European Pharmacopoeia Commission, 2020e; Steiner et al., 2016).

ChewTs need to have specific mechanical properties to ensure durability and low friability after compression, packaging, shipping, and handling. They should also be readily chewable without posing a risk to teeth, dentures, or mandibular joints. Chewability is assessed through mechanical tests, such as tablet breaking force. The hardness of a ChewT should generally lower than that of conventional tablets to enable chewing of the dosage form. The satisfactory hardness of uncoated tablets is considered to be 30–50 N/cm^2 (Arora & Arora Sethi, 2013).

The FDA recommends a ChewT having a hardness of less than 12 kp (FDA & CDER, 2018); this corresponds to 118 N.

c) *Palatability*

Palatability, defined as the acceptability and pleasantness of taste and texture of orally administered products, is crucial in solid oral dosage forms, ensuring patient adherence and optimizing therapeutic outcomes. The FDA released a guidance in 2018 which outlined important quality attributes to consider when developing ChewTs. These include taste, after-taste, odor, flavor, texture, mouthfeel, and visual aesthetics (U.S. Food and Drug Administration, 2018). To ensure a comfortable mouthfeel, it is preferable for the salivary pH of a dosage form to be administered orally to be as close to the physiological saliva range of 5.8-7.4 as possible. Administration of a dosage form with a pH outside this range may cause local mucosal irritation and discomfort (Nair et al., 2013; Patel et al., 2006; Pechová et al., 2018; Woertz et al., 2013). Furthermore, the taste is a significant determinant of patient adherence, especially in pediatric and geriatric populations. Ensuring that the bitter taste of APIs is effectively masked requires organoleptic assessments by trained panelists (Nyamweya & Kimani, 2020). ChewTs are also commonly used in veterinary products for dogs and cats, and palatability is an important factor for acceptance, often requiring the use of complex palatants (U.S. Food and Drug Administration, 2018).

d) *Moisture content*

Moisture content in pharmaceutical products plays a pivotal role in determining the stability and handleability of the final product. While the presence of excessive moisture can jeopardize the physico-chemical, chemical, and microbiological integrity of the product (Szakonyi & Zelkó, 2012), completely dry dosage forms, especially ODFs, risk becoming brittle, reducing their manageability. Some moisture in ODFs is often desirable, leveraging water's inherent plasticizing properties to enhance the dosage form's flexibility. To optimize this, excipients such as glycerol, propylene glycol (PG), polyethylene glycol (PEG), sorbitol, low molecular mass macrogols, citrates, and phthalates are incorporated due to their capability to enhance the ODF's plasticity (Hoffmann et al., 2011; Liew et al., 2014). However, while plasticizers enhance flexibility, they may also modify other attributes of the ODF, such as taste and mechanical strength. Excessive plasticizer content can also introduce stability concerns, given their propensity to absorb water. Additionally, ODFs with too high a moisture content has been described as sticky (Pechová et al., 2018). Similarly, the moisture balance is crucial for tablets. Insufficient moisture can result in hard and brittle tablets, while excessive moisture might produce overly soft, breakable tablets. Although there's no universally defined moisture content threshold for pharmaceuticals, studies suggest that an ideal buccal film should have less than 5% moisture (Nair et al., 2013), and the optimal moisture content for tablets sits around 4–5% (Tomar et al., 2017).

e) Disintegration

When considering the disintegration of ODFs, their ability to swiftly dissolve in the oral cavity is paramount, typically within a span of 5–30 seconds. Despite the crucial nature of this attribute, there remain no official pharmacopeial guidelines specifically dedicated to any specific method or acceptance limits for testing and determining the disintegration behavior of ODFs (Salawi, 2022). According to the Ph. Eur., an orodispersible dosage form should disintegrate within 3 min, an uncoated dosage form within 15 min, and an immediate release dosage form, a capsule, and a film-coated dosage form within 30 min (European Pharmacopoeia Commission, 2020a). The limit of 3 min set for ODTs has generally also been used for the novel ODFs (Thabet et al., 2018). Rapid disintegration is not only a matter of drug release but also of patient safety and comfort, particularly in pediatric and veterinary contexts. A fast disintegration time minimizes the risk of the dosage form being spit out or lodged in the esophagus. This rapid dissolution is especially vital for chewable dosage forms, where there is a potential risk of gastrointestinal obstruction should the ChewT not be entirely consumed or chewed (U.S. Food and Drug Administration, 2018). The current prevalent methods to evaluate ODF disintegration times include the Petri dish method and the slide frame methods, with the former being the preferred choice for most researchers (Salawi, 2022). The disintegration time of ChewTs is studied in the same manner as conventional tablets, with a tablet disintegrator (Deon et al., 2022).

f) Drug content and content uniformity

Maintaining consistency in drug content and ensuring uniform distribution of the API is of paramount importance, as it directly correlates to therapeutic efficacy and patient safety. The analysis of drug content is traditionally performed by dissolving the dosage form in a known amount of media. This solution is then subjected to sophisticated techniques like ultraviolet-visible (UV-Vis) spectrophotometry or high-performance liquid chromatography (HPLC), to accurately quantify the API. Such methodologies are not only used to ensure dose consistency across different units but also to gauge the effective blending during the manufacturing process. In the context of printed formulations, the drug content assay takes on additional significance. It serves as an essential step in quality control, providing insights into unit dosing, the efficacy of blending during production, and monitoring potential drug degradation throughout the process, which could be triggered by factors such as heat, light, or laser sources (Deon et al., 2022). Pharmacopeias usually provide rigorous standards for content uniformity, often demanding that each unit dosage form (e.g., tablet, capsule, or film) should deliver between 85% to 115% of the intended API dose (European Pharmacopoeia Commission, 2020c).

g) Drug release

In vitro dissolution tests are performed to characterize and describe the release profile of dosage forms. This importance is particularly accentuated for oral solid

and semisolid dosage forms, where the drug must be effectively released to facilitate absorption within the gastrointestinal tract (Deon et al., 2022). Compendial dissolution apparatuses, both paddles and baskets, are utilized in the analysis (European Pharmacopoeia Commission, 2020b). However, neither the Ph. Eur. nor the USP has established specific dissolution test setups and requirements for ODFs. There is no specific dissolution time requirement for ChewTs either, but according to the FDA, ChewTs should meet the same dissolution specifications as immediate-release tablets (U.S. Food and Drug Administration, 2018), which is 80% drug release within 30 min (European Pharmacopoeia Commission, 2020b).

h) Solid-state characterization

Solid-state characterization is crucial in the development of printed pharmaceuticals to ensure the intended properties and performance of the printed dosage forms. It provides insights into the solid-state forms of the API, the polymer matrix, and their combined structure in the final printed form. This characterization can determine if the drug remains in its original solid-state form or undergoes transitions, such as from crystalline to amorphous, during the formulation and printing process. Differential scanning calorimetry (DSC) provides insight into heat flow and transitions, such as a drug's crystallinity and melting point. However, its sensitivity can be influenced by sample changes during heating. Fourier transform infrared spectroscopy (FTIR) examines molecular interactions between the drug and polymer. Yet, it can sometimes overlook subtle changes that other methods might capture. Raman spectroscopy offers a non-destructive approach to understand molecular vibrations but can be susceptible to fluorescence interference. Another widely utilized method is X-ray powder diffraction (XRPD), which is particularly effective for identifying the crystalline nature of the components, however, it may lack sensitivity. For rapid and non-destructive quality control, NIR spectroscopy stands out as an invaluable tool in characterizing the solid-state of printed pharmaceuticals. Due to the various limitations that the techniques are facing, they are often employed in tandem to ensure a comprehensive understanding of the drug's solid-state (Deon et al., 2022).

3. Aims of the thesis

The research presented in this thesis aimed to investigate the potential of SSE 3DP as a manufacturing technique for producing customized dosage forms near the point-of-care. The main focus of the thesis was to develop printed dosage forms for patient populations that currently lack suitable dosage forms and strengths, specifically pediatric patients and animals. The overall goal of the research was to investigate the feasibility of the printing technology to produce suitable dosage forms enabling enhanced patient compliance and satisfaction by providing tailored doses that meet their individual needs.

The specific aims of the thesis were to:

- Formulate and characterize a wide range of drug-loaded printing inks (I-VI)
- Develop a nanoformed API printing ink (VI)
- Investigate the printability of the prepared inks (I-VI)
- Evaluate the content uniformity and dosing flexibility of the printing technology for oral dosage forms (I-VI)
- Compare printed dosage forms with a dosage form prepared by a conventional manufacturing technique utilized at hospital pharmacies (II)
- Compare different SSE 3D printers' ability to produce uniform and tailored doses (III)

4. Materials

The section below gives an overview of the materials used in the studies included in the thesis. A more detailed description of the materials can be found in the respective original publications (I-VI).

4.1   Active pharmaceutical ingredient (I-VI)

In Figure 4, the chemical structures of the API used in the studies are visualized. The APIs were all, except for piroxicam (PRX) in study VI, selected based on a lack of currently appropriate doses for the specific patient populations. The different APIs used for printing tailored dosage forms were warfarin sodium (WS) (Sigma-Aldrich, St. Louis, MO, USA) (I, II), prednisolone (PRE) (Sigma-Aldrich, 99%, Shanghai, China) (III), gabapentin (GBP) (Fagron Services B.V. Uitgeest, Netherlands) (IV), theophylline (TPH) (Fluka Biochemika, Sigma Aldrich, Steinheim, Germany) (V), and nanoformed piroxicam (nanoPRX) (Nanoform Finland Oy, Helsinki, Finland) (VI).

A. Warfarin sodium   B. Prednisolone

C. Gabapentin   D. Theophylline   E. Piroxicam
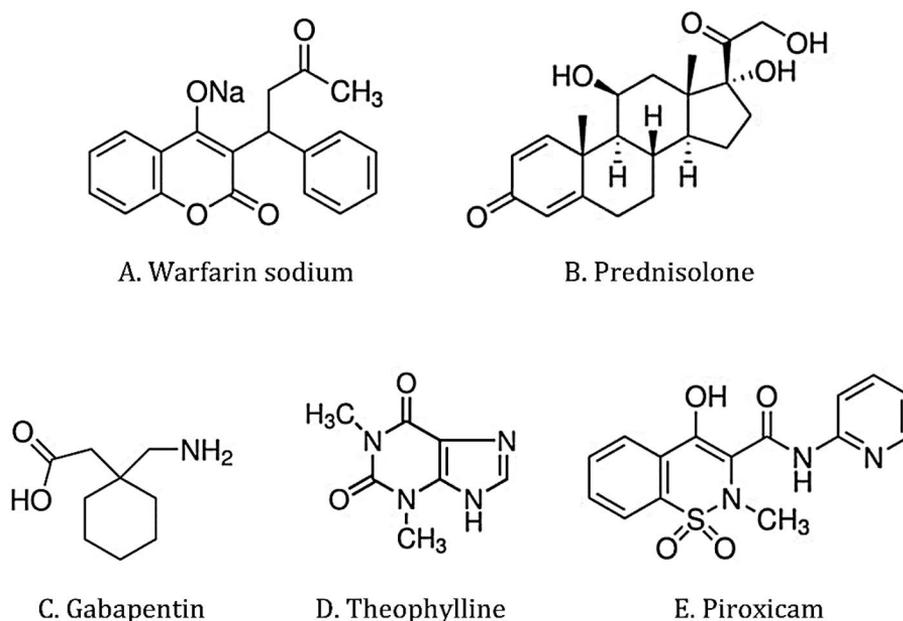
Figure 4. *Chemical structures of warfarin sodium (WS) (**A**), prednisolone (PRE) (**B**), gabapentin (GBP) (**C**), theophylline (TPH) (**D**), and piroxicam (PRX) (**E**).*

4.2   Inks (I-VI)

Pharmaceutical-grade polymers and excipients were used in the preparation of the printing inks in all studies. Drug-loaded inks with suitable properties for SSE 3DP and IJP were prepared.

The WS ink for SSE 3DP contained WS, hydroxypropyl cellulose (HPC, Klucel™ EXF, molecular weight (MW) 80,000, Ashland, Schaffhausen, Switzerland), and a mixture of ethanol (EtOH, ≥94%, Etax A, Altia, Helsinki, Finland) and purified water (Milli-Q water, Millipore SA-67120, Millipore, Molsheim, France) (I, II). The WS ink for IJP was prepared by dissolving WS in a mixture of EtOH, purified water, and PG (≥99.5%, Sigma-Aldrich, St. Louis, MO, USA). Quinoline yellow (Sigma-Aldrich, Bangalore, India) was added to the ink for visualization purposes. In addition, a blue drug-free IJP ink was prepared to imprint drug-loaded films with QR codes. The blue color originated from adding brilliant blue G (pure, Sigma-Aldrich, St. Louis, MO, USA) to the mixture of PG, purified water, and EtOH (II).

The PRE ink consisted of PRE, liver powder (LP) (CC Moore & Co Ltd., Stalbridge, UK), and HPC in a purified water and EtOH mixture. LP was added as a taste-enhancing agent to render the dosage form more appealing to animals (III).

The GBP and TPH inks consisted of either GPB (IV) or TPH (V), respectively, in addition to hydroxypropyl methylcellulose (HPMC, Methocel K3 Premium LV, MW <10,000, Dow Chemical Company, Bomlitz, Germany), crospovidone (Kollidon CL, BASF, Ludwigshafen, Germany), mannitol (Ph. Eur., Merck, Darmstadt, Germany), glycerol (85%, Fagron, Barsbüttel, Germany), and LP in a purified water and EtOH mixture.

In study VI, four different inks were prepared, but only two of them were further analyzed. The two analyzed inks contained nanoPRX, HPMC (Tylopur 605, MW 18-22,000, SE Tylose GmbH & Co.KG Wiesbaden, Germany), and Tween 80 (Sigma Aldrich, Steinheim, Germany), ink 2 also contained HPC and glycerol.

4.3 Substrate for inkjet printing (II)
The substrates for IJP consisted of the film-forming polymer HPC in a mixture of EtOH and purified water.

4.4 Oral powders in unit dose sachets (II)
For the preparation of the oral powders in unit dose sachets (OPSs), commercially available Marevan forte® 5 mg tablets (Orion Pharma, Espoo, Finland) were mixed with lactose monohydrate (parve granules, Oriola, Espoo, Finland).

5. Methods

An overview of the methods used in the studies included in the thesis is described in the sections below. In addition, detailed descriptions of the methods used for each research work are presented in the respective original publications (I-VI).

5.1 Preparation

5.1.1 Inks for semi-solid extrusion-based 3D printing (I-VI)

In Table 3, the compositions of the drug-loaded SSE 3DP inks are summarized.

The SSE 3DP inks for studies I-III were prepared by mixing the API and additives in a 1:1 (v/v) mixture of EtOH and purified water on a magnetic stirrer overnight. The WS ink for study I consisted of 1.3% (w/w) WS and 16% (w/w) HPC. The WS ink for study II consisted of 1.5% (w/w) WS and 15% (w/w) HPC. The PRE ink consisted of 1% (w/w) PRE, 1% (w/w) LP, and 24% (w/w) HPC (III).

The SSE 3DP inks for studies IV and V were prepared in the same manner but with two different APIs. Firstly, a 15% (w/v) aqueous HPMC K3 gel was prepared and kept in the fridge overnight. The dry powders, 20% GPB (IV) or TPH (V), 27% mannitol, 6% crospovidone, and 3% LP were first mixed using a mortar and pestle, upon a homogenous powder mixture was obtained, 8% glycerol, 35% pre-made HPMC K3 gel, and 1% purified water were added all in a w/w ratio.

The nanoPRX inks were formulated by first preparing a nanoPRX suspension and a polymer dispersion separately and then mixing two parts of the suspension with three parts of the polymer dispersion with a microfluidic device (publication VI, Figure A.2.), obtaining printing inks with a 3% (w/w) drug load. The suspension consisted of 7.5% (w/w) nanoPRX, 3.75% (w/w) HPMC 605, and 1% (w/w) Tween 80 in purified water. Two different polymer dispersions were used to prepare two different printing inks. For printing ink 1, the polymer dispersion consisted of 25% (w/w) HPMC 605 in purified water. For printing ink 2, the polymer dispersion consisted of 25% HPC and 4% glycerol in purified water (VI).

All the placebo formulations were prepared in the same manner as the drug-loaded printing inks without adding the said API (I-VI).

Table 3. *Composition of the drug-loaded inks used for semi-solid extrusion (SSE) 3D printing of oral solid dosage forms in studies I-VI.*

Study	Ink base	API	Concentration (w/w)
I	HPC, EtOH, purified water	WS	1.3%
II	HPC, EtOH, purified water	WS	1.5%
III	HPC, LP, EtOH, purified water	PRE	1%
IV	HPMC K3, mannitol, crospovidone, glycerol, LP, purified water	GBP	20%
V	HPMC K3, mannitol, crospovidone, glycerol, LP, purified water	TPH	20%
VI	HPMC 605, Tween 80, purified water	nanoPRX	3%
	HPMC 605, Tween 80, HPC, glycerol, purified water	nanoPRX	3%

HPC: hydroxypropyl cellulose; EtOH: ethanol; WS: warfarin sodium; LP: liver powder; PRE: prednisolone; HPMC: hydroxypropyl methylcellulose; GBP: gabapentin; TPH: thephylline; nanoPRX: nanoformed piroxicam

5.1.2 Ink for inkjet printing (II)

Various inks for IJP, both drug-loaded and drug-free placebo formulations for analytical purposes, were prepared. More precisely, an inkjet printable ink solution was prepared by dissolving 100 mg/g WS in the ink base consisting of a mixture of 5% purified water (w/w), 27% PG (w/w), 57.99% EtOH (w/w), and 0.01% (w/w) of quinoline yellow. The colorant was added to the ink to improve the printed area's visualization. A placebo ink was prepared similarly with a composition of 5% (w/w) purified water, 27% (w/w) PG, 67.99% (w/w) EtOH, and 0.01% (w/w) quinoline yellow.

A placebo ink containing 1% (w/w) brilliant blue G dissolved in the ink base consisting of 27% (w/w) PG, 5% (w/w) purified water, and 67% (w/w) EtOH was used for printing QR codes on dried ODFs prepared by SSE 3DP and IJP.

5.1.3 Substrate for inkjet printing (II)

HPC-based substrates for IJP were prepared from a dispersion containing 15% (w/w) HPC dispersed in a 1:1 mixture of EtOH and purified water and solvent-cast utilizing a film applicator (Multicator 411, Erichsen, Hemer, Germany). The polymeric dispersion was cast on top of transparency sheets (clear transparent X-10.0, Folex, Germany) with a wet thickness of 600 μm. The cast substrates

were allowed to dry at ambient conditions overnight before imprinting with the drug-loaded ink.

5.1.4 Oral powders in unit dose sachets (II)

OPSs were extemporaneously prepared according to the standard operating procedure at the hospital pharmacy of Helsinki University Hospital (HUS) and were used as a comparator to the printed dosage forms. First, 5 mg Marevan forte® tablets were crushed in a mortar and ground with a pestle to a fine powder. Next, lactose monohydrate was added in geometric amounts to receive the final concentration needed for each dose. Finally, 200 mg of the prepared powder blend was weighed (analytical balance, Mettler Toledo XP204, Greifensee, Switzerland) into waxed powder papers (Herra Järvisen Verstas Oy, Helsinki, Finland). The OPSs were finally labeled and further packed in plastic Ziplock bags.

5.2 Printing

5.2.1 Semi-solid extrusion-based 3D printing (I-VI)

SSE 3DP was utilized in all studies. The inks were placed in disposable syringes, attached with dispensing precision tips, and printed on transparency sheets according to pre-determined designs.

In study I, the first WS study, the drug-loaded HPC-based dispersion was inserted into 10 mL single-use syringes (BD Plastipak TM Luer-Lok, Becton Dickinson S.A., Madrid, Spain) equipped with a disposable 21 G electro-polished tip (Techcon TE Needle, Ellsworth adhesives, Norsborg, Sweden). The Biobots 1 (Biobot, Philadelphia, PA, USA) printer coupled to an ultra-quiet and oil-free air compressor (California air tools, San Diego, California, US) was used to print both drug-free ODFs and ODFs containing WS. Four different sizes were designed in Autodesk Inventor® Professional 2019 (Autodesk Inc., San Rafael, CA, USA), sliced with RepetierHost V1.61 (Hot-World GmbH and Co. KG, Willich, Germany), and printed one at a time on top of transparency sheets. They were fabricated with a layer height of 0.5 mm, a printing speed of 8 mm/s, and a pressure of 10.4 PSI. The printlets were left to dry at ambient conditions overnight.

Four different-sized ODFs for the second WS study (II) were designed and sliced with the same software as in the first study, as well as printed with the same printer and in a similar manner. One difference was that the ODFs were printed with a layer height of 0.1 mm, requiring a more precise tip of 25 G, resulting in raising the pressure to 25 PSI to obtain therapeutic doses. The ODFs were printed as one vertical shell and filled using a rectilinear fill pattern with a 45° fill angle, an infill density of 100%, and an infill overlap of 15%. All printing steps were conducted with a speed of 8 mm/s. The printlets were left to dry at ambient conditions overnight.

For the PRE study (III), six different-sized designs were made in Fusion 360 (version 2.0.10446, 2020, Autodesk, San Rafael, CA, USA), and printing with three different SSE 3D printers was investigated. The ink was placed in 10 mL single-use syringes when printing with the pneumatic Biobot printer, and 50 mL disposable syringes (Henke-Ject Luer-Lok, Henke sass wolf GmbH, Tuttlingen, Germany) were used when printing with Bocusini 3D food printer (Procusini, Freising, Germany) and Zmorph multitool 3D printer (Zmorph, Wrocław, Poland), of which both operates through the addition of mechanical pressure to a plunger. All syringes were equipped with 1.5-inch 20 G precision dispensing tips (Quantx precision dispense tips, Fisnar, Germantown, WI, USA). With the Biobot printer, drug-loaded ODFs were successfully printed in two layers, with specific printing parameters including a 1 mm layer height, one vertical shell, and a rectilinear fill pattern with a 45° fill angle. The printing process employed 100% infill density and 100% infill overlaps, with printing performed at 96 PSI with a print speed of 5 mm/s. The Bocusini food printer has limited settings that can be adjusted, primarily allowing for the selection of materials which in turn determines the temperature. In this case, we opted to utilize the "pasta" setting and print without applying heat. The design was printed in a single layer. The Zmorph printer was set to print with 100% thickness, 1-layer count, 2 mm layer height, 2 mm path width, no retraction, and a print speed of 10 mm/s.

Compounding of personalized medicines through the utilization of 3DP requires the capability to efficiently produce small batches of accurately measured drug quantities in real-time, tailored to the specific needs of individual patients (Szakonyi & Zelkó, 2012); hence, the manufacturing time of six squares for each printer was recorded and compared (III). The drug-free placebo dispersions were extruded by hand to be used as a reference in the performed analysis. The printed films were left to dry for two days under ambient conditions before analysis. The Biobot 1 SSE 3D printer was chosen for further studies based on the uniformity of the content results. For the second print, the print time was decreased by exchanging the tip to a shorter one (0.25-inch 21 G tip Quantx precision dispense tips, Fisnar Europe, South Lanarkshire, Scotland, UK) in order to increase the flow. The designs were then printed in a single layer instead of two, using a pressure of 84 PSI and a print speed of 10 mm/s.

The GBP (VI) and TPH (V) studies were printed in a similar manner with the exception of the applied pressure. The ChewTs were designed using Fusion 360, encompassing seven different GBP doses, and four different TPH doses. The designs were sliced in the browser-based Brinter printing software and printed with a Brinter 1 3D BioPrinter (Brinter Ltd, Turku, Finland) attached with a Pneuma Tool print head (Brinter Ltd, Turku, Finland) and a compressor. The prepared printing inks were transferred into 10 mL Optimum® clear barrel syringes with Optimum® clear pistons (Nordson EFD LLC, Rhode Island, USA) attached with 16 G precision tips (Nordson EFD LLC, USA) and left to stand for 2 h prior to printing. In the browser-based Brinter printing software, the print

settings were set to 1 mm layer height, 1 shell, and a solid fill with a 45° fill angle. The print speed was set to 8 mm/s, and the pressure was set to 290 mbar for the GBP-loaded ink (VI) and 1500 mbar for the TPH-loaded ink (V) during printing to achieve therapeutic doses.

The nanoPRX inks were printed with the Biobot printer according to the four circles designed in Fusion 360 and sliced with RepertierHost (VI). The inks were placed in 10 mL disposable syringes and attached with a 21 G dispensing precision tip. The printlets were printed with a layer height of 0.5 mm, using a rectilinear fill pattern with a 45° fill angle, and the infill density and infill overlap were both set to 80%. To achieve therapeutic doses by printing with both printing ink 1 and 2, the pressure had to be adjusted to fit the different viscosities of the dispersions. Printing ink 1 was printed at 17 PSI and printing ink 2 at 28 PSI, with a print speed of 8 mm/s. The drug-free placebo dispersions were manually extruded.

5.2.2   Inkjet printing (II)

ODFs were prepared by imprinting the prefabricated HPC substrates with the WS IJP ink according to a premade digital design made in PowerPoint (II). A PixDro LP50 PIJ (Roth and Rau, Eindhoven, Netherlands) equipped with a 128-nozzle printhead (SL-128 AA, Fujifilm, Tokyo, Japan), and a camera for visualization of the jetted droplets was used for the preparation of personalized WS doses. Before printing, the prepared ink (drug and drug-free) was filtered (0.45 μm polypropylene membrane syringe filter, VWR International, Radnor, PA, USA). The used printing resolution was 720 DPI, and the IJP was conducted with a jetting frequency of 1400 Hz, a voltage of 80 V, an ink pressure of – 18 mbar, and a pulse shape of 3-16-5 μs. One printing pass resulted in 32 ODFs, which were allowed to dry at ambient conditions overnight before manually being cut into the final size using a scalpel and an in-house designed cutting template.

Furthermore, IJP was utilized to imprint dried SSE 3DP and IJP ODFs with readable QR codes containing vital information about the dosage form, such as type of dosage form, API and strength, manufacturing date, expiration date, as well as batch number. The QR code was generated utilizing the free online QR generator (goQR.me, Foundata GmbH, Karlsruhe, Germany), saved as a .bmp file, and imported into the printing software. The same PIJ, printhead, and similar settings were used to print the QR code on the prepared dosage forms. More details can be found in the corresponding publication (II). The readability of the imprinted QR code on the ODFs was evaluated using QR readers on mobile phones.

5.3   Manufacturing times (II, III)

One of the key aspects of personalized medicines is the ability to tailor doses to the patient's need at a specific time, hence, the time of production is an important

factor. In study II, the manufacturing times for the three different manufacturing methods were recorded to better understand how time-consuming the different processes are. In study III, the time it took to print with the different SSE 3D printers was recorded and compared.

5.4 Drying process (III, VI)

If a cross-linking agent and curing process is not utilized as a step in the SSE 3DP process, a drying step is required post-printing to obtain the final dosage form. Under ambient conditions, it can take up to 48 h until the dosage form is completely dry. Hence in studies III and VI, expedited drying was investigated.

In study III, drying at elevated temperatures was investigated, namely, the dosage forms were placed in an oven heated up to 40, 60, 80, or 100 °C, and the time it took for the ODFs to completely dry was recorded and compared to drying at ambient conditions. A tack test was conducted at regular intervals until the films were completely dry, indicated by their easy detachment from the transparency sheet. The dried films were evaluated in regard to their appearance, flexibility, smoothness of the films' surface, and the presence of air bubbles.

In study VI, freeze-drying was explored. The freeze-drying process was carried out by first placing the freshly printed samples in an ultra-low temperature freezer set to -80 °C (SANYO Electric Biomedical Co., Ltd, Nakamura-Ku, Japan) for 15 min, followed by freeze-drying for 15 h, utilizing the Heto CT 60 e (Allerod, Denmark) freeze-drying system, equipped with oil mist filter EMF10 vacuum (Edwards high vacuum international, West Sussex, England). Characterization was performed on both room-temperature dried (RTD) and freeze-dried (FD) films.

5.5 Characterization

5.5.1 Printing inks (I-VI)

All printing inks were visually inspected and manually extruded to determine their ability to keep their shape upon printing. The SSE 3D printers were used to print accurate doses of the drug-loaded inks and not to print elaborate shapes. The printing inks prepared in studies III-VI were investigated with a rheometer, and the nanoparticles in the nanoPRX ink (VI) were investigated through DLS and TEM.

5.5.1.1 Rheology (III-VI)

Rheology measurements were performed on the PRE-loaded ink and drug-free placebo dispersion with and without LP, as well as on the drug-loaded and drug-free nonprintable dispersions (III). The measurements were conducted by an MCR 702 MultiDrive rheometer (Anton Paar GmbH, Ashland, VA, USA) with a PP25 parallel plate (plate diameter and measuring gap of 25 mm and 0.5 mm, respectively) at 23 °C. Viscosity curves were obtained through shear flow

measurement of shear rate with a logarithmic ramp of 0.01–1000 s^{-1}, with 1 s per data point. The thixotropic behavior of the formulations was also analyzed.

Rheology measurements were performed on the GBP-loaded printing ink and the drug-free placebo paste to investigate their viscosity under the influence of shearing and time (IV). The measurements were performed at 0, 2, 4, 6, 8, 10, 12, and 24 h after preparation to investigate the viscosity vs. shear rate over time. The measurements were carried out with the HAAKE™ MARS™ Modular Advanced Rheometer system equipped with a plate rotor of 35 mm in diameter (P35/Ti) and a matching lower plate (TMP35), all by Thermo Fischer Scientific (Karlsruhe, Germany). The measuring gap was set to 1 mm and the temperature to 23 °C.

The rheology measurements for the TPH printing ink with the corresponding drug-free placebo paste (V) were performed once daily in the same manner as in the GBP study. The aim was to investigate the viscosity of the drug-loaded printing ink and the drug-free placebo paste under shear rate for seven days to study the ink's stability and possible change in viscosity over time, which would influence the printing results.

In the nanoPRX study (VI), rheology was utilized to investigate the viscosity of the printing inks under the influence of shearing properties to determine their rheological properties for SSE 3DP. The rheological properties of the dispersions were analyzed with a HAAKE MARS 40 Rheometer equipped with a 35 mm in diameter rotor plate (P35/Ti) and a lower plate (TMP 35). The measuring gap was set to 0.5 mm, and the temperature was kept at 23 °C.

5.5.1.2 Dynamic light scattering characterization (VI)
The particle size of the prepared dispersed systems was measured utilizing DLS (Zetasizer Nano series, Malvern Instruments (Worcestershire, UK) and analyzed with Zetasizer software 7.11 (Malvern instruments limited). The prepared nanoPRX suspensions were diluted with water and sonicated for 30 s, followed by vortexing for a few seconds prior to DLS measurement. Each sample was analyzed with 20 s of equilibrium time before measuring using ZEN0040 disposable cuvettes at 25 °C. Average and standard deviation were calculated in triplicate. The measurement is affected by the polymer in the suspension as the Z-average includes the adsorbed or hydrated layer around the nanoparticle. Therefore, the intrinsic viscosity of the polymer concentration was calculated to obtain the actual particle size of nanoPRX in the suspensions.

5.5.1.3 Transmission electron microscopy (VI)
The nanoPRX' morphology in the prepared nanoPRX suspensions was analyzed by TEM imaging (JEM-1400 Plus Electron Microscope, JEOL, Musashino, Akishma, Tokyo, Japan) in bright-field mode with an accelerating voltage of 80 kV. The prepared nanoPRX suspension was diluted to a concentration of 0.01 wt%, sonicated for 1 min, and a sample of 5 µL was transferred onto a

carbon-coated copper grid (Ted Pella Inc., Redding, CA, USA) and incubated for 3 min at ambient temperature. Excess liquid was removed prior to imaging. The particle size of a single particle TEM image was manually measured using the open-source image analysis software (Fiji version 2.11.0, National Institutes of Health, Maryland, USA).

5.5.2 Dosage forms (I-VI)

5.5.2.1 Weight, thickness, and appearance (I-VI)

The appearance of the substrate for IJP (II) and the SSE 3D-printed dosage forms (I-VI) were visually evaluated. Moreover, the weight was determined with an analytical balance (AND GH-252, A and D Instruments Ltd., Tokyo, Japan (I-III) or Radwag Wagi Elektroniczne by Radwag, Radom, Poland (IV-VI)), and the thickness was determined using a digital caliper (Absolute Digimatic, CD-6 "CX, Mitutoyo, Kawasaki, Japan).

5.5.2.2 Microscopic analysis (III, VI)

Microscopy images of the surface of the PRE dosage form (III) were captured using a handheld 5 MP digital microscope (Bodelin technologies, Oregon, OR, USA) and MicroCapture Pro version 2.2 software. The surface morphology of the prepared films was further examined using SEM (LEO Gemini 1530, Carl Zeiss AG, Oberkochen, Germany) with a Thermo Scientific UltraDry Silicon Drift Detector. Prior to scanning, all samples were coated with carbon using a vacuum evaporator. SEM images were obtained at an accelerated voltage of 8 kV with 50x magnification, using the secondary electron detector, and under a pressure of 2×10^{-5} mbar.

SEM images of the printed nanoPRX-loaded dosage forms and drug-free placebo samples (VI) were captured by a field emission SEM Sigma 300 VP Carl Zeiss Microscopy Deutschland GmbH, Germany). The samples were frozen using liquid nitrogen, cracked, and transferred to a 90° aluminum SEM sample holder equipped with double-sided carbon tape. Subsequently, the samples were coated with a 5 nm thick layer of platinum to render the material conductive prior to imaging.

5.5.2.3 Mechanical properties (I-VI)

Sufficient mechanical strength is required to ensure the ability to pack, handle, and administer the dosage form. Various mechanical properties of the prepared substrates and the printed dosage forms were studied using a TA-XTplus (Stable Micro Systems, Godalming, UK) texture analyzer equipped with a 10 kg load cell utilizing different setups. The prepared films were investigated with suitable setups, namely puncture test (I-III, VI), tensile strength (III), and folding endurance (III). The mechanical strength of the prepared ChewTs (IV, V) was determined by measuring the crushing strength.

a) Puncture test (I-III, VI)

The burst strength and elongation at break of the drug-free and drug-loaded films prepared in study I (n = 3), in studies II and VI (n = 5), and in study III (n = 6) (with and without LP), were investigated using a film puncture setup. The setup consisted of a Perspex film support platform and an aluminum circular top plate (film support rig HDP/FSR, Stable Micro Systems, Surrey, UK), which together clamps the film in place. A spherical probe (ø 5 mm, SMS P/5S, TA.XT.Plus Texture Analyser, Godalming, UK) was used to puncture the film. The acquisition of data was initiated when the trigger force of 0.049 N was reached, and the measurement was conducted at a constant speed of 1 mm/s. The maximum applied force (N) and penetration depth (mm) into the film before rupturing was recorded using Stable Micro Systems software (2013 version 6.1.4.0, TA.XT.Plus Texture Analyser, Surrey, UK). Experiments were conducted at ambient conditions.

b) Tensile strength (III)

The resistance to longitudinal pulling of drug-free and PRE-loaded films was evaluated using a texture analyzer equipped with two self-tightening roller grips (Stable Micro Systems, Surrey, UK). The films were securely positioned between the roller grips, with an exposing area of 10 × 80 mm. The lower clamp remained stationary, while the upper clamp pulled the film apart at a speed of 0.10 mm/s to a distance of 60 mm, triggered at a load of 0.029 N. The maximum tensile force and the distance at which the maximum force occurred were recorded. The percentage of elongation was calculated by comparing the elongation amount to the original sample length of 80 mm. All measurements were conducted under ambient conditions, with a sample size of 6.

c) Folding endurance (III)

The folding endurance test was conducted manually in study III, where the film was repeatedly folded at a 180-degree angle at the same location until visible signs of breaking or cracking were observed. Both drug-free and PRE-loaded films were subjected to this test in triplicate, under ambient conditions.

d) Crushing strength (IV, V)

The hardness of the drug-loaded printed ChewTs was measured with a heavy-duty platform (Stable Micro Systems, Surrey, UK) and a 5 mm cylinder probe (SMS P5 probe, Stable Micro Systems, Surrey, UK). The probe was brought down with a speed of 2 mm/s until a trigger force of 0.981 N was achieved, after which the probe continued with a speed of 0.10 mm/s for 1 mm. The software recorded the maximum force (N) at the crushing point. The hardness was measured 48 h after printing (n = 5) under ambient conditions.

5.5.2.4   Salivary pH (I-V)

For a comfortable mouthfeel, the salivary pH of the prepared ODFs (I-III), OPSs (II), and ChewTs (IV, V) should be close to neutral. The salivary pH of both drug-free and drug-loaded dosage forms (n = 3) was measured. The dosage form was

wetted with 1 mL purified water (I-III) or sterile water (IV, V) in a glass vial, after 30 s, the electrode of the pH meter (Mettler Toledo FE20, Mettler Toledo AG, Zurich, Switzerland for studies I-III or Edge R pH by HANNA Instruments, Inc, Woonsocket, USA for studies IV and V) was brought to the water surface. Equilibrium was allowed for 1 min for the prepared ODFs and ChewTs, and 15 min for the prepared OPSs prior to recording the reading. The average and standard deviations of the three measurements were calculated.

5.5.2.5 Moisture content (I-VI)

The moisture present in the fabricated drug-free and drug-loaded dosage forms (n = 3) was evaluated using a moisture analyzer (Radwag Mac 50/NH by Radwag, Radom, Poland). Samples were placed on an aluminum pan and heated up to 120 °C. The test was considered complete when the mass change was less than 1 mg/min and equilibrium was reached. The mass-% weight loss due to moisture evaporation was recorded. All measurements were conducted under ambient conditions, and average values with corresponding standard deviations were calculated.

5.5.2.6 Disintegration (I-VI)

Rapid disintegration is crucial for ODFs, but it is challenging to mimic in-use conditions.

For study I, the drop method was utilized. In the film support rig, one film at a time (n = 3) was attached, upon 0.2 mL of purified water was placed in the hole on top of the film, and the time until the film broke, and the drop dropped through was recorded.

In study II, the disintegration time of the ODFs (n = 3) was determined by using the Petri dish method, in which 10 mL of purified water was pipetted into a Petri dish, and the ODF was subsequently dropped on top of the liquid surface using tweezers. The time for the film to completely rupture in the middle into smaller film pieces was recorded and reported as the time for the film to disintegrate. In other words, swelling (in any direction) of the film or small pieces wearing off at the edges was not defined as the endpoint.

In study III, a custom-made apparatus (publication III, Figure 1) based on the slide frame and ball measurement device (Steiner et al., 2016) was designed and built. The apparatus was positioned in a shaking incubator (Unitron plus Incubator shaker, INFORS AG, Bottmingen, Switzerland) set to 37 °C and 50 rpm. The test involved placing a set of three 30 × 40 × 1 mm films between the frames of the device. On each film, 100 µL of purified water was added, followed by the placement of a 10 mm bearing steel ball (Kento OY, Kokkola, Finland) in the center. Subsequently, 3 mL of purified water was added on top of each film. The time taken for the ball to break the film and activate the timer switch was recorded. Average values and corresponding standard deviations were calculated (n = 6).

For studies IV-VI, a Sotax DT2 tablet disintegrator (Sotax, Allschwil, Switzerland), which corresponds to Ph. Eur. Apparatus A (basket-rack assembly) was utilized. The dosage forms were placed in the disintegration apparatus, and plastic discs were placed on top of each dosage form to prevent them from floating. The test was conducted in 37 °C purified water in a 1-liter glass beaker. The time was recorded until the dosage forms were completely dissolved. Average and standard deviations were calculated (n = 6).

5.5.2.7   Drug content (I-VI)
When determining the suitability of a method for the production of tailored doses at or close to the point-of-care, the ability of the said method to produce dosage forms with an accurate amount of drug is of the highest importance and was hence analyzed in all studies (I-VI) and on all prepared dose sizes. Complete descriptions can be found in corresponding publications. Still, briefly, the content determination was performed by immersing the dosage forms in 250 mL flasks containing 100 mL of purified water (I-V) or in a 100 mL flask containing 50 mL of a 1:1 purified water and EtOH mixture (VI). The flasks were then placed on an orbital shaker (Multi-shaker PSU 20, Biosan, Latvia) set to 50 rpm (I, II) or 150 rpm (III-VI) for a minimum of 3 h until the dosage forms were completely dissolved. The samples were diluted and derivatized when necessary. The absorbance was subsequently spectrophotometrically analyzed at 207 nm (I, II), 246 nm (III), 376 nm (IV), 272 nm (V), and 357 nm (VI) with an UV-Vis spectrophotometer (Lambda 35, PerkinElmer, Singapore, Singapore for studies I and II, and UV-6300PC Double Beam Spectrophotometer, VWR International BVBA, Leuven, Belgium for studies III-VI). The system was zero-calibrated before measurement with corresponding drug-free placebo samples treated in the same manner as the drug-loaded samples in order to omit any potential absorbance from the excipients.

Average drug content and standard deviations were calculated against a pre-determined calibration curve, and the correlation between the designed sizes and obtained drug amounts was established. Furthermore, for studies II and III, the uniformity of content of single-dose preparations (UC) was calculated according to the Ph. Eur. 2.9.6, test B (European Pharmacopoeia Commission, 2020c). For study III also the acceptance values (AV) were calculated, and for study V the content uniformity (CU) was calculated, both described in Ph. Eur. 2.9.40 (European Pharmacopoeia Commission, 2020d).

In contrast to the other APIs investigated, GBP cannot directly be spectrophotometrically measured. Hence in study IV, the literature was extensively reviewed, and over ten UV-Vis spectrophotometric methods (publication IV, Table 1) were thoroughly analyzed and assessed to find the best-performing method to accurately and precisely quantify GBP in the prepared dosage forms. A full description of the materials and procedures of each method can be found in the corresponding article (IV).

5.5.2.8 *In vitro* drug release (I-VI)

The drug release profile was determined on all prepared dosage forms. Manual dissolution was performed in studies I, II, and IV, and an automated dissolution setup was utilized in studies II, III, V, and VI. In the manual dissolution, samples were accurately weighed, placed in spiral capsules to prevent them from floating, and immersed into 250 mL flasks containing 100 mL of purified water. The flasks were placed in a shaking water bath (Julabo SW22, Germany), set to 37 °C and 50 rpm. Aliquots were manually withdrawn and spectrophotometrically measured according to the wavelengths mentioned in section 5.5.2.7.

An automated dissolution setup (Sotax AT 7 Smart, Basel, Switzerland) was utilized in studies II, III, and V. The dosage forms were placed in vessels containing 500 mL (II, III) or 900 mL (V) of media equipped with baskets set to 50 rpm (II) or paddles set to 100 rpm (III, V), and immersed into a water bath set to 37 °C. At specified time intervals, the release media samples were automatically withdrawn using a pump (Sotax CY 6, Basel, Switzerland). Prior to absorbance measurement, the withdrawn samples were filtered using a glass microfiber filter GF/B (GE Healthcare Life Sciences, Cheshire, UK). The absorbance measurements were performed using an online UV-Vis spectrophotometer (Lambda 35, PerkinElmer, Singapore). The wavelengths used were 207 nm, 247 nm, and 272 nm for studies II, III, and V, respectively. A USP type 1 apparatus (Erweka, Langen, Germany), along with the *in-situ* fiber optic concentration monitoring system Pion Rainbow R6 UV probe (East Sussex, England) with a path length of 2 mm was utilized in study VI. The second derivative spectrum was used for the analysis to minimize the effect of non-dissolved nanoparticles, and the area under the curve at the wavelength range of 300-320 nm was used to quantify the adsorption. The samples were placed in baskets rotating at 100 rpm situated in dissolutions vessels containing 900 mL of phosphate buffer pH 6.5, set to 37±0.5 °C, and the study was carried out for 120 min. The average normalized cumulative % drug released vs. time was plotted (n = 3).

Additionally, in study III, the drug release kinetics was determined by applying mathematical models to the drug release process, and the obtained drug release was plotted against various models.

5.5.2.9 Thermal properties (I-V)

Thermal analyses were performed using differential scanning calorimetry (Q2000 instrument by TA Instruments, New Castle, DE, USA). Data were analyzed with the TA Universal Analysis software v. 4.5A by TA Instruments. Samples were weighed, placed, and sealed in aluminum Tzero pans equipped with lids (TA instruments, Switzerland) and measured with a heating ramp at a heating rate of 10 °C/min under nitrogen purge gas with a flow rate of 50 mL/min. The samples were measured from 40 °C to 230 °C, -20 °C to 230 °C, 40 °C to 260 °C, 20 °C to 200 °C, and 20 °C to 300 °C for study I, II, III, IV, and V,

respectively. Each sample was measured two times, and a third measurement was carried out if differences were observed during the first two runs.

5.5.2.10   Infrared spectroscopy (I-VI)
On all prepared dosage forms, attenuated total reflectance Fourier transform infrared (ATR-FTIR) spectroscopy measurements were carried out utilizing a UATR-2 Spectrum Two instrument by PerkinElmer (Beaconsfield, UK). A force of 75 N was applied to the samples placed on the diamond to ensure optimal signal quality. The samples were measured over a range of 4000 cm^{-1} to 400 cm^{-1} with four accumulations at a resolution of 4 cm^{-1}. Each sample was analyzed twice, with a third measurement performed if any discrepancies were observed between the initial runs. The acquired spectra were processed using the PerkinElmer software Spectrum v. 10.03.02, applying functions such as baseline correction, normalization to 3%T, and data tune-up to enhance smoothness and correct the baseline.

5.5.2.11   Raman spectroscopy (V, VI)
In studies V and VI, a Raman spectrometer (Nicolet iS50 Raman by Thermo Fisher Scientific, Waltham, MA, USA) equipped with a 1064 nm diode laser (500 mW) and an InGaAs detector was utilized. The sample was placed on a gold plate, focused through OMNIC µView (v. 9.1.0) software prior to measurement, and measured with 128 scans at 0.25 W and the aperture set to 50. Spectra were acquired using OMNIC iS50 Raman software (v. 9.1.0) at a spectral range of 3600–100 cm^{-1}. Two measurements were performed on each sample.

5.5.2.12   X-ray powder diffraction (VI)
XRPD measurements were performed on the nanoPRX-containing SSE 3D-printed films using Malvern PANalytical Empyrean X-ray diffractometer (Malvern Panalytical Ltd, Malvern, UK), equipped with a Cu Kα (1.54 Å) source, MultiCore optics, and a solid-state PIXcel3D detector. A full description can be found in the corresponding article. Shortly, the printed films were attached to aluminum sample holders and measured in the reflection geometry in a spinning stage with a 5-40 (2θ) measurement range.

5.5.2.13   Stability (II, V, VI)
In study II, the stability of the prepared SSE 3D-printed ODFs, IJP ODFs, and OPSs was investigated over four weeks. The dosage forms' mechanical properties, disintegration, drug content, and solid-state were evaluated weekly.

In study V, the printing ink's stability was examined over seven days using daily rheology and ATR-FTIR analysis. Additionally, the produced ChewTs were assessed over three months to determine shelf life, evaluating drug content, moisture content, mechanical strength, and solid-state (DSC, ATR-FTIR, and Raman spectroscopy) at specified intervals.

In study VI, the nano-PRX' stability in the prepared RTD and FD dosage forms were stored in closed Petri dishes at ambient conditions for one month after preparation, and the solid state was evaluated by ATR-FTIR and Raman spectroscopy. In addition to the one-month stability study, the stability of the nanoPRX in the prepared dosage forms stored for three months at room temperature and 75% RH was investigated by XRPD.

All the measurements have been performed in the same manner as mentioned in the corresponding sections above.

6. Results and discussion

In the thesis, SSE 3DP was investigated as a novel technology to produce tailored doses close to the point-of-care to substitute the current manual compounding techniques. APIs with a specific need for tailoring were formulated into printed solid oral dosage forms, namely ODFs (I-III) and ChewTs (IV-V). PRX was used as a model drug to explore the ability of SSE 3DP a poorly soluble drug to produce drug-loaded oral films with personalized doses of nanoparticles, namely nanoPRX. An overview of the six studies is listed in Table 4.

Table 4*. Overview of the manufacturing methods, APIs, and the prepared dosage forms used in studies I-VI.*

Study	Manufacturing method	API	Feedstock material(s)	Dosage form
I	SSE	WS	Viscous ink	ODF
II	SSE	WS	Viscous ink	ODF
	IJP		Substrate & low-viscous ink	ODF
	Tablet manipulation		Commercial tablet	OPS
III	SSE	PRE	Viscous ink	ODF
IV	SSE	GBP	Viscous ink	ChewT
V	SSE	TPH	Viscous ink	ChewT
VI	SSE	nanoPRX	Viscous ink	Oral film

SSE: semi-solid extrusion-based 3D printing; IJP: inkjet printing; WS: warfarin sodium; PRE: prednisolone; GBP: gabapentin; TPH: theophylline; nanoPRX: nanoformed piroxicam; ODF: orodispersible film; OPS: oral powders in unit dose sachet; ChewT: chewable tablet

6.1 Preparation and characterization

6.1.1 Printing inks (I-VI)

6.1.1.1 Semi-solid extrusion-based 3D printing inks (I-VI)

For the preparation of the ODFs, a film-forming polymer was dispersed in a suitable solvent to render inks suitable for SSE 3DP. Several polymers in combination with suitable solvents and solvent mixtures have been studied throughout the studies.

In study I, the pre-formulation indicated that poly(vinyl alcohol) (PVA) and HPC were efficient film-forming polymers. Inks suitable for SSE 3DP were obtained and were thus printed. Upon drying, the PVA films turned out curved and rigid; hence, PVA was considered an unsuitable polymer as a film-forming agent to

produce printing inks for the production of ODFs. On the contrary, HPC rendered clear, smooth, and flexible films without the need of additional plasticizers, suitable as ODFs. Purified water is the first choice for the production of safe ODFs for pediatric use. Still, EtOH was added to the formulation to speed up the drying as well as to prevent bubbles from forming in the printing ink, consequently resulting in inconsistent printing. The most suitable HPC concentration was evaluated, and 16% was chosen. A lower polymer percentage rendered printing inks too runny, and a higher polymer concentration caused ink back draw during the printing process causing bubbles to form. The final printing ink for the production of ODFs for pediatric use in study I consisted of 1.3% (w/w) WS and 16% (w/w) HPC dissolved or dispersed in a 1:1 (w/w) purified water and EtOH mixture (MQ:EtOH). A clear, visually homogenous dispersion was obtained.

A polymer screening process initiated study II, and around 60 different formulations were screened regarding their film-forming capacity and suitability to be processed into personalized ODFs by SSE 3DP. A conversation had been held with medical doctors at HUS, and they expressed their preference on using as few excipients as possible. However, disintegrants, saliva stimulating agents, sweeteners, taste masking agents, flavors, colorants, etc., may be introduced in the formulation to further tailor the ODF's properties or to fulfill a patient's individual preferences. Despite a thorough screening of multiple polymers in different solvents and solvent combinations, the conclusion was drawn that the ink prepared in study I performed the best in terms of printability and characteristics of the final dosage form. The chosen SSE 3DP ink for study II was almost identical to study I. However, the amounts slightly differed, and the printing ink in study II consisted of 1.5% (w/w) WS and 15% (w/w) HPC dissolved or dispersed in a 1:1 (w/w) MQ:EtOH mixture. The printing ink looked identical to the printing ink prepared in study I.

In study III, animals were the target patient population; hence, LP was investigated as a taste enhancer to facilitate administration. Different polymers were screened, but HPC again showed the best results. A more pronounced 3D structure was desired, and hence the polymer amount was increased. Different drug concentrations were evaluated, but with a drug load of 2% (w/w) and above, the dispersions became cloudy, and crystallization of the drug occurred in the dried films, making the ODFs brittle and possessing decreased handleability. The printing ink for producing the final dosage form, therefore, consisted of 1% (w/w) PRE, 1% (w/w) LP, and 24% (w/w) HPC, all dissolved or dispersed in a 1:1 (w/w) MQ:EtOH mixture. The prepared printing ink was visually determined to be homogenous, had a rich brown color (publication III, Figure 2) and scent of liver due to the addition of the LP, and possessed good viscosity for SSE 3DP.

The printing ink base for the preparation of printed ChewTs for veterinary use in studies IV and V were identical and consisted of 35% pre-made HPMC-gel (15% w/v), 27% mannitol, 6% crospovidone, 8% glycerol, 3% LP, and 1%

purified water (all in w/w). The formulation also contained 20% drug, either GBP or TPH, in studies IV and V, respectively. Palatability is an important attribute of a chewable dosage form in order to achieve voluntary acceptance in animals (European Medicines Agency, 2014). GBP is known to be a bitter agent, and additives are necessary to add to the formulation to mask the taste of the API. Mannitol is widely used as an excipient in chewable dosage forms for its non-hygroscopic nature, sweet flavor, and smooth consistency (Dahiya et al., 2015), and LP is generally liked by both cats and dogs as a flavoring agent. In order to prevent poor palatability of the dosage form, these two additives were added to the formulation. The obtained drug-loaded inks had a brown color and scent of liver, and the inks were thick, bubble-free pastes suitable for SSE 3DP.

In study VI, after extensive screening, two different drug-loaded printing inks were chosen and prepared for analysis: printing ink 1 and printing ink 2. In comparison to studies I-V, the preparation method of the printing inks in study VI was different. Firstly, a base dispersion was prepared in order to mix the nanoPRX into the dispersion while maintaining the drug as nanoparticles and producing a drug suspension. Many different polymers and amounts of polymer were investigated to find the best-performing polymer to disperse and stabilize the nanoparticles (publication VI, Table A.1.). HPMC polymers performed the best, specifically type E HPMC polymers, due to the ratio of hydrophobic and hydrophilic substitution compared to type K polymers; type E polymers are considered more effective crystallization inhibitors. Ashland reported that higher hydrophobic substitution is essential in stabilizing the drug in a suspension (Y. Yang et al., 2016). Among all type E polymers that were investigated, Tylopur 605 showed the best performance based on visual inspection and DLS results (publication VI, Table A.2.). A more detailed description of the performance of the different polymers can be found in the corresponding publication.

As the drug suspension prepared in study VI, is not directly printable due to too low viscosity, polymer dispersions were prepared to be mixed with the drug suspension in order to obtain a printable printing dispersion. Three different polymers were investigated for the preparation of the polymer dispersion, namely Kollicoat Protect (PEG-PVA), Klucel EXF (HPC), and Tylopur 605 (HPMC); 25% (w/w) polymer dispersions were prepared with all three polymers, with and without glycerol. PEG-PVA was found to be an unsuitable polymer for the purpose, and no further studies were conducted on the said polymer. As the nanoparticles dissolve in EtOH, only purified water was used as a solvent in the printing ink. Due to the absence of EtOH, the HPC dispersion became foamy and contained air bubbles and lumps. The presence of lumps in a printing ink is unacceptable as it causes clogging and uneven printing. Air bubbles also complicates the printing process, causing uneven printing. Hence glycerol was added to the solution, and a clear, smooth HPC solution was obtained. HPMC often requires a plasticizer to render flexible films, but the HPMC dispersion with

glycerol took a long time to disperse, and the obtained dispersion was foamy and contained bubbles and lumps. In contrast, the HPMC dispersion without glycerol gave a smooth and clear solution.

Two final polymer dispersions were chosen for further studies in study VI, namely a 25% (w/w) HPMC dispersion and a 25% (w/w) HPC dispersion with 4% (w/w) glycerol. Two different printing inks were prepared by combining the prepared nanoPRX-containing suspension with the two different polymer dispersions in a ratio of two parts of drug suspension with three parts of polymer dispersion and mixed together with a microfluidic device (publication VI, Figure A.2.). A complete description can be found in the corresponding publication. The obtained drug-loaded printing inks were homogenous with white color.

Drug-free dispersions and pastes were prepared for all studies in the same manner as the drug-loaded printing inks without the addition of the corresponding drug. All the drug-free dispersions and pastes possessed a visually thinner consistency compared to their matching drug-loaded printing ink.

a) Rheology (III-VI)
The rheology properties of the SSE 3DP inks prepared in studies III-VI were evaluated to investigate the viscosity differences between the prepared printing inks within the studies and possible changes in viscosity over time, as well as providing information regarding their printability.

In study III, the rheological behavior of four different dispersions were investigated, namely drug-free and drug-loaded dispersions with and without the addition of LP. As a comparison, two unprintable dispersions (due to too high viscosity), one with and one without the drug, were also measured. All formulations exhibited Newtonian fluid behavior at a low shear rate, where the viscosity is independent of the shear rate. However, at higher shear rates (10 s^{-1}), shear-thinning behavior was observed, confirming the suitability of the ink for SSE 3DP (publication III, Figure 3). The viscosity of the drug-free dispersion increased when 1% PRE or LP was added due to increased solid fraction. Moreover, as LP has a larger spatial scale and more irregular shape than PRE, hindering the interaction of the HPC molecular chains, resulting in the increase of the zero-shear viscosity. However, the incorporation of 1% PRE into the drug-free dispersion with LP resulted in a decrease in viscosity; this might be due to the small particle size of PRE acting as a lubricant between the HPC and LP molecules during shearing, leading to a decrease in viscosity. In addition, the ability to maintain the structure after extrusion is also important for SSE 3DP; hence the recovery of the dispersions was evaluated. The drug-free dispersion showed the slowest viscosity recovery speed. The viscosity recovery speed was increased with the incorporation of PRE and LP. Overall, the HPC-based

formulations had a fast viscosity recovery speed that regained 75% of their maximum viscosity in 10 s, thus ensuring their suitability for SSE 3DP.

The required pressure while SSE 3DP is dependent on the formulation's viscosity, hence, a change in viscosity over time can detrimentally affect the printing results. In study IV, rheology measurements were performed on both the drug-free and drug-loaded pastes in order to evaluate if the formulation exhibits a change in viscosity over time. The inks exhibited non-Newtonian fluid behavior with shear-thinning properties (publication IV, Figure 3). The lower viscosity of the drug-free paste compared to the drug-loaded printing ink was affirmed by the rheological analysis. The intermolecular interactions and increased volume fraction will generally occur between the drug and other excipients in the formulation (Nicoud et al., 2015). The increased viscosity observed in the drug-loaded paste is due to the addition of GBP, which increases the solid fraction in the paste. Viscosity changes were observed during the first two hours after preparation and again after 12 h, hence, a window of 2-12 h after preparation was considered optimal for printing.

For study V, the rheological properties of the drug-loaded printing ink and the drug-free placebo paste stored at room temperature and in the fridge were examined against shear rate once a day for up to a week. Printing inks stored at different temperatures and measured at different time points all exhibited a shear-thinning behavior (publication V, Figure 1). The drug-loaded inks exhibited higher viscosities compared to the drug-free placebo pastes. The stability of the printing paste was investigated, and an increase in viscosity for each day was observed. Still, no difference between the two storing temperatures was noticed. This increase in viscosity could affect the printing result, and further investigation is needed. A correlative study should be conducted, where the time from preparation and the pressure required to reach therapeutic doses would be investigated. Increased pressure is required to achieve the same print result with higher viscosity formulations.

In study VI, the rheological behavior of the two prepared drug-loaded printing inks and their corresponding drug-free placebo dispersions was determined. The HPC used in printing ink 2 has four times higher MW compared to the HPMC used in printing ink 1, causing printing ink 2 to have a higher viscosity than printing ink 1 (publication VI, Figure 3). This was also observed during the preparation and printing of the inks. While printing ink 2 contained glycerol, our study found no correlation between its presence and effect on viscosity. The drug-loaded formulations exhibited a higher viscosity than the placebo formulations due to the intermolecular interactions and the increased volume fraction between the drug and the other excipients. All printing inks showed shear-thinning behavior, which is crucial for SSE 3DP.

In all studies, all inks exhibited shear-thinning behavior, which is a requirement for SSE 3DP to allow for smooth extrusion of the material without blocking the

nozzle (Cheng et al., 2020). When comparing the obtained viscosities in the prepared inks (Table 5), the inks in study VI showed the lowest viscosity, followed by the inks in study III, IV, and V. Despite the inks in study IV and V having the same ink base, the TPH ink in study V had a much higher viscosity compared to the GBP ink prepared in study IV. The higher viscosity of the TPH ink might be associated with the API's MW and particle size. TPH has a MW of 180.16 g/mol and a particle size of >500 microns in diameter (Shukla & Price, 1989), which is higher than GBP's MW and particle size of 171.24 g/mol and 28.8 μm, respectively. However, more importantly, GBP is freely soluble in water, whereas TPH is only slightly soluble in water (PubChem, n.d.-b, n.d.-a), giving rise to an increased viscosity. Due to the different viscosities, the inks were printed with different nozzles as well as different applied pressures.

Table 5. *Summary of the drug-loaded inks used in studies I-VI regarding their % of solvent in ink, viscosity measured at 0.01 shear rate (1/s), the inner diameter of nozzle used in printing, required applied pressure during printing, and printer utilized.*

Study	Solvent % in ink	Viscosity (Pa·s)	Nozzle (ID mm)	Pressure (PSI)	Print speed (mm/s)	Printer
I	82.7	-*	0.51	10.4	8	Biobot
II	83.5	-*	0.26	25	8	Biobot
III	74	31.46	0.51	84	10	Biobot**
IV	30.75	307.3	1.19	4.21***	8	Brinter
V	30.75	483.4	1.19	21.76***	8	Brinter
VI	79.8	2.0	0.51	17	8	Biobot
	77.4	4.8	0.51	28	8	Biobot

* = not measured, ** = best performing printer in the study, *** = converted from mbar to PSI. ID: inner diameter; PSI: pounds per square inch

b) Dynamic light scattering characterization (VI)
In study VI, several nanoPRX suspensions were evaluated with DLS for facilitating the choice of suspension to be used in the preparation of the printing ink (publication VI, Table A.2.). The chosen base dispersion was an aqueous dispersion containing 3.75% (w/w) Tylopur 605 and 1% (w/w) Tween 80. NanoPRX was mixed with the base dispersion to obtain a drug loading of 7.5% (w/w). The drug-loaded nanoPRX suspension exhibited a good PDI value of 0.168 ± 0.095 and a Z-average of 388 ± 16 nm.

c) Transmission electron microscopy (VI)
TEM was utilized to characterize the size of the nanoPRX particles in the prepared final suspension. Agglomeration is hard to avoid and both single particles and agglomerates were found in the suspension (publication IV, Figure 2). A Fiji software was utilized to measure the size of a single particle

found in the drug suspension and was found to be 375 nm, this confirms the DLS findings and indicates that the nanoPRX is in its original nanosized form of PRX and that the suspension preparation was successful.

6.1.1.2   Inkjet printing inks (II)

Both a drug-loaded WS ink and a placebo color ink for QR code imprinting were successfully prepared and printed without causing clogging of the nozzles. The drug-loaded WS ink was prepared to contain a high drug load of 100 mg/g, enabling imprinting of the desired dose in a single layer compared to performing multiple printing cycles.

6.1.2   Printing

6.1.2.1   Semi-solid extrusion-based 3D printing (I-VI)

The drug-loaded printing inks prepared for the different studies were successfully SSE 3D-printed according to the pre-made designs. Throughout the studies it was observed that the viscosity of the ink plays a crucial role in achieving optimal printing results, whereby higher viscosity requires more applied pressure. Moreover, the printing speed also influences the required applied pressure, with higher speed necessitating more pressure. However, in some cases, increasing the pressure may not suffice, and nozzle size may also need to be increased. Table 5 outlines the solvent percentage in the ink, measured viscosity, inner diameter of the nozzle used, and the required pressure for printing therapeutic doses in the different studies.

The drug-loaded inks in studies I and II were very similar, and the same printer was used to print the ODFs. However, in study II, a smaller nozzle size was used to achieve a higher resolution, which required increased printing pressure. Rheology measurements were not performed on the inks prepared in these studies but compared to the printing inks prepared in the other studies, they had the highest solvent percentage and exhibited the lowest apparent viscosity. In study II, the use of an SSE 3D printer to produce personalized doses was evaluated and compared to using an IJP or preparing OPSs. SSE 3DP was successfully utilized to print personalized ODFs with the printing inks prepared in studies I and II.

Study III aimed to evaluate three different SSE 3D printers and their ability to produce tailored doses for veterinary care. The speed of printing and the printers' user-friendliness was evaluated. But primarily, the obtained content uniformity of the dosage forms printed with the different printers was compared to determine which printer could best be employed in a pharmacy or an animal clinic setting. Of the three, the Bocusini printer is the simplest to use. But the simplicity makes personalization unfeasible as it offers no modification possibilities regarding printing speed or pressure. Instead of adjusting the settings according to the properties of the prepared ink, the ink has to be prepared in a manner that is suitable to the pre-determined print settings.

Moreover, the printer produced uneven printing, as evident from the varying sizes observed of the printed films despite using identical designs. It was observed that slightly more material was printed for each film, rendering films of different sizes and hence different drug loadings (publication III, Table 3). As a result, the Bocusini printer is not suitable for producing accurate drug doses in a pharmacy or animal clinic setting.

The second printer investigated in study III, was the Zmorph printer. One of the functionalities of the three-in-one printer is the thick paste extruder making it into an SSE 3D printer. The printer is manufactured to fit 100 mL syringes with no Luer lock function. We were interested in using the same tip for all printers, so the Zmorph printer was altered to accommodate a 50 mL syringe with a Luer lock function. The Voxelizer 2 software permits the adjustment of settings such as the thickness of the gel/paste, the layer count and height, the path width, the travel and printing speed, and retraction. One major problem was encountered with the said printer. Uneven final films were observed due to inconsistent ink extrusion caused by uneven plunger rotation, resulting in variations in drug content (publication III, Table 3). Based on the findings of this study, it can be concluded that the Zmorph printer is not suitable for use in a pharmacy or animal clinic setting. However, the Zmorph printer could yield better results with some engineering adjustments.

With the final printer investigated in study III, the Biobot printer, there is the ability to change the pressure, travel, print speed, printing pattern, layer count and height, infill, and overlap, among other parameters. The Biobot printer offers versatility in printing various gels/pastes, with adjustable settings to accommodate ink properties. However, a limitation of the Biobot printer lies in its scale-up capability, as it is designed to accommodate a 10 mL syringe, and challenges have been observed in maintaining consistent pressure. Of the three investigated printers, the Biobot printer operating with pneumatic pressure proved to be the superior candidate for utilization in a pharmacy or animal clinic setting (publication III, Table 3). For the second print, the Y-axis of the film design was adjusted to acquire Biobot-printed drug-loaded ODFs of different sizes. In order to reduce the printing time, the tip was exchanged for a shorter one, enabling an increase of the printing speed and decrease of the printing pressure. The printing speed was increased to 10 mm/s to decrease the printing time. As can be seen in Table 5, the solvent percentage in the ink was lower compared to printing ink I and II leading to a printing ink with a higher viscosity. The higher viscosity, combined with increased print speed and a demand for a higher extrusion to obtain thicker ODFs in order to reach therapeutic doses, caused the required printing pressure to be eight-fold increased.

Studies IV and V had the same ink base but contained different APIs. As can be seen in Table 5, the printing ink in study V had a higher viscosity compared to the printing ink in study IV, causing the need to increase the printing pressure in study V compared to IV in order to achieve therapeutic doses. Nevertheless, both

inks were successfully printed to prepare drug-loaded ChewTs of different doses for veterinary use.

Both printing ink 1 and 2 prepared in study VI were successfully SSE 3D-printed, and different-sized drug-loaded films were obtained. However, printing ink 1 exhibited a lower viscosity than printing ink 2, resulting in lower required pressure for printing ink 1 compared to printing ink 2.

Three different SSE 3D printers were compared in study III and based on the content uniformity   presented in Table 9 in section 6.1.4.8, the Biobot printer performed the best. If the Brinter printer had been a comparator at that time, I speculate that the Brinter printer would have prevailed. In general, SSE 3D printers have some technical limitations that need to be addressed to ensure their optimal use in producing personalized dosage forms. One of the most significant issues currently is that they can only accommodate 10 mL syringes, which limits the size of the batches that can be printed. Additionally, changing the syringe causes a need for recalibration of the printer. However, these are technical issues that can be improved. One of the specific problems encountered with the Biobot printer is the fluctuation in pressure during printing, which can lead to dosage forms with varying drug amounts. Moreover, when printing inks with higher viscosities, the plunger used in the syringes may tilt, resulting in complete print failure. In contrast, the plunger used in the Brinter printer is sturdier, leading to fewer printing failures and more consistent pressure.

Other factors that may impact the accuracy and precision of drug loading in SSE 3DP include the distance between the syringe tip and the build platform, the length of the nozzle, and the amount of material in the syringe. Therefore, it is crucial to standardize or monitor these factors to achieve personalized dosage forms with accurate and precise drug loading. Despite these technical challenges, SSE 3DP remains a promising technology for producing personalized dosage forms. By addressing these issues, SSE 3DP can be a valuable tool in the pharmaceutical industry, allowing for the production of tailored doses for human and veterinary care.

6.1.2.2   Inkjet printing (II)
IJP was successfully used to imprint the solvent-casted substrate with one layer of drug-loaded ink. Upon imprinting, the imprinted polymer sheet was left to dry overnight and cut to the final size using a cutting template and scalpel. Clogging of the nozzles is a common failure in IJP but was not observed during the printing.

IJP was successfully used to imprinted both dried SSE 3DP and IJP ODFs with readable QR codes (Figure 5). The information included in the QR code can easily be tailored according to the requirements or desires of a hospital, pharmacy, or animal clinic.
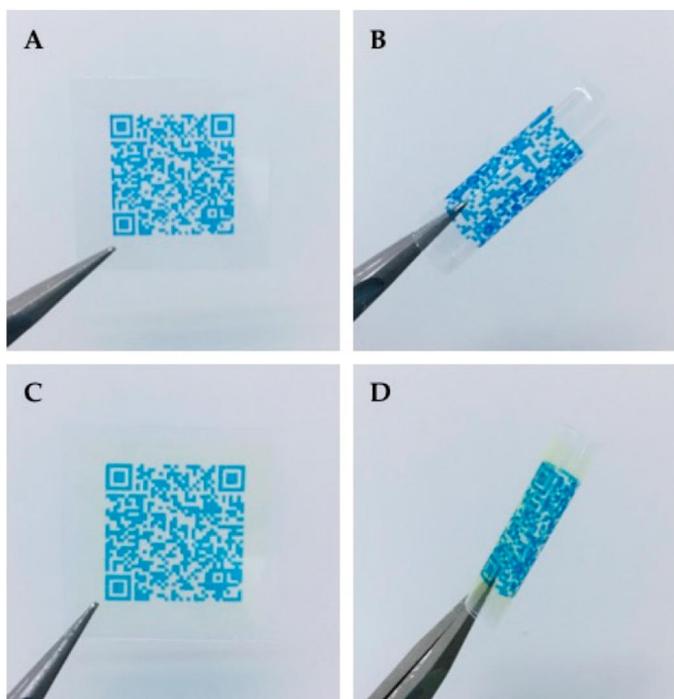
Figure 5. A) *Semi-solid extrusion-based 3D-printed (SSE 3DP) drug-loaded orodispersible film (ODF) imprinted with a quick response (QR) code containing information about the dosage form and **B)** the same SSE 3DP ODF rolled up to visualize the flexibility of the film. **C)** Inkjet-printed (IJP) drug-loaded ODF with a printed QR code and **D)** the flexible IJP ODF is subsequently coiled up for illustrative purposes. The size of the films is approximately 2x2 cm. Reproduced from (II), with permission from MDPI.*

6.1.3 Manufacturing time

In study II, the manufacturing time was recorded for each method and compared. However, comparing the manufacturing times is challenging due to the variations in their respective processes. For the printing techniques, only the actual printing step was recorded. This is due to that in the case that these novel techniques would become an established manufacturing method at, e.g., a pharmacy, a hospital pharmacy, or an animal clinic setting, it would be desirable that the substrates, printing formulations, etc., would be contract-manufactured and delivered to the site, where only minor preparation steps such as addition of the desired API would be performed. Therefore, only the time it took to print one SSE 3D-printed ODF was recorded. The time it took to print one ODF with the target size of 2 mg was almost 3 min, this is the time from pressing start until the printhead returned to its starting positions. This is much longer than the printing of ODFs using IJP and the preparation of OPSs. The SSE 3DP time could be decreased by printing several ODFs in one step. While IJP, 32 doses were printed

at a time, only taking 18 s on average to imprint the pre-prepared substrate with 2 mg drug-loaded ink. The IJP time is dependent on the number of used nozzles but also the placement of the specific nozzles. IJP is clearly a much faster printing technique if only considering the printing step in itself. But IJP is a highly labor-intensive technique as it requires maintenance and cleaning especially in a laboratory setting where the printer is not constantly running. A benefit for SSE 3DP is that is utilizes disposable syringes, requiring minimum cleaning. For the preparation of the OPSs, the recorded manufacturing times included the time to prepare the powder mass as well as the time to weigh all individual doses into powder papers and subsequently closing and labeling them. Preparation of the powder mass took around 11 min and the weighing of 30 units took around 32 min.

In study III, the printing times were recorded for the three different printers, and the time it took to print six squares in one printing was 5 min 40 s, 10 min 26 s, and 13 min 44 s for the Bocusini, Biobot, and Zmorph printers, respectively. The Bocusini printer was the fastest but did provide uneven printing. For the second print, the Y-axis of the film design was adjusted to acquire Biobot-printed drug-loaded ODFs of different sizes. To decrease the printing time, the tip was exchanged for a shorter one, enabling an increase the printing speed and decrease the printing pressure. The printing speed was increased to 10 mm/s to decrease the printing time. The printing time was hence reduced from 10 min and 26 s to 5 min and 52 s which equals to approximately 1 min per ODF. This could further be reduced by increasing the size of the printing bed allowing for higher number of films to be printed at a time.

The printing time was also recorded in study IV, it took 2 min and 12 s to print 8 ChewTs of size 10.

6.1.4   Dosage forms (I-VI)

SSE 3DP was successfully utilized to prepare different doses of drug-loaded dosage forms to provide tailored doses close to the point-of-care. ODFs were prepared in studies I-III, ChewTs in studies IV and V, and oral films in study VI.

6.1.4.1   Appearance

The SSE 3D-printed ODFs prepared in study I can be seen in Figure 6. The ODFs prepared in study II are identical to the ones prepared in study I, and the ODFs prepared in study III look similar to the ODFs in the two previous studies but with the exception of the color. In study III, LP was added to the printing ink to increase adherence through voluntary uptake of the animals. As a result, the ODFs prepared in studies I and II were clear, while the ODFs prepared in study III had a brown hue. All prepared ODFs were thin and flexible.
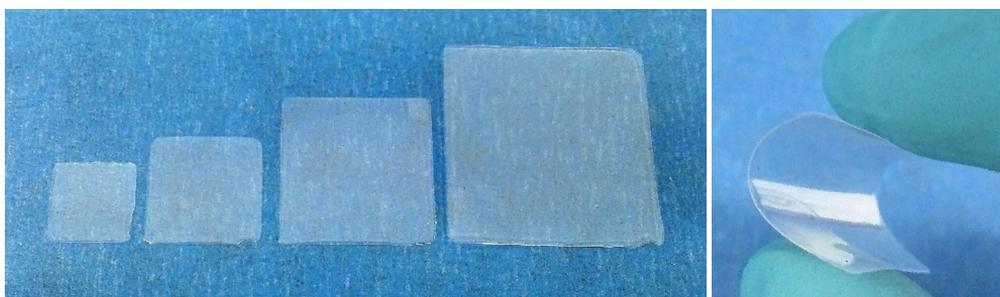
Figure 6. *Picture of the semi-solid extrusion (SSE)-based 3D-printed orodispersible films prepared in study I. The size of the films ranges from 10 mm to 30 mm. Reproduced from (I), with permission from Elsevier.*

Figure 7 presents the SSE 3D-printed ChewTs prepared in study IV. The printed dosage forms have a rectangular shape as designed, with rounded corners due to the surface tension-dominated behavior of the printing ink. ChewTs of escalating sizes of seven different doses corresponding to the CADs were obtained. As animals dislike too chewy dosage forms (Aleo et al., 2018), the prepared hard ChewTs in this study, with a brown color and an apparent liver scent resembling a dog or a cat treat, are expected to have a high voluntary acceptance, which is the cornerstone of success in the medicinal treatment of animals (European Medicines Agency, 2014). As the ChewTs in study V were prepared with the same printing ink base, the obtained dosage forms, as expected, were identical to the ones seen in Figure 7, with the exception that only four different doses were prepared.
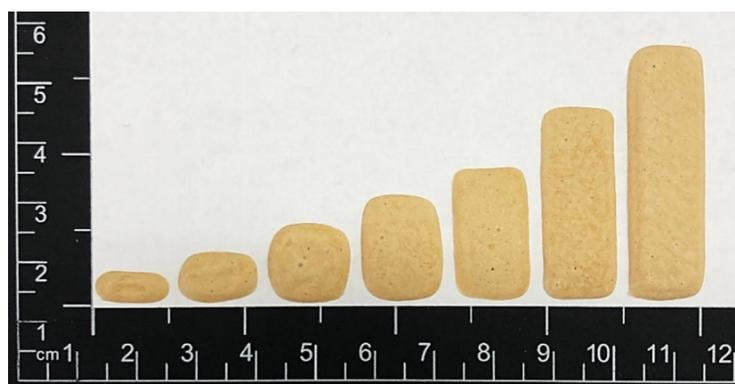

Figure 7. *Photographic image of the semi-solid extrusion (SSE)-based 3D-printed gabapentin-containing chewable tablets of different doses. Reproduced from (IV), with permission from Elsevier.*

In study VI, as can be seen in Figure 8, the films dried at room temperature had a smooth surface, while freeze-drying the film gave the film a porous structure with an uneven surface. The films obtained from printing ink 1 were hard and brittle while printing ink 2 yielded flexible films; this is most likely due to the

addition of glycerol in printing ink 2, which acts as a plasticizer. All films had a white color due to the addition of nanoPRX. However, the films dried at room temperature exhibited a slight color change to light yellow. This slight color change, even though not bright yellow, raised concerns regarding the stability of nanoPRX in a formulation for prolonged times, as PRX is known to crystallize to the monohydrate form in the presence of water (G. Liu et al., 2014). After freeze-drying, the films from printing ink 1 became white, while the films from printing ink 2 still exhibited a slight yellow hue.

Figure 8. *Semi-solid extrusion (SSE)-based 3D-printed films containing nanoparticles of piroxicam. Films printed with printing ink 1 and (**A**) dried at room temperature and (**B**) freeze-dried. Films printed with printing ink 2, (**C**) dried at room temperature, and (**D**) freeze-dried. Reproduced from (VI), with permission from Elsevier.*

6.1.4.2 Drying process (III, VI)

One of the most time-consuming steps in SSE 3DP is the drying of the printed dosage forms to obtain the final product. To eliminate this step, one approach is to add curing agents to the formulation and perform a curing step. However, the purpose of all the studies was to develop safe dosage forms in the simplest manner, so adding a curing agent was deemed undesirable. Therefore, two studies, namely study III and VI, investigated and evaluated different drying conditions for the printed dosage forms.

In study III, the time it took for the film to dry at different temperatures was recorded, and the appearance and flexibility upon drying were investigated. It took 24 h for the films to dry at room temperature, resulting in smooth, flexible films without bubbles. When drying the ODFs at elevated temperatures, the drying time was decreased, but bubbles emerged in the films. As expected, the higher the temperature, the lower the required drying time was, resulting in required drying times for films dried at 60, 80, and 100 °C to be 3, 2, and 1 h, respectively, but at all aforementioned drying temperatures yielded bubbly, uneven, and brittle films (Figure 9). In order to decrease the drying time but maintain the film's flexibility and durability, the films were dried for 5 h at 40 °C.

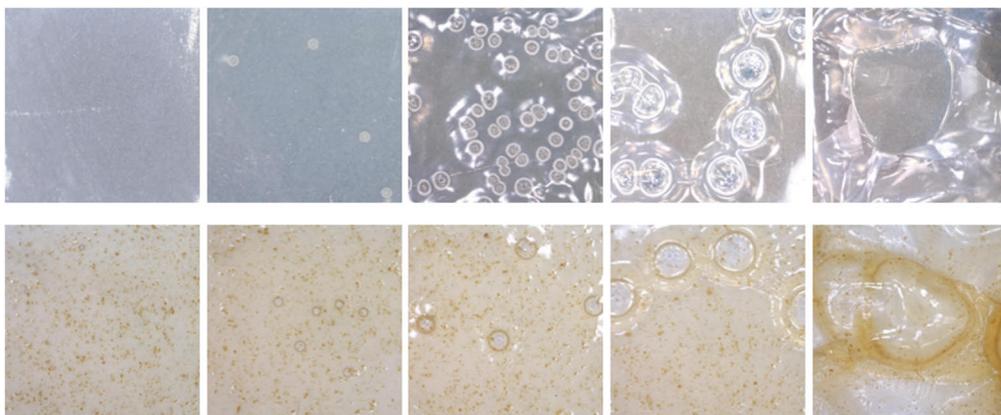In the figure, it is evident that the addition of LP yielded brown-colored films with tangible particles.

Figure 9. *Pictures of drug-loaded films without liver powder (upper row) and drug-loaded films with liver powder (lower row). From the left, after drying at room temperature, 40, 60, 80, and 100 °C. Reproduced from (III), with permission from MDPI.*

The films prepared from printing ink 1 and 2 in study VI took 48 h to completely dry at ambient conditions. Exposing nanoPRX for long durations to water may lead to Ostwald ripening and recrystallization of anhydrous form I to monohydrate; this change causes a bright yellow color (publication VI, Figure A.1.) (R. Sheth et al., 2005). Due to a slight color change to light yellow was observed in the RTD films, freeze-drying was investigated to decrease the time that nanoPRX was subjected to water. Freeze-drying gave the films a more porous structure, as can be seen in Figure 8. As time is often a crucial attribute to value, decreasing the time from order to delivery is important. Freeze-drying decreased the time to obtain the final dosage form from 48 h to around 16 h. This would provide the customer with the product one day earlier. Of course, this requires the manufacturing site to have access to a freeze-drier and potentially increases the cost of the product but decreasing the drying time would decrease the required space for storage which is a cost in itself. Both RTD and FD films were further analyzed.

6.1.4.3 Microscopic analysis (III, VI)
Microscopic analysis of ODFs prepared in study III was performed with a handheld digital microscope and through SEM. As can be seen in Figure 10, ODFs without LP are smooth, transparent, and have a blueish tone. The addition of LP altered the film color to brown, and the liver particles are both tangible and visible in the films. When printing the 1% PRE-loaded printing ink, no drug crystals were visible in the obtained ODFs, but when the 2% PRE-loaded printing ink was printed, ODFs with visible drug crystals emerged upon drying. SEM pictures were obtained, and the same characteristics were observed as in the

microscopy pictures. As can be seen in the bottom row of Figure 10, the drug-free and drug-loaded ODFs without LP have a smooth surface, the ODFs printed with the 2% PRE-loaded ink shows drug crystals, and the drug-free and drug-loaded ODFs with LP exhibit a rough surface due to presence of LP particles.
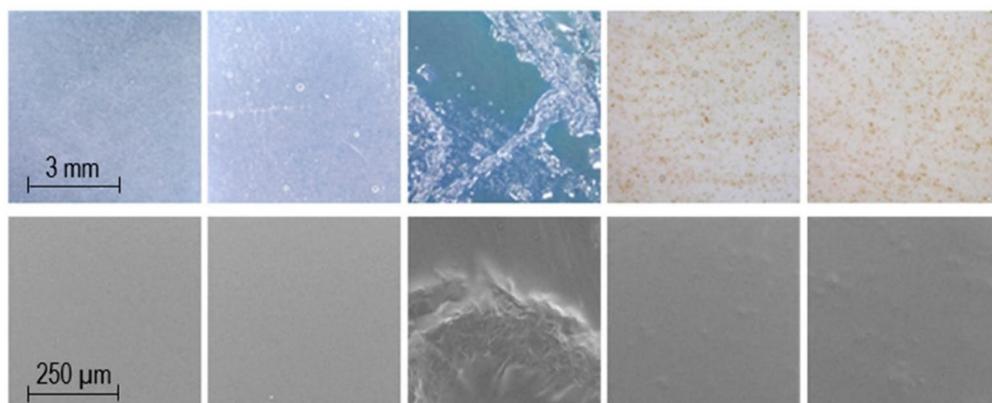

Figure 10. *Microscopy images of semi-solid extrusion (SSE)-based 3D-printed orodispersible films (ODFs). From the left, drug-free film, 1% prednisolone-loaded film, 2% prednisolone-loaded film, drug-free film with liver powder, and 1% prednisolone-loaded film with liver powder. The images in the upper row were captured using a handheld digital microscope, while the lower row showcases scanning electron microscopy (SEM) images. Reproduced from (III), with permission from MDPI.*

The SEM images obtained in study VI (publication VI, Figure 5) showed that the nanoPRX particles were clearly visible in the RTD and FD films prepared from printing ink 1. The observed particles not only indicate the presence of nanoPRX but also that the particles are not highly agglomerated but mainly distributed as individual primary particles. However, particles are not visible in films prepared from printing ink 2. This is potentially due to the excellent film-forming properties of HPC coating the nanoparticles, rendering them concealed.

6.1.4.4   Mechanical properties (I-VI)

a) Puncture test (I-III, VI)
Mechanical properties play a crucial role in the physical integrity of ODFs. Hence, a puncture test was performed on all films prepared in the studies. Extensive results can be found in the corresponding publications.

In study I, the film burst strength of the drug-free and drug-loaded ODFs were very similar at 16.0 ± 1.8 N and 16.5 ± 2.2 N, respectively, the results were statistically insignificant. The result indicates that the ODFs were equally strong and that the addition of the WS did not affect the durability of the dosage form. But the addition of WS statistically significantly affected the flexibility of the ODFs as the distance at burst decreased from 2.45 ± 0.32 mm for the drug-free

films to 1.93 ± 0.09 mm for the drug-loaded films. This decrease in flexibility was also noticeable while handling. However, the drug-loaded ODFs exhibited a high burst strength and high distance at burst, indicating that the WS-loaded ODFs are adequately durable and flexible to prevent deformation during handling.

In study II, ODFs prepared by SSE 3DP were compared to ODFs prepared by solvent casting and imprinted by IJP (publication II, Figure 4). The drug-free solvent-cast films used as placebo reference for the IJP ODFs were stronger than the ODFs prepared by SSE 3DP, with a high statistical significance, primarily due to an increased thickness of the solvent-cast ODFs compared to the SSE 3D-printed ODFs. In line with the result found in study I, the addition of WS did not affect the burst strength of the SSE 3D-printed ODFs but did decrease the flexibility of the dosage form. While the IJP imprinted ODFs were not stronger than the SSE 3D-printed ODFs, the flexibility increased more than double the amount. This effect might be due to PG, which is present in the IJP printing ink, having a plasticizing effect. Plasticizers typically interact with the polymer chains present in the formulation resulting in increased chain mobility and, consequently, a decreased glass transition temperature, which in terms of mechanical properties is seen as ODFs with improved plastic and elastic properties (Boateng et al., 2009). However, all ODFs showed sufficient mechanical properties.

In study III, drug-free and drug-loaded ODFs, with and without LP, were investigated (publication III, Table 5). The addition of PRE slightly weakened the film from 42.4 ± 1.0 N to 35.3 ± 0.7 N for films without LP and from 29.1 ± 0.8 N to 26.0 ± 1.2 N for films with LP, the changes were statistically highly significant. The presence of undissolved LP particles in the film resulted in a significant reduction in burst strength of the formulation. While the flexibility of the films remained unaffected by the addition of the drug, a statistically significant decrease in flexibility was observed with the addition of LP to the ODFs. Despite these variations, all the films exhibited high burst strength and an adequate distance at burst, ensuring no issues with the handling of the ODFs.

Films prepared from printing ink 1 and 2 and their corresponding drug-free placebo dispersions were investigated in regard to their durability and handleability in study VI (publication VI, Tables 2 and 3). Films printed with printing ink 1 were generally stronger but less flexible than those printed with printing ink 2. Drug-loaded films commonly exhibit lower strength and flexibility than drug-free placebo films due to particles' presence in the matrix, as noticed in studies (I-III). This was also observed for films printed with printing ink 1. Films printed with drug-loaded printing ink 2 again had a higher strength but lower flexibility than their corresponding placebo. Films printed with the drug-free printing ink were measured on another day when the relative humidity was higher, and hence the results can be explained by this. Both HPC and HPMC are hygroscopic polymers (Panraksa et al., 2020), meaning that they take up moisture from the air affecting their physical and possibly chemical properties.

It was expected that the FD films would exhibit both lower strength and flexibility due to their porous structure. The strength of the FD films compared to RTD films was lower, as expected, but the flexibility was maintained even after freeze-drying, extensive results can be found in study VI, Table 2.

b) Tensile strength (III)

A tensile strength test was performed on the SSE 3D-printed ODFs in study III. A high percentage of extension equals higher flexibility. The tests show that a higher fraction of solid material present in the film results in lower mechanical strength. The drug-free films without LP had the highest maximum forces of breakage, followed by the drug-loaded ODFs without LP, the drug-free films with LP, and the drug-loaded ODFs with LP (publication III, Table 5). The presence of PRE and/or LP resulted in a slightly lower maximum stretch distance in the tensile test. For satisfactory handling properties, a percentage of elongation greater than 10% is preferred (Lir et al., 2007). All ODFs showed adequate tensile strength with a percentage of elongation higher than 10%.

c) Folding endurance (III)

A folding endurance test was manually performed on the ODFs prepared in study III. According to the test, the drug-loaded ODFs without LP could withstand the highest number of folds, cracking at 40 and breaking at 46. The drug-free films without LP could also withstand a substantial number of folds, but less than the drug-loaded ODFs without LP, indicating that PRE could contribute to a plasticizing effect. Both the drug-free films and the drug-loaded ODFs with LP were very sensitive to folds; the drug-free films cracked after the first fold, while the drug-loaded ODFs could withstand 6 folds without cracking. Both films broke at 8 folds. All the prepared films failed to comply with this standard, but all ODFs endured handling well without any damage, fulfilling the Ph. Eur. requirements for ODFs (Elmeshad & El Hagrasy, 2011).

d) Crushing strength (IV, V)

The crushing strength of the prepared ChewTs in studies IV and V was measured to ensure sufficient hardness for packing, handling, and administration of the dosage form. In a study by Nyamweya et al., the tablet breaking force of various commercially available ChewTs was studied with a hardness tester, and obtained values ranged between 70 N and 150 N (Nyamweya et al., 2020). A hardness tester was also attempted to be used in the current study; however, the test was not applicable due to the shape of the dosage form, and hence a texture analyzer was utilized.

The results obtained from the measurement performed on the GBP-loaded ChewTs (IV) were 9.24 ± 0.61 N/19.63 mm^2 equaling 47.07 ± 3.11 N/cm^2, which is right in line with the proposed strength by Arora and Arora Sethi (2013). The prepared ChewTs in this study obtained a hardness well below the FDA threshold as well as lower than all commercially available ChewTs studied by Nyamweya et al. However, the ChewTs were hard enough to not break during

handling, indicating that the prepared dosage form is suitable to be used as a chewable dosage form.

The TPH-containing ChewTs prepared in study V required a much higher crushing strength compared to the GBP-containing ChewTs prepared in study IV. The TPH-containing ChewTs exhibited a crushing strength of 45.87 ± 7.46 N/19.63 mm^2. The results can not directly be compared between the two prepared ChewTs as different probes were used. However, the study indicates that the TPH-containing ChewTs had a much higher crushing strength compared to the GBP-containing ChewTs, which was also observed when handling. However, the prepared ChewTs still exhibited a crushing strength in line with the FDA's recommendation.

6.1.4.5 Salivary pH (I-V)

The surface pH was determined for the dosage forms prepared in studies I-V in order to ensure a comfortable mouthfeel. The results are summarized in Table 6.

Table 6. *Salivary pH of the printed orodispersible films (ODFs) and chewable tablets (ChewTs), and the manually prepared oral powders in unit dose sachets (OPSs). Data presented as average ± SD, n = 3.*

Study	Dosage form	Technique	API	Salivary pH	
				1 min	**15 min**
I	ODF	SSE	WS	7.1 ± 0.3	N/A
			Drug-free	6.8 ± 0.3	
II	ODF	SSE	WS	7.1 ± 0.1	7.1 ± 0.1
			Drug-free	6.9 ± 0.1	6.4 ± 0.3
	ODF	IJP	WS	7.4 ± 0.3	7.1 ± 0.0
			Drug-free	7.0 ± 0.2	6.4 ± 0.2
	OPS	Manual	WS	9.4 ± 1.6	7.3 ± 0.2
III	ODF with LP	SSE	PRE	6.6 ± 0.1	N/A
			Drug-free	7.2 ± 0.3	
	ODF without LP	SSE	PRE	4.6 ± 0.7	N/A
			Drug-free	4.8 ± 0.2	
IV	ChewT	SSE	GBP	7.0 ± 0.4	N/A
V	ChewT	SSE	TPH	6.3 ± 0.0	N/A

API: active pharmaceutical ingredient; ODF: orodispersible film; SSE: semi-solid extrusion-based 3D printing; WS: warfarin sodium; IJP: inkjet printing; OPS: oral powders in unit dose sachet; LP: liver powder; PRE: prednisolone; ChewT: chewable tablet; GBP: gabapentin; TPH: theophylline; N/A: not applicable

As is evident in the table, all final dosage forms exhibited a pH within the range of physiological saliva and should hence not cause any discomfort or local irritation upon administration. In studies I and II, the addition of WS slightly

increased the pH compared to drug-free ODFs. The OPSs prepared in study II showed an alkaline pH after 1 min, but the pH decreased to a neutral range when allowing the OPS to dissolve further. This indicates that to avoid local irritation, the OPSs should be fully dissolved/dispersed before administration directly in the oral cavity.

The results from study III shows that without the addition of LP, the dosage forms exhibit an acidic salivary pH, but the addition of LP increases the pH to a neutral range making it a suitable formulation for oral administration. The ChewTs prepared in studies IV and V, both show a neutral pH; TPH causes a slightly lower pH compared to GBP.

6.1.4.6   Moisture content (I-VI)
The drug-free films and the drug-loaded ODFs prepared in study I exhibited a slightly higher moisture content than suggested by Nair et al., namely, 5.9 ± 1.6% and 6.5 ± 2.2%, respectively. In study II, the prepared ODFs showed a moisture content of around 10%. Despite the high moisture content, the films were handleable and not sticky. Many studies in preparation of ODFs have shown higher moisture content than 5% but still lower than 10% (Elmeshad & El Hagrasy, 2011; Foo et al., 2018; Visser et al., 2015). The ODFs prepared in study III all showed a moisture content of close to 3%; still, the films were flexible enough and demonstrated good handleability. The drug-loaded films prepared in study VI exhibited a moisture content of less than 5%. The two different drying techniques did not significantly affect the result, as all dosage forms were stored at ambient conditions.

The prepared ChewTs in studies IV and V had a moisture content of 3.7 ± 0.6% and 3.2 ± 0.6%, respectively, which is slightly below the recommended moisture content range of 4-5% (Tomar et al., 2017), however, the ChewTs were not found to be brittle despite the lower moisture content.

The moisture present in the prepared dosage forms may originate from residual solvents from the formulation development or due to the hygroscopic nature of one or multiple components present in the formulation. The biggest reason for the difference in moisture content seems to be the changes in relative humidity.

6.1.4.7   Disintegration (I-VI)
The results of the disintegration results obtained from all the studies can be found in Table 7. The dosage forms in studies I-III are considered ODFs, and a fast disintegration is deemed crucial due to the nature of the dosage form. The obtained results are not directly comparable because a different disintegration method was used in each study. The results indicate that the disintegration time is dependent on the thickness of the film; the thicker the film, the slower the disintegration. The drug-loaded ODFs in studies I and II complied with the disintegration limit set for orodispersible dosage forms, namely, the dosage form had to disintegrate within 3 min (European Pharmacopoeia Commission,

2020a). The addition of LP increased the presence of particles in the dosage form of the prepared ODFs in study III. This decreased the disintegration time to almost comply with the disintegration time set for an orodispersible dosage form. The disintegration time could additionally be decreased by adding a disintegrator, increasing the LP amount, or preparing thinner films.

Table 7. *Disintegration time of the printed orodispersible films (ODFs) and chewable tablets (ChewTs) analyzed utilizing different methods. Data presented as average ± SD, n = 3.*

Study	Sample	DIS method	Thickness (mm)	DIS time (s)
I	Drug-free ODF	Drop-through	0.11 ± 0.01	185 ± 5
	Drug-loaded ODF		0.11 ± 0.01	139 ± 29
II	SSE drug-free ODF	Petri dish	0.04 ± 0.00	28 ± 9
	SSE drug-loaded ODF		0.04 ± 0.00	39 ± 4
	IJP drug-free ODF		0.05 ± 0.00	90 ± 1
	IJP drug-loaded ODF		0.05 ± 0.00	123 ± 5
III	Drug-free ODF without LP	Slide frame and ball	0.23 ± 0.02	300 ± 196
	Drug-loaded ODF without LP		0.26 ± 0.04	710 ± 277
	Drug-free ODF with LP		0.22 ± 0.03	192 ± 17
	Drug-loaded ODF with LP		0.24 ± 0.01	212 ± 30
IV	Drug-loaded ChewT	Tablet disintegrator	1.61 ± 0.12	202 ± 34
V	Drug-loaded ChewT	Tablet disintegrator	1.43 ± 0.09	467 ± 39
VI	Drug-loaded RTD film 1	Tablet disintegrator	0.50 ± 0.12	495 ± 44
	Drug-loaded FD film 1		1.51 ± 0.09	558 ± 52
	Drug-loaded RTD film 2		0.27 ± 0.01	939 ± 138
	Drug-loaded FD film 2		0.41 ± 0.04	480 ± 138

DIS: disintegration; ODF: orodispersible film; LP: liver powder; ChewT: chewable tablet; SSE: semi-solid extrusion-based 3D printing; RTD: room temperature dried; FD: freeze-dried

The ChewTs prepared in studies IV and V, disintegrated within the time limit set for immediate-release tablets. Nyamweya et al. studied the disintegration time of several commercially available ChewTs in a similar setup. They found that the mean disintegration times ranged from 6 to more than 60 min in distilled water (Nyamweya et al., 2020). The TPH-loaded ChewTs (V) took almost 8 min to disintegrate. The obtained result is in the lower end of the spectrum found by Nyamweya et al., but more than double the time it took for the GBP-loaded ChewTs (IV), which took around 3 min to disintegrate. These ChewTs contain the same ink base, but the poorer solubility of TPH compared to GBP might attribute

to the difference in the disintegration time between the two printed dosage forms. However, the disintegration time of the prepared dosage forms in both studies is lower than that of commercially available chewable dosage forms found by Nyamweya et al. and is hence considered sufficient.

In study VI, the FD films had a more porous structure, and the assumption was that it would contribute to faster disintegration. Films printed with printing ink 1 and dried at different conditions had similar disintegration times despite the different morphology, while the disintegration time was cut in half for FD films printed with printing ink 2 compared to RTD films. Printing ink 1 consist mostly of HPMC and printing ink 2 of HPC, both polymers are hydrophilic cellulosic polymers, where HPMC is substituted with methoxy and hydroxypropyl groups, and HPC is substituted with only hydroxypropyl groups (Viridén et al., 2009). It has been found that hydrophilicity affects the drug release and swelling performance of matrix tablets (Alderman, 1984). None of the films disintegrated within 3 min, which is the limit for an orodispersible dosage form, but they all disintegrated within the 30 min limit set for immediate-release dosage forms (European Pharmacopoeia Commission, 2020a). Adding a disintegrant to the formulation could expedite the disintegration.

6.1.4.8   Drug content (I-VI)

One of the biggest criteria for producing tailored drug dosage forms is precise and accurate drug content. It is important that the dose can easily be adjusted by adjusting the design; hence, a high correlation between the designed size and obtained drug amount is crucial.

In study I, pediatric ODFs with therapeutic doses of WS with the targeted drug amounts of 1, 2, 4, and 8 mg were prepared. To achieve different drug amounts, different-sized films were designed, namely, films were designed to have a volume of 25, 50, 100, and 200 mm^3. The achieved drug amounts were 0.9 ± 0.0, 1.8 ± 0.1, 3.8 ± 0.1, and 7.4 ± 0.1 mg, respectively, which were close to the targeted drug amounts, but could further be optimized by a slight increase in pressure. Low standard deviation and good correlation ($R^2 = 0.9996$) between designed sizes and obtained drug amounts were achieved.

In study II, pediatric therapeutic doses of WS were prepared, with the target drug amounts of 0.1, 0.5, 1, and 2 mg, and ten dosage forms of each dose of the prepared batch and preparation method were analyzed to determine the UC and AV as described in the Ph. Eur., the results are presented in Table 8. A full analysis can be found in the corresponding publication. But in general, the study revealed that based on the fulfillment of AV, SSE 3DP was the manufacturing method with the best accuracy and precision of the incorporated drug for most prepared batches and dosage units. Both printing methods were superior to OPSs, which is the method being used today at the hospital pharmacy for dose manipulation of WS dosage forms for clinical use. SSE 3DP was further found to have a linear correlation between the dry weight of the film and the drug content (mg) (R^2

values of 0.9996, 1.00, and 0.9999 for batches 1, 2, and 3, respectively), which could be an easy quality control that could be used in a hospital pharmacy, pharmacy, or animal clinic setting. Additionally, the conducted stability study did not show drug degradation, indicating that the moisture content in the formulations did not affect the drug's stability during the study period.

Table 8. *Drug content, content uniformity (UC), uniformity of dosage units (acceptance value (AV), according to Ph. Eur. 9th ed.), and dose accuracy compared to target doses for the various batches prepared by different manufacturing techniques. Drug content is expressed as average ± SD, n = 10, and AV and UC are calculated based on ten dosage forms from each batch. Note that the weight of the oral powders in unit dose sachets (OPSs) is given without a decimal, as that is how it is routinely done when manufacturing OPSs in the hospital pharmacy. However, the weight of the orodispersible films (ODFs) is given with one decimal to show differences between the dosage forms. Modified and reproduced from (II), with permission from MDPI.*

Dosage form; Batch	Weight (mg)	Drug amount (mg)	Maximum deviation (%)	Acceptance value
0.1 mg				
SSE ODF				
1	1.5 ± 0.0	0.14 ± 0.00	+ 2.9 [a]	41.0 [d]
2	1.3 ± 0.1	0.11 ± 0.00	+ 1.1 [a]	10.9 [c]
3	1.2 ± 0.2	0.10 ± 0.02	- 30.0 [b***]	47.1 [d]
IJP ODF				
1	2.1 ± 0.1	0.07 ± 0.01	+ 25.9 [b***]	55.0 [d]
2	2.3 ± 0.2	0.09 ± 0.00	- 9.0 [a]	17.6 [d]
3	2.2 ± 0.0	0.09 ± 0.01	+ 21.4 [a*]	25.4 [d]
OPS				
1	200 ± 0	0.05 ± 0.01	- 22.5 [e***]	67.8 [d]
2	200 ± 0	0.09 ± 0.01	- 23.3 [a*]	29.0 [d]
3	200 ± 0	0.08 ± 0.01	+ 18.3 [a*]	37.6 [d]
0.5 mg				
SSE ODF				
1	6.2 ± 0.1	0.59 ± 0.00	+ 1.2 [a]	17.5 [d]
2	5.2 ± 0.1	0.48 ± 0.01	- 1.8 [a]	4.9 [c]
3	5.5 ± 0.1	0.52 ± 0.01	- 2.5 [a]	4.5 [c]
IJP ODF				
1	8.6 ± 0.1	0.51 ± 0.04	- 13.8 [a]	20.8 [d]
2	9.3 ±0.2	0.51 ± 0.03	- 13.7 [a]	16.1 [d]
3	9.5 ± 0.0	0.52 ± 0.02	- 4.6 [a]	11.6 [c]

OPS				
1	200 ± 0	0.47 ± 0.05	- 18.9 [e**]	30.4 [d]
2	200 ± 0	0.54 ± 0.02	+ 5.7 [a]	15.5 [d]
3	200 ± 0	0.48 ± 0.06	- 26.1 [b**]	32.5 [d]
1 mg				
SSE ODF				
1	12.2 ± 0.1	1.16 ± 0.01	+ 1.2 [a]	16.6 [d]
2	10.7 ± 0.1	1.01 ± 0.05	- 14.8 [a]	13.7 [c]
3	11.5 ± 0.1	10.9 ± 0.01	+ 1.3 [a]	9.9 [c]
IJP ODF				
1	17.1 ± 0.6	1.09 ± 0.07	- 11.1 [a]	23.4 [d]
2	17.2 ± 0.3	1.06 ± 0.07	- 12.0 [a]	21.3 [d]
3	18.2 ± 0.6	1.05 ± 0.03	- 4.2 [a]	10.3 [c]
OPS				
1	200 ± 0	1.01 ± 0.03	- 6.0 [a]	6.9 [c]
2	200 ± 0	1.10 ± 0.06	+ 8.0 [a]	22.7 [d]
3	200 ± 0	1.11 ± 0.06	+ 7.1 [a]	23.5 [d]
2 mg				
SSE ODF				
1	23.0 ± 0.7	2.12 ± 0.06	- 5.4 [a]	12.5 [c]
2	22.4 ± 0.1	2.11 ± 0.01	+ 1.5 [a]	5.4 [c]
3	22.7 ± 0.2	2.13 ± 0.03	- 2.4 [a]	8.2 [c]
IJP ODF				
1	34.7 ± 0.2	2.06 ± 0.10	- 9.8 [a]	14.8 [c]
2	34.9 ± 0.8	2.13 ± 0.10	- 12.7 [a]	17.6 [d]
3	40.1 ± 1.2	2.10 ± 0.02	+ 1.5 [a]	5.8 [c]
OPS				
1	200 ± 0	2.17 ± 0.07	+ 14.9 [a]	16.0 [d]
2	200 ± 0	2.24 ± 0.03	+ 2.8 [a]	14.3 [c]
3	200 ± 0	2.25 ± 0.05	+ 3.5 [a]	17.1 [d]

The number of individual doses outside ± 15% limits: * = 1 dose, ** = 2 doses, *** = 3 doses. a = complies with the requirements for UC, b = does not comply with the requirements for UC, c = complies with the requirements for AV, d = does not comply with the requirements for AV, e = an additional 20 units should be tested to reveal if the test passed or failed. SSE ODF: semi-solid extrusion-based 3D-printed orodispersible film; IJP ODF: inkjet-printed orodispersible film; OPS: oral powders in unit dose sachet

In study III, three different SSE 3D printers were assessed for content uniformity within and between batches. The AV and UC were calculated with results in Table 9. Extensive results and analysis can be found in the corresponding publication (publication III, Table 3). The Bocusini printer failed the UC and AV

criteria for all three batches. Only one batch from the Zmorph printer met the requirements. Conversely, the Biobot printer consistently met the UC and AV criteria across all batches, making it the selected printer for subsequent studies. In the second print with the Biobot printer, different-sized films were printed to obtain different doses, i.e., tailored doses. All films had a designed width of 15 mm and a height of 1 mm, but with an increasing length of 10, 15, 20, 25, and 30 mm. The obtained drug amounts for the designed sizes were 2.7, 4.1, 5.4, 6.3, and 7.3 mg, respectively, all with a small standard deviation of 0.1 mg. Again, a great correlation (R^2 = 0.9934) between the designed size and obtained drug amount was achieved, further confirming that altering the design enables tailoring of the dose and thus proving that SSE 3DP is a suitable method for the production ODFs with tailored doses.

Table 9. *Weight, calculated drug amount, the maximum deviation of content uniformity (UC), and uniformity of dosage units (acceptance value) of the orodispersible films' (ODFs) batches printed with different semi-solid extrusion (SSE)-based 3D printers. Modified and reproduced from (III), with permission from MDPI.*

Printer; Batch	Weight (mg)	Drug amount (mg)	Maximum deviation (%)	Acceptance value
Bocusini				
1	63.6 ± 10.5	5.5 0.7	- 34.8 [b***]	44.8 [d]
2	69.0 ± 8.5	6.0 ± 0.8	- 26.5 [b**]	56.4 [d]
3	79.8 ± 10.9	6.8 ± 0.8	+ 33.0 [b***]	72.2 [d]
Biobot				
1	65.1 ± 0.2	4.8 ± 0.1	+ 6.6 [a]	6.5 [c]
2	62.2 ± 1.6	4.6 ± 0.2	- 8.4 [a]	15.0 [c]
3	63.2 ± 0.2	4.6 ± 0.1	- 5.5 [a]	11.2 [c]
Zmorph				
1	69.2 ± 7.2	5.0 ± 0.5	- 23.2 [b***]	24.7 [d]
2	66.7 ± 3.1	4.9 ± 0.2	- 15.9 [e**]	12.2 [c]
3	81.3 ± 8.2	6.0 ± 0.6	+ 30.1 [b***]	48.8 [d]

Number of individual doses outside ± 15% limits: * = 1 dose, ** = 2 doses, *** = 3 doses. a = complies with the requirements for UC, b = does not comply with the requirements for UC, c = complies with the requirements for AV, d = does not comply with the requirements for AV, e = an additional 20 units should be tested to reveal if the test passed or failed.

For study IV, seven different doses were designed with constant width and height but with increasing length. GBP (IV) cannot directly be UV-Vis spectrophotometrically analyzed in order to quantify the drug amount. Hence, various methods were extensively assessed to find and develop a reliable

quantification method for GBP. A full description of methods, analysis, and assessment can be found in the corresponding publication (publication IV, Table 2 and Figure 2), including a detailed description of the best-performing method. The ascorbic acid method exhibited the best performance throughout each assay and was used to quantify both the drug content and drug release profile of GBP. The obtained drug amount reached from around 10 mg for the smallest ChewT to over 200 mg for the biggest dosage form, with a great correlation of $R^2 = 0.9935$ between obtained drug amount and designed size. Good content uniformity was obtained, with the highest variation from average being less than or equal to 10%.

In study V, four different sizes were printed with a TPH content between 30 mg and 120 mg, and a high correlation ($R^2 = 0.9973$) between the designed size and obtained drug amount was attained. The achieved CU for sizes 5, 10, 15, and 20 were 6.78, 13.75, 8.62, and 8.48. The requirements are met if the CU is less or equal to 15, all prepared sizes meet the Ph. Eur. and USP criteria for uniformity of dosage units (European Pharmacopoeia Commission, 2020d). No significant changes in drug content were observed during the three-month stability study, and the dosage form met the uniformity criteria (≥ 15) at all time points.

In study VI, the drug content of the different-sized films (diameter of 7.5, 10, 15, and 20 mm) printed with printing ink 1 and 2 and dried at ambient conditions was measured (n = 5). The obtained PRX amounts for printing ink 1 were therapeutic doses of 4.78 ± 0.17, 6.90 ± 0.48, 12.26 ± 0.47, and 21.90 ± 1.73 mg with a correlation of $R^2 = 0.9965$ between the designed size and obtained drug amount. Similar drug content was obtained for printing ink 2; 4.40 ± 0.24, 6.36 ± 0.26, 13.62 ± 0.75, 21.01 ± 0.89 mg ($R^2 = 0.9946$). The study shows that a homogenous printing ink of nanoparticles was obtained, applicable for the production of tailored doses.

6.1.4.9 *In vitro* drug release (I-VI)

Drug release behavior *in vitro* was assessed for the printed oral dosage forms, utilizing both manual (studies I, II, and IV) and automatic (studies II, III, V, VI) dissolution setups. The choice between manual and automatic dissolution setups is influenced by various factors. Manual dissolution setups are preferred when the aim is to replicate conditions involving a lower volume of dissolution media. They are also chosen for investigating drug release profiles related to small drug doses that might challenge detection in automatic dissolution setups with larger media volumes. Additionally, manual dissolution is the practical choice when an intermediate step, like derivatization for UV-Vis analysis, is required for each sample. In contrast, automatic dissolution setups are favored for their standardized and reliable nature. They offer consistency and reliability in drug release testing and minimizes the potential for human error. Overall, the choice between manual and automatic dissolution setups depends on several factors, including the need to replicate specific conditions, the detection of small drug doses, and the necessity of intermediate steps like derivatization. It's notable

that both the Ph. Eur. and the USP lack specific dissolution test setups and criteria for ODFs. A harmonized dissolution method specifically designed for ODFs is needed and would excel the research.

In study I, all but one size exhibited a drug release that met the requirements of immediate release (publication I, Figure 3). In general, the smaller sizes exhibited a more rapid dissolution profile. All sizes exhibited a burst release of drug particles present on the surface of the dosage form allowing for the water-soluble drug to rapidly release, followed by a relatively slow drug release due to the gelation of HPC in contact with water which entraps the drug that is slowly released by gel erosion (Klančar et al., 2015). As the drug release was investigated through manual sampling, a more accurate drug release profile would be obtained by automatic sampling at more frequent time points. The choice of performing the study manually was the desired low amount of media, which is impossible with the available automatic setup.

In study II, the dissolution behavior of SSE 3D-printed and IJP ODFs, and OPSs was compared through manual dissolution (publication II, Figure 8). As expected, the OPSs exhibited the fastest drug release, as the drug in this formulation was present in ground tablets, thus enabling a rapid release of the water-soluble drug due to a large surface area. On the contrary, for the ODFs, a slower drug release was observed in accordance with study I. The thin manufactured ODFs were seen to disintegrate quickly. However, a complete drug release was not observed until around 30 min, suggesting that the drug particles were still embedded in the polymer matrix after the ODF ruptured into smaller pieces. The size of the ODFs or OPSs was not observed to have a pronounced impact on the drug release, which is in line with the results obtained in the disintegration study.

Additionally, in study II, an automatic dissolution was performed on the biggest size of all dosage forms (publication II, Figure 9). The dissolution of the drug was faster for all formulations due to the increased amount of liquid and improved stirring compared to the manual setup. The SSE 3D-printed ODF and the OPS with a target dose of 2 mg displayed an 80% drug release within the first 2 min of the experiment. The corresponding drug release for the IJP ODF was 4 min. This underpins the difference in results gained from the different setups, as previously discussed. An automated setup is a more robust method due to decreased human errors and would, therefore, be favorable. However, the online dissolution setup could not be used for the smallest dosage forms in this study due to a low dose in the dosage form and the large volume of media required.

In study III, an automatic dissolution setup both in water and in phosphate buffer was utilized, and the dissolution profiles between ODFs with LP and without LP were compared (publication III, Figure 7). The pure drug released quickly in water and was fully dissolved within minutes, pure PRE had a slower drug release in buffer (pH 6.8), and 80% drug release was obtained first at 40 min.

The drug release of the drug-loaded ODFs without LP in water was slightly slower compared to the pure substance at first due to the gelation of the HPC, but the ODFs rapidly dissolved and reached 80% drug release within 50 min. In buffer, the drug release of PRE from the ODFs is slow due to potential cross-linking of the polymer, and only 90% drug release was achieved. Films containing LP generally had a slightly faster drug release profile due to the presence of solid particles expediting the disintegration of the film. It was noticed during the dissolution studies in buffer, that the films remained intact and turned opaque. An immersion study was conducted to assess the behavior of HPC films in both water and buffer solutions, and the dried films were analyzed using ATR-FTIR spectroscopy. Films immersed in buffer at elevated temperatures exhibited an additional FTIR peak which might correspond to the phosphate crosslinking of HPC, causing a delayed release (publication III, Figure 12).

Additionally in study III, the obtained dissolution data up to 80% drug release for the prepared dosage forms were fitted to various kinetic models, and the correlation coefficient and release exponent values were calculated (complete details can be found in the publication III, Figure 8 and Table 7). All ODFs exhibited a strong correlation with the Korsmeyer-Peppas drug diffusion model, demonstrating N values exceeding 0.5. This indicates a non-Fickian diffusion release mechanism, suggesting that drug release occurs through a combination of diffusion and swelling, and that the release is dependent on time. These findings align with the behavior of HPC, where drug release from the polymer matrix is facilitated by HPC swelling, resulting in erosion and subsequent diffusion from the gel layer (Klančar et al., 2015). In water, the drug release of the ODFs without LP showed a good correlation ($R^2 > 0.99$) for all tested models except the zero order. In comparison, the addition of LP altered the dissolution profile to fit zero order release kinetic in water. Drug-loaded ODFs with and without LP followed a Higuchi release kinetic in buffer.

The dissolution of the ChewTs prepared in study IV had to be analyzed by manual dissolution setup due to every sample requires a derivatization step to be analyzed by UV-Vis. The study investigated several derivatization methods and found that the ascorbic acid method was accurate and robust; hence this method was utilized to quantify GBP in the dosage forms. As GBP is freely soluble, the pure drug exhibited complete drug release within minutes. As expected, the drug release from the prepared ChewTs was slightly slower but still rapid, and more than 90% of the drug was released within 15 min (publication IV, Figure 5). The prepared ChewTs met the Ph. Eur. specification of releasing at least 80% drug within 30 min (European Pharmacopoeia Commission, 2020b). An automated test setup that allows for an increased number of sampling time points would yield a more accurate dissolution profile, but due to the required derivatization step, this was not feasible.

An automatic setup was utilized for analyzing the drug release profile of the ChewTs prepared in study V. Pure TPH achieved 100% drug release within

minutes, but as encountered for all the previous dosage forms, the drug release from the printed dosage forms was slightly slower. Still, complete drug release was obtained at 5 min (publication V, Figure 4). The drug release between the TPH dosage forms and the GBP dosage forms cannot be compared as the dissolution setups are different and hence not comparable. However, both dosage forms exhibit rapid drug release appropriate for a chewable dosage form.

In study VI, all dosage forms were tested by automatic dissolution (publication VI, Figure 6). Printed films of ink 1 showed a fast drug release, with a small delay if freeze-dried. Films printed with ink 2 had a slower drug release, but freeze-drying giving a porous structure, expedited the drug release. Printing ink 1 consist of mostly HPMC while printing ink 2 consists of HPC. Mohammed et al. reported that HPC polymers are non-ionic, which releases the drug by a mechanism of swelling and erosion (Mohammed et al., 2012). Furthermore, the viscosity of the polymers also affects drug release. In our study, the HPMC-based polymer's viscosity is lower than the HPC-based polymer, which was observed in the rheological results of the polymer-based dispersions (Table 5). Therefore, it could be concluded by the substitution amount of methoxy and hydroxypropyl in the HPMC-based polymer and its lower MW and viscosity might expedite the drug release in printing ink 1 compared to printing ink 2 that consists of HPC. The dissolution rate acceptance criteria by the Ph. Eur. for an immediate release dosage form, is that more than 75% or 80% of the drug must be released within 15 min or 30 min, respectively (European Pharmacopoeia Commission, 2020b). The criteria are met for three out of the four tested dosage forms. The dissolution result corresponds to the disintegration results obtained for the prepared dosage forms.

6.1.4.10 Thermal properties (I-V)

The thermal properties of all the prepared dosage forms in the different studies were analyzed with a DSC. In the prepared drug-loaded ODFs from studies I-III, there is no melting point characteristic of the drug observed, indicating that the drug can be found in an amorphous state in the ODFs (publication I, Figure 11; publication III, Figure 13). In study IV, a melting point characteristic of GBP can be found in the prepared ChewTs, proving that the crystals in the dosage form are crystallized GBP (publication IV, Figure 6). A concern when manufacturing GBP dosage forms is the degradation of GBP to gabapentin lactam. This degradation product should display a distinct melting point approximately at 87–91 °C (Braga et al., 2008; Cutrignelli et al., 2007). This melting point was not found in the thermograms of the prepared ChewTs, indicating that GBP did not degrade into gabapentin lactam during the manufacturing process. TPH (study V) is polymorphic, i.e., exhibits several polymorphs of the drug, which of the anhydrous TPH form II is desired. The drug-loaded ChewTs did not show an endothermic event corresponding to the melting of TPH (publication V, Figure 6). Usually this could indicate that the drug is in an amorphous form or that the drug has dissolved in the polymer during heating. Moreover, the

presence of drug crystals observed under microscope confirm that no amorphous form was present. Ultimately, DSC could not be used to analyze the polymorph in the final dosage form in study V.

6.1.4.11 Infrared spectroscopy (I-VI)

In order to investigate possible interactions between the drug and the additives, or possible changes in the drugs due to the manufacturing, ATR-FTIR was performed on all prepared dosage forms. The full analysis including graphs of the findings can be found in the corresponding publications.

a) Warfarin

In studies I and II, the characteristic bands of WS could be found in the pure substance and the physical mixtures at around 1663 cm^{-1}, 1453 cm^{-1}, 1323 cm^{-1}, 1720 cm^{-1}, 761 cm^{-1}, and 702 cm^{-1} (Parfenyuk & Dolinina, 2017; Vuddanda et al., 2018; M. L. Yang & Song, 2015). Only a few of the aforementioned peaks could be found in the drug-loaded SSE 3D-printed dosage forms (publication I, Figure 5; publication II, Figure 10), of which all peaks are attributed to HPC. As not all characteristic peaks could be found, it confirms the finding made in the DSC analysis that WS might be present in amorphous form in the printed dosage forms. No significant spectral shifts, changes in band intensity, or complete dilution of bands were observed in any of the dosage forms during the one-month stability study performed in study II, suggesting that there were no significant changes in the intermolecular interactions during storage.

b) Prednisolone

In study III, characteristic peaks of PRE could be found in the pure substance and the physical mixtures at 3497 cm^{-1}, 3453 cm^{-1}, 3350 cm^{-1}, 1711 cm^{-1}, 1652 cm^{-1}, and 1612 cm^{-1} (Nguyen et al., 2017; Palanisamy & Khanam, 2011). Some of the aforementioned characteristic peaks are hidden by the peaks associated with HPC, however, the carbonyl groups in PRE are present in both the physical mixtures and the drug-loaded SSE 3D-printed films and at 1712–1708 cm^{-1} and 1657–1651 cm^{-1} (publication III, Figure 11), indicating that PRE is present in crystalline form in the printed dosage forms. Furthermore, these peaks are more profound in the drug-loaded film with 2% PRE compared to the 1% PRE-loaded film, suggesting that infrared spectroscopy could be utilized in quality assurance for drug quantification.

The ODFs did not fully dissolve in the dissolution study performed in buffer and only 90% drug release was obtained. Hence, an immersion study was performed where the films after immersion were measured with ATR-FTIR as it was suspected that a crosslinking of HPC occur in the presence of phosphate. In the ATR-FTIR measurement a new peak at around 1650 cm^{-1} was observed for films immersed in buffer at elevated temperatures (publication III, Figure 12). The emergence of the new peak observed in the study could potentially be attributed to either the cross-linking of HPC or the presence of water. It is known that phosphate can act as a cross-linking agent for cellulose, and this process can be

facilitated by elevated temperatures (da Silva Peixoto et al., 2019). However, characteristic FTIR peaks of phosphate could not be found in the samples.

c) Gabapentin

GBP exhibits polymorphism and is prone to degrade to beta lactam, the purpose of the ATR-FTIR analysis in study IV was to determine the drug's form in the prepared dosage and to assess any potential degradation. Some of the characteristic peaks are hidden by the additives in the formulation, but characteristic peaks of GBP form II could be found in the SSE 3D-printed ChewTs (publication IV, Figure 7), namely 1534 cm^{-1}, 1396 cm^{-1}, and 1165 cm^{-1} (Lin et al., 2010; Ranjous & Hsian, 2013). Despite the additives in the formulation having strong peaks in the region where the characteristic peaks of gabapentin lactam are found (3202 cm^{-1}, 2928 cm^{-1}, and 1699 cm^{-1}), no changes in the spectra at these wavelengths were found confirming the DSC findings that the manufacturing process did not degrade the drug.

d) Theophylline

In study V, ATR-FTIR analysis was performed for seven days on the printing inks stored at different temperatures and of the prepared ChewTs at set time points up to three months after printing. TPH is known to exist as a crystalline monohydrate and three anhydrous polymorphs (the stable forms I and II and the metastable form III), and a fourth anhydrous form IV has also been identified. The anhydrous form II is most commonly used as an API in pharmaceutical dosage forms, but monohydrate products are also on the market. Phase transition during pharmaceutical processing can occur, e.g., anhydrous TPH transforms into TPH monohydrate in the presence of water at ambient conditions (Khamar et al., 2011; Shukla & Price, 1989). Characteristic peaks of anhydrous TPH of polymorph II was found in the printing ink and the final dosage forms, and no changes to the drug was observed throughout the stability study on the ink nor the ChewTs (publication V, Figure 7). The studies indicate that the active and stable form of TPH is present in both the ink and the ChewTs and that neither the storage conditions nor the preparation method caused a phase transition, furthermore, the drug stayed stable in the ChewTs for at least three months.

e) Piroxicam

PRX also exhibit different polymorphs, namely α, β, and monohydrate, and was investigated in study VI with ATR-FTIR. The following peaks were found in the pure nanoPRX and the printed films; 1633 cm^{-1}, 1300 cm^{-1}, 1352 cm^{-1}, 832-729 cm^{-1}, and 685 cm^{-1} and 654 cm^{-1} (publication VI, Figure 7), all corresponding to the β form of PRX (Adibkia et al., 2007; Redenti et al., 1999; Taddei et al., 2000). This confirms that the nanoformed API has remained unchanged throughout the process. Furthermore, no change in the infrared spectra was observed after one month of storing (publication VI, Figure A.5.).

6.1.4.12   Raman spectroscopy (V-VI)

In study V, Raman spectroscopy was utilized to further analyze the polymorphic character of TPH in the prepared ChewTs and whether changes were observed over the stability study period of three months. Characteristic peaks of TPH form II are observed in the spectra of the pure drug and in the drug-loaded ChewTs, additionally, no variation in the spectra is observed throughout the three-month stability study (publication V, Figure 8). Specifically, the absence of the characteristic peak of TPH form I at 1329 cm^{-1} and the presence of the characteristic peak of TPH form II at 1662 cm^{-1} (Zhu et al., 2019) in all the prepared samples and throughout the stability study, confirms the results found in the ATR-FTIR spectra, namely, that anhydrous TPH of polymorph II is present in the printed ChewTs and that it is stable for at least three months.

Raman spectroscopy was also performed in study VI to investigate the polymorphic form of PRX (publication VI, Figure 8) and whether the ATR-FTIR results could be confirmed which indicated that the nanoPRX was found unchanged and stable throughout the manufacturing process. Neither characteristic peaks of PRX monohydrate at 1462 cm^{-1} and 1398 cm^{-1}, nor the characteristic peak of PRX form α at approximately 1543 cm^{-1} can be found in the printed films. However, the characteristic strong band for the β form of PRX is present at 1521 cm^{-1} (Adibkia et al., 2007; Redenti et al., 1999). The findings confirm the ATR-FTIR findings that PRX form β is found in the printed films and that the drug has not changed form while formulating or one month after printing.

6.1.4.13   X-ray powder diffraction (VI)

XRPD was performed in study VI to confirm the findings made by ATR-FTIR and Raman analysis regarding the polymorphic form of nanoPRX in the prepared films. The obtained XRPD patterns in all printed films were similar to the one obtained from pure nanoPRX (publication VI, Figure 9). The results indicate no changes had occurred in the drug's crystallinity, which confirms the findings made by ATR-FTIR and Raman analysis that the formulation preparation was successful in keeping the nanoformed drug stable. The analysis was performed again three months after printing and no changes have occurred indicating that the dosage forms are stable for at least three months after printing.

7. Summary and conclusions

This thesis explored the utilization of SSE 3DP as a novel approach for manufacturing customized drug-loaded solid oral dosage forms close to the point-of-care, aiming to replace traditional manual compounding techniques. Semi-solid high-viscous inks in form of gels or pastes were formulated, which were employed to successfully produce tailored dosage forms of five model drugs investigated within the thesis. The research focused on various aspects of personalization, including the customization of dosage, size, and type of solid oral dosage forms. Personalization was achieved through the careful selection of printing inks and the printing of dosage forms of different sizes. The printed dosage forms underwent rigorous analysis using established pharmaceutical analytical methods to assess their quality and to ensure the reliability and success of the printing process. By exploring the quality of the printing materials and gaining insights into the characteristics of the prepared dosage forms, this study contributes to a deeper understanding of the printing process and its potential for producing tailored medicines. The findings shed light on the feasibility and viability of SSE 3DP as an innovative approach to revolutionize drug manufacturing, bringing us closer to the realization of personalized medicine and enhanced patient care.

In the first study (I), the research focused on the successful printing of thin and flexible yet durable ODFs of various sizes, containing therapeutic doses ranging from approximately 1 mg to 8 mg. Notably, the low standard deviation in drug content indicates the suitability of this method for drugs with a narrow therapeutic index, such as WS. The printed films demonstrated rapid disintegration and immediate drug release. Furthermore, the films exhibited a neutral salivary pH, which is crucial for ensuring compatibility with orodispersible drug administration. These findings highlight the potential of the prepared ODFs as a practical choice for delivering a tailored and accurate amount of a potent API that demands rapid disintegration and immediate drug release.

In the second study (II), two printing techniques, namely SSE 3DP and IJP, were compared to each other and to OPS prepared at the hospital pharmacy using a standard operating procedure for the preparation of personalized doses. The printed ODFs demonstrated superior characteristics compared to OPSs, with the ODFs produced using SSE 3DP showing the best results. The printed ODFs were formulated with various therapeutic doses of WS, ranging from 0.1 mg to 2 mg, specifically tailored for pediatric patients. Additionally, a stability study conducted over a 4-week period at room temperature confirmed the stability of both the ODFs and OPSs during this time. These findings highlight the favorable attributes of the printed ODFs, including content uniformity, mechanical properties, and stability. Overall, these findings support the potential of printed

ODFs as a viable option for delivering personalized and stable doses of WS to pediatric patients.

In the third study (III), the focus was on evaluating the capability of three different SSE 3D printers to produce tailored doses for veterinary care. The printers were assessed and compared based on their suitability for printing drug-loaded veterinary dosage forms, printing speed, and user-friendliness. The primary objective was to compare the content uniformity of the printed dosage forms using the different printers to determine which printer would be most suitable for use in a pharmacy or an animal clinic setting. To enhance the taste and encourage voluntary uptake, LP (a taste-enhancer) was added to the formulation, resulting in films with a neutral salivary pH suitable for oral delivery in veterinary patients. The films exhibited rapid disintegration and immediate drug release. A strong correlation ($R^2 = 0.9934$) between the designed size and the achieved drug amount with therapeutic doses of TPH up to 7.4 mg was observed with the best-performing 3D printer. This correlation further confirmed that modifying the design allows for tailored dosing, highlighting the suitability of SSE 3DP for producing ODFs with tailored doses. One of the most time-consuming steps in SSE 3DP is the post-drying process to obtain the final product. Therefore, the drying time was investigated under different drying conditions. It was observed that higher temperatures resulted in shorter drying times; however, temperatures above 40 °C led to the formation of brittle films. Overall, the findings from this study demonstrate the feasibility of using SSE 3DP to produce drug-loaded ODFs with tailored doses for veterinary care. The study provides valuable insights into printer selection, dosage form characteristics, and drying conditions, contributing to the advancement of SSE 3DP in veterinary medicine.

In the fourth study (IV), the application of SSE 3DP was explored for producing hard ChewTs intended for veterinary care. To enhance acceptance and appeal to animals, LP was added to the formulation, resulting in ChewTs with a brown color and an apparent liver scent, resembling treats for dogs or cats. The ChewTs were printed in various sizes corresponding to CADs, offering escalating doses. The printed ChewTs demonstrated favorable characteristics, including fast disintegration, immediate drug release, and a neutral salivary pH. The GBP amount in the ChewTs varied, with around 10 mg for the smallest ChewT and over 200 mg for the largest dosage form, showing a high correlation ($R^2 = 0.9935$) between the designed dose and the achieved drug amount. The content uniformity of the ChewTs was excellent, with the highest variation from the average being less than or equal to 10%. These findings highlight the suitability of SSE 3DP for producing hard ChewTs with tailored doses for veterinary applications. The ability to customize the size, drug content, and flavor of the ChewTs offers potential for personalized medicines for animals. The study provides valuable insights into the dosage form characteristics and content uniformity, contributing to the advancement of SSE 3DP in veterinary medicine.

In the fifth study (V), the focus was on investigating the loading of the same ink base used in study IV with a different drug, namely TPH. The printed dosage forms exhibited fast disintegration, although slightly slower than those in study IV. Four different sizes of TPH-loaded ChewTs were successfully printed, ranging from 30 mg to 120 mg of drug content, with a high correlation between the designed size and the obtained drug amount. All doses met the content uniformity requirements specified by the Ph. Eur. and USP. The results demonstrated that the same ink base used in a previous study was suitable for preparing TPH-containing dosage forms. The printed ChewTs, which incorporated LP for improved acceptance, remained stable throughout the three-month stability study. These findings have practical implications, as they showcase the feasibility of manufacturing pet-friendly ChewTs of different API utilizing the same ink base.

In the sixth study (VI), oral thin films containing therapeutic doses of nanoPRX particles were successfully prepared using SSE 3DP. The primary objective of this study was to stabilize the nanoPRX particles in an aqueous dispersion (ink base) and maintain their original form throughout the manufacturing process. Tylopur-605 was identified as a superior stabilizer based on DLS results and was selected for suspension preparation. Two printing inks were prepared with the ink suspension. Printing ink 1 demonstrated ease of manufacturing, and the corresponding thin films exhibited fast disintegration, dissolution rate, and suitable mechanical properties, albeit being harder and more brittle compared to films prepared from printing ink 2. The study achieved a high correlation ($R^2 = 0.9965$) between the designed size and the obtained drug amount, confirming the second objective of the study that personalized doses can be achieved by modifying the film's area. Ultimately, printing ink 1 was preferred over printing ink 2. The study also compared two drying methods, with freeze-drying reducing the drying time from 24 hours to 15 hours compared to ambient conditions. Importantly, freeze-drying improved the disintegration and dissolution properties of the films. Solid-state analysis was extensively conducted to examine the drug's polymorphic form, which confirmed that the prepared thin films maintained the nanoPRX particles in their original form. The dosage form remained stable for at least three months after printing. This study successfully demonstrates the concept of SSE 3DP nanoformed particles to obtain personalized doses. The findings have implications for other poorly water-soluble drugs requiring dose personalization, particularly in pediatric and geriatric populations, with the potential to improve treatment outcomes.

In culmination, the success of the SSE 3DP as a pioneering method for tailored drug manufacturing is intricately tied to pivotal parameters such as nozzle diameter, travel speed, extrusion rate, printing temperature, and the nozzle-to-build plate distance. The viscosity and homogeneity of the ink play a decisive role in influencing the precision and quality of the printed product. Ensuring proper

calibration of these parameters and maintaining consistent ink properties are fundamental for achieving optimal results.

SSE 3DP holds immense potential for revolutionizing the healthcare industry and transforming medicine manufacturing. This highly versatile technology enables the preparation of medicine with tailored characteristics including dosage form, dosing, and flavoring to be catered to the need of individual patients. One of the notable advantages of SSE 3DP is the utilization of disposable syringes, which enhances the manufacturing process by ensuring adherence to stringent quality control requirements. This feature contributes to the production of safe and reliable medicines while maintaining compliance with regulatory standards. By harnessing the capabilities of SSE 3DP, the healthcare industry can unlock new possibilities for personalized medicine, optimizing treatment outcomes and enhancing patient experiences. The ability to create customized dosage forms with specific properties showcases the potential of SSE 3DP to shape the future of pharmaceutical manufacturing and medicine delivery.

8. Future perspective

The successful implementation of tailored 3D-printed oral dosage forms close to the point-of-care on a larger scale necessitates a paradigm shift, the establishment of new regulatory guidelines, and the development of innovative business models to ensure efficient delivery of these enhanced drug products to patients, preferably through a mass customization approach. Several distribution chain scenarios have been proposed for on-demand printed dosage forms, with large hospital pharmacies or compounding facilities emerging as the most feasible options, followed by small hospital pharmacies and community pharmacies. The potential for 3DP in patients' homes has also been recognized, emphasizing the importance of safety, regulatory compliance, and reliable control mechanisms.

To address these challenges, it has been proposed that licensed manufacturing facilities prepare the drug-loaded feedstock used for printing under GMP conditions, which would then be shipped to the printing location for the production of tailored doses using in-line analytical techniques. Alternatively, a mass-produced printing ink base could be shipped to the printing facility, where the appropriate drug and dosage would be added according to a prescription, blended, and then printed into tailored doses using a 3D printer equipped with built-in analytical equipment.

However, despite the FDA and EMA's interest in personalized medicine, decentralized manufacturing, and innovative drug delivery technologies, there is currently a lack of a regulatory framework for oral dosage forms with flexible doses that can be manufactured on-demand using 3DP technologies. This regulatory gap poses challenges and risks for pharmaceutical companies venturing into the development of 3D-printed oral dosage forms. The approval process for printed dosage forms remains uncertain, whether it will encompass the entire printing process or solely the final dosage form. The classification and production location of printed products may influence future regulatory guidelines.

This thesis focused on exploring the use of SSE 3DP to produce tailored doses suitable for pediatric and veterinary patients. The study compared different SSE 3D printers, investigated the use of the same ink base with different drugs, examined the printing of nanoparticles, and explored the stability of both printing inks and prepared dosage forms. However, given the limitations of a thesis, there is room for further exploration. Future studies could explore additional SSE 3D printers with built-in analytical tools to ensure the safety and efficacy of tailored doses. Investigating the printing of various drugs in a standard ink base with rheological properties determining the printing pressure required for accurate doses would also be valuable. Additionally, studying children's and animals' voluntary acceptance of the printed dosage forms would provide insights into the most appropriate formulations.

In order for SSE 3DP to become the preferred method for producing on-demand tailored doses, it is imperative to meet the requirements of cost-effectiveness, scalability, speed, robustness, reliability, accuracy, safety, and ease of operation. This requires careful material optimization, establishing education and training, the development of appropriate equipment, rigorous quality control protocols, automating the translation of prescription information into dose designs, fast and safe post-processing, and suitable packaging and labeling. To achieve these goals and overcome the associated challenges, collaboration between academia, industry, regulatory bodies, and healthcare professionals is imperative. This collaborative effort fosters innovation, enables the sharing of best practices, and facilitates the exchange of knowledge, research findings, and experiences. By working together, stakeholders can address the regulatory and technological barriers associated with SSE 3DP, ultimately accelerating its adoption and implementation in healthcare.

9. Acknowledgements

References

Adibkia, K., Shadbad, M. R. S., Nokhodchi, A., Javadzedeh, A., Barzegar-Jalali, M., Barar, J., Mohammadi, G., & Omidi, Y. (2007). Piroxicam nanoparticles for ocular delivery: Physicochemical characterization and implementation in endotoxin-induced uveitis. *Journal of Drug Targeting*, *15*(6), 407–416. https://doi.org/10.1080/10611 860701453125

Ahmed, I., & Kasraian, K. (2002). Pharmaceutical challenges in veterinary product development. *Advanced Drug Delivery Reviews*, *54*(6), 871–882. https://doi.org/10.1016/S0169-409X(02)00074-1

Ahmed, T. A., Alotaibi, H. A., Alharbi, W. S., Safo, M. K., & El-Say, K. M. (2022). Development of 3D-Printed, Liquisolid and Directly Compressed Glimepiride Tablets, Loaded with Black Seed Oil Self-Nanoemulsifying Drug Delivery System: In Vitro and In Vivo Characterization. *Pharmaceuticals*, *15*(1), 68. https://doi.org/10.3390/ph150 10068

Ahmed, T. A., Felimban, R. I., Tayeb, H. H., Rizg, W. Y., Alnadwi, F. H., Alotaibi, H. A., Alhakamy, N. A., Abd-Allah, F. I., Mohamed, G. A., Zidan, A. S., & El-Say, K. M. (2021). Development of Multi-Compartment 3D-Printed Tablets Loaded with Self-Nanoemulsified Formulations of Various Drugs: A New Strategy for Personalized Medicine. *Pharmaceutics*, *13*(10), 1733. https://doi.org/10.3390/pharm aceutics13101733

Alderman, D. A. (1984). A review of cellulose ethers in hydrophilic matrices for oral controlled-release dosage forms. *International Journal of Pharmaceutical Technology and Product Manufacture*, *5*, 1–9.

Aleo, M., Ross, S., Becskei, C., Coscarelli, E., King, V., Darling, M., & Lorenz, J. (2018). Palatability Testing of Oral Chewables in Veterinary Medicine for Dogs. *Open Journal of Veterinary Medicine*, *8*, 107–118. https://doi.org/10.4236/ojvm.2 018.88011

Alhnan, M. A., Okwuosa, T. C., Sadia, M., Wan, K. W., Ahmed, W., & Arafat, B. (2016). Emergence of 3D Printed Dosage Forms: Opportunities and Challenges. In *Pharmaceutical Research*. https://doi.org/10.1007/s1109 5-016-1933-1

Allahham, N., Fina, F., Marcuta, C., Kraschew, L., Mohr, W., Gaisford, S., Basit, A. W., & Goyanes, A. (2020). Selective laser sintering 3D printing of orally disintegrating printlets containing ondansetron. *Pharmaceutics*, *12*(2), 110.

https://doi.org/10.3390/pharmaceutics12020110

Ameeduzzafar, Alruwaili, N. K., Rizwanullah, Md., Abbas Bukhari, S. N., Amir, M., Ahmed, M. M., & Fazil, M. (2019). 3D Printing Technology in Design of Pharmaceutical Products. *Current Pharmaceutical Design*, *24*(42), 5009–5018. https://doi.org/10.2174/13816 12825666190116104620

Anderson, W., Kozak, D., Coleman, V. A., Jämting, Å. K., & Trau, M. (2013). A comparative study of submicron particle sizing platforms: Accuracy, precision and resolution analysis of polydisperse particle size distributions. *Journal of Colloid and Interface Science*, *405*, 322–330. https://doi.org/10.1016/J.JCIS.2 013.02.030

Aprecia. (2020). *Aprecia Establishes a Long-Term Partnership with Battelle [Press release]*. https://www.aprecia.com/news /aprecia-establishes-a-long-term-partnership-with-battelle

Aprecia. (2021a). *Glatt Pharmaceutical Services and Aprecia to Advance Patient Focused Pharmaceuticals with Aprecia's 3D-Printing Technology [Press release]*. https://www.aprecia.com/news /glatt-pharmaceutical-services-and-aprecia-to-advance-patient-focused-pharmaceuticals-with-aprecias-3d-printing-technology

Aprecia. (2021b). *Nanoform and Aprecia Collaborate to Advance 3D Printed Nanomedicines [Press release]*. https://www.aprecia.com/news /nanoform-and-aprecia-collaborate-to-advance-3d-printed-nanomedicines

Arora, P., & Arora Sethi, V. (2013). ORODISPERSIBLE TABLETS: A COMPREHENSIVE REVIEW. *International Journal of Research and Development in Pharmacy and Life Sciences*, *2*(2), 270–284.

Batchelor, H. K., & Marriott, J. F. (2015). Formulations for children: problems and solutions. *British Journal of Clinical Pharmacology*, *79*(3), 405–418. https://doi.org/10.1111/bcp.12 268

Beer, N., Hegger, I., Kaae, S., De Bruin, M. L., Genina, N., Alves, T. L., Hoebert, J., & Kälvemark Sporrong, S. (2021). Scenarios for 3D printing of personalized medicines - A case study. *Exploratory Research in Clinical and Social Pharmacy*, *4*, 100073. https://doi.org/10.1016/J.RCSO P.2021.100073

Beer, N., Kaae, S., Genina, N., Sporrong, S. K., Alves, T. L., Hoebert, J., De Bruin, M. L., & Hegger, I. (2023). Magistral Compounding with 3D Printing: A Promising Way to Achieve Personalized Medicine. *Therapeutic Innovation & Regulatory Science*, *57*(1), 26–36.

https://doi.org/10.1007/s4344
1-022-00436-7

Boateng, J. S., Stevens, H. N. E.,
Eccleston, G. M., Auffret, A. D.,
Humphrey, M. J., & Matthews, K.
H. (2009). Development and
mechanical characterization of
solvent-cast polymeric films as
potential drug delivery systems
to mucosal surfaces. *Drug
Development and Industrial
Pharmacy*, *35*(8), 986–996.
https://doi.org/10.1080/03639
040902744704

Braga, D., Grepioni, F., Maini, L.,
Rubini, K., Polito, M., Brescello, R.,
Cotarca, L., Duarte, M. T., André,
V., & Piedade, M. F. M. (2008).
Polymorphic gabapentin:
Thermal behaviour, reactivity
and interconversion of forms in
solution and solid-state. *New
Journal of Chemistry*, *32*(10),
1788–1795.
https://doi.org/10.1039/b8096
62g

Cailleaux, S., Sanchez-Ballester, N.
M., Gueche, Y. A., Bataille, B., &
Soulairol, I. (2021). Fused
Deposition Modeling (FDM), the
new asset for the production of
tailored medicines. *Journal of
Controlled Release*, *330*, 821–841.
https://doi.org/10.1016/j.jconr
el.2020.10.056

Carlota, V. (2019, January 28).
*Multiply Labs 3D Prints
Personalised Daily Pills.*
3Dnatives.
https://www.3dnatives.com/en
/multiply-labs-3d-prints-pills-
280120194/#!

Cerda, J. R., Arifi, T., Ayyoubi, S.,
Knief, P., Ballesteros, M. P.,
Keeble, W., Barbu, E., Healy, A. M.,
Lalatsa, A., & Serrano, D. R.
(2020). Personalised 3D Printed
Medicines: Optimising Material
Properties for Successful Passive
Diffusion Loading of Filaments
for Fused Deposition Modelling
of Solid Dosage Forms.
Pharmaceutics, *12*(4), 345.
https://doi.org/10.3390/pharm
aceutics12040345

Chachlioutaki, K., Karavasili, C.,
Mavrokefalou, E. E.,
Gioumouxouzis, C. I., Ritzoulis, C.,
& Fatouros, D. G. (2022). Quality
control evaluation of paediatric
chocolate-based dosage forms:
3D printing vs mold-casting
method. *International Journal of
Pharmaceutics*, *624*, 121991.
https://doi.org/10.1016/J.IJPHA
RM.2022.121991

Chaiwarit, T., Aodsab, N., Promyos,
P., Panraksa, P., Udomsom, S., &
Jantrawut, P. (2022). Fabrication
of Hydroxypropyl
Methylcellulose Orodispersible
Film Loaded Mirtazapine Using a
Syringe Extrusion 3D Printer.
Scientia Pharmaceutica, *90*(4),
68.
https://doi.org/10.3390/scipha
rm90040068

Charoo, N. A., Barakh Ali, S. F.,
Mohamed, E. M., Kuttolamadom,
M. A., Ozkan, T., Khan, M. A., &
Rahman, Z. (2020). Selective
laser sintering 3D printing – an
overview of the technology and
pharmaceutical applications.
Drug Development and Industrial

Pharmacy, *46*(6), 869–877. https://doi.org/10.1080/03639 045.2020.1764027

Chatzitaki, A.-T., Eleftheriadis, G., Tsongas, K., Tzetzis, D., Spyros, A., Vizirianakis, I. S., & Fatouros, D. G. (2023). Fabrication of 3D-printed octreotide acetate-loaded oral solid dosage forms by means of semi-solid extrusion printing. *International Journal of Pharmaceutics*, *632*, 122569. https://doi.org/10.1016/j.ijphar m.2022.122569

Chatzitaki, A.-T., Mystiridou, E., Bouropoulos, N., Ritzoulis, C., Karavasili, C., & Fatouros, D. G. (2021). Semi-solid extrusion 3D printing of starch-based soft dosage forms for the treatment of paediatric latent tuberculosis infection. *Journal of Pharmacy and Pharmacology*, 1–9. https://doi.org/10.1093/jpp/rg ab121

Chen, P., Liu, J., Zhang, K., Huang, D., Huang, S., Xie, Q., Yang, F., Huang, J., Fang, D., Huang, Z., Lu, Z., & Chen, Y. Z. (2021). Preparation of clarithromycin floating core-shell systems (CSS) using multi-nozzle semi-solid extrusion-based 3D printing. *International Journal of Pharmaceutics*, *605*, 120837. https://doi.org/10.1016/J.IJPHA RM.2021.120837

Cheng, Y., Qin, H., Acevedo, N. C., Jiang, X., & Shi, X. (2020). 3D printing of extended-release tablets of theophylline using hydroxypropyl methylcellulose

(HPMC) hydrogels. *International Journal of Pharmaceutics*, *591*, 119983. https://doi.org/10.1016/J.IJPHA RM.2020.119983

Choong, Y. Y. C. (2022). Additive manufacturing for digital transformation. *Digital Manufacturing: The Industrialization of "Art to Part" 3D Additive Printing*, 145–182. https://doi.org/10.1016/B978-0-323-95062-6.00002-4

Cilurzo, F., Cupone, I. E., Minghetti, P., Selmin, F., & Montanari, L. (2008). Fast dissolving films made of maltodextrins. *European Journal of Pharmaceutics and Biopharmaceutics*, *70*(3), 895–900. https://doi.org/10.1016/j.ejpb.2 008.06.032

Clayton, K. N., Salameh, J. W., Wereley, S. T., & Kinzer-Ursem, T. L. (2016). Physical characterization of nanoparticle size and surface modification using particle scattering diffusometry. *Biomicrofluidics*, *10*(5). https://doi.org/10.1063/1.4962 992

Conceição, J., Farto-Vaamonde, X., Goyanes, A., Adeoye, O., Concheiro, A., Cabral-Marques, H., Sousa Lobo, J. M., & Alvarez-Lorenzo, C. (2019). Hydroxypropyl-β-cyclodextrin-based fast dissolving carbamazepine printlets prepared by semisolid extrusion 3D printing. *Carbohydrate*

Polymers, *221*, 55–62. https://doi.org/10.1016/J.CARBPOL.2019.05.084

Craft Health. (n.d.). *CraftMake*. Retrieved May 29, 2023, from https://www.crafthealth.me/support

Croitoru-Sadger, T., Mizrahi, B., Yogev, S., & Shabtay-Orbach, A. (2019). Two-component cross-linkable gels for fabrication of solid oral dosage forms. *Journal of Controlled Release*, *303*, 274–280. https://doi.org/10.1016/J.JCONREL.2019.04.021

Cui, M., Pan, H., Fang, D., Qiao, S., Wang, S., & Pan, W. (2020). Fabrication of high drug loading levetiracetam tablets using semi-solid extrusion 3D printing. *Journal of Drug Delivery Science and Technology*, *57*, 101683. https://doi.org/10.1016/J.JDDST.2020.101683

Cui, M., Yang, Y., Jia, D., Li, P., Li, Q., Chen, F., Wang, S., Pan, W., & Ding, P. (2019). Effect of novel internal structures on printability and drug release behavior of 3D printed tablets. *Journal of Drug Delivery Science and Technology*, *49*, 14–23. https://doi.org/10.1016/J.JDDST.2018.10.037

CurifyLabs. (n.d.). *CurifyLabs Technology*. Retrieved May 29, 2023, from https://curifylabs.com/technology

Curti, C., Kirby, D. J., & Russell, C. A. (2021). Stereolithography Apparatus Evolution: Enhancing Throughput and Efficiency of Pharmaceutical Formulation Development. *Pharmaceutics*, *13*(5), 616. https://doi.org/10.3390/pharmaceutics13050616

Cutrignelli, A., Denora, N., Lopedota, A., Trapani, A., Laquintana, V., Latrofa, A., Trapani, G., & Liso, G. (2007). Comparative effects of some hydrophilic excipients on the rate of gabapentin and baclofen lactamization in lyophilized formulations. *International Journal of Pharmaceutics*, *332*(1–2), 98–106. https://doi.org/10.1016/j.ijpharm.2006.09.053

da Silva Peixoto, T., Yamashita, F., Bilck, A. P., Carvalho, G. M., & Grossmann, M. V. E. (2019). Crosslinking starch/oat hull mixtures for use in composites with PLA. *Polimeros*, *29*(3), 1–8. https://doi.org/10.1590/0104-1428.02519

Dabbagh, S. R., Sarabi, M. R., Rahbarghazi, R., Sokullu, E., Yetisen, A. K., & Tasoglu, S. (2021). 3D-printed microneedles in biomedical applications. *IScience*, *24*(1), 102012. https://doi.org/10.1016/j.isci.2020.102012

Dahiya, J., Jalwal, P., & Singh, B. (2015). Chewable Tablets: A Comprehensive Review. *The Pharma Innovation Journal 2015:*

4(5): 100-105, *4*(5), 100–105. www.thepharmajournal.com

Daly, R., Harrington, T. S., Martin, G. D., & Hutchings, I. M. (2015). Inkjet printing for pharmaceutics - A review of research and manufacturing. *International Journal of Pharmaceutics*. https://doi.org/10.1016/j.ijpharm.2015.03.017

Danaei, M., Dehghankhold, M., Ataei, S., Hasanzadeh Davarani, F., Javanmard, R., Dokhani, A., Khorasani, S., & Mozafari, M. R. (2018). Impact of particle size and polydispersity index on the clinical applications of lipidic nanocarrier systems. In *Pharmaceutics* (Vol. 10, Issue 2). https://doi.org/10.3390/pharmaceutics10020057

Davidson, G. (2017). Veterinary compounding: Regulation, challenges, and resources. *Pharmaceutics*, *9*(1), 5. https://doi.org/10.3390/pharmaceutics9010005

Davies, P. (2009). Oral Solid Dosage Forms. In M. Gibson (Ed.), *Pharmaceutical Preformulation and Formulation* (2nd Edition, pp. 367–430). CRC Press.

de Oliveira, T. V., de Oliveira, R. S., dos Santos, J., Funk, N. L., Petzhold, C. L., & Beck, R. C. R. (2022). Redispersible 3D printed nanomedicines: An original application of the semisolid extrusion technique. *International Journal of Pharmaceutics*, *624*, 122029.

https://doi.org/10.1016/J.IJPHARM.2022.122029

Deon, M., dos Santos, J., de Andrade, D. F., & Beck, R. C. R. (2022). A critical review of traditional and advanced characterisation tools to drive formulators towards the rational development of 3D printed oral dosage forms. *International Journal of Pharmaceutics*, *628*, 122293. https://doi.org/10.1016/j.ijpharm.2022.122293

DiHeSys. (n.d.). *DiHeSys*. Retrieved May 29, 2023, from https://www.digital-health-systems.com/kopie-von-start

Dong, X., Zhang, W., Wang, X., Liu, S., Liang, J., Liufu, C., Zeng, S., Pang, J., Li, S., Xiong, L., Zhou, G., Zhu, W., Lao, H., Lin, Z., & Yang, F. (2022). A Novel Preparation Method for Effervescent Tablets of Xianganfang Containing Fresh Juice using a Semi-Solid Extrusion 3D Printer with Three Cartridge Holders. *AAPS PharmSciTech*, *23*(6), 193. https://doi.org/10.1208/s12249-022-02336-3

Dores, F., Kuźmińska, M., Soares, C., Bohus, M., A Shervington, L., Habashy, R., Pereira, B. C., Peak, M., Isreb, A., & Alhnan, M. A. (2020). Temperature and solvent facilitated extrusion based 3D printing for pharmaceuticals. *European Journal of Pharmaceutical Sciences*, *152*, 105430. https://doi.org/10.1016/J.EJPS.2020.105430

Doser. (2021, October 18). *Doser MedPrint 3D printer added to LUMC Hospital pharmacy GMP licenc [Press release]*. https://dosermedical.com/news /doser-medprint-3dprinter-added-to-lumc-hospital-pharmacy-gmp-licence/

Edinger, M., Bar-Shalom, D., Sandler, N., Rantanen, J., & Genina, N. (2018). QR encoded smart oral dosage forms by inkjet printing. *International Journal of Pharmaceutics*, *536*(1), 138–145. https://doi.org/10.1016/j.ijphar m.2017.11.052

Eduardo, D. T., Ana, S. E., & José B., F. (2021). A micro-extrusion 3D printing platform for fabrication of orodispersible printlets for pediatric use. *International Journal of Pharmaceutics*, *605*, 120854. https://doi.org/10.1016/J.IJPHA RM.2021.120854

El Aita, I., Breitkreutz, J., & Quodbach, J. (2019). On-demand manufacturing of immediate release levetiracetam tablets using pressure-assisted microsyringe printing. *European Journal of Pharmaceutics and Biopharmaceutics*, *134*, 29–36. https://doi.org/10.1016/J.EJPB. 2018.11.008

El Aita, I., Breitkreutz, J., & Quodbach, J. (2020). Investigation of semi-solid formulations for 3D printing of drugs after prolonged storage to mimic real-life applications. *European Journal of Pharmaceutical Sciences*, *146*, 105266. https://doi.org/10.1016/J.EJPS. 2020.105266

Elbl, J., Gajdziok, J., & Kolarczyk, J. (2020). 3D printing of multilayered orodispersible films with in-process drying. *International Journal of Pharmaceutics*, *575*, 118883. https://doi.org/10.1016/J.IJPHA RM.2019.118883

Elder, D. P., Kuentz, M., & Holm, R. (2016). Pharmaceutical excipients — quality, regulatory and biopharmaceutical considerations. *European Journal of Pharmaceutical Sciences*, *87*, 88–99. https://doi.org/10.1016/J.EJPS. 2015.12.018

Eleftheriadis, G. K., Kantarelis, E., Monou, P. K., Andriotis, E. G., Bouropoulos, N., Tzimtzimis, E. K., Tzetzis, D., Rantanen, J., & Fatouros, D. G. (2021). Automated digital design for 3D-printed individualized therapies. *International Journal of Pharmaceutics*, *599*, 120437. https://doi.org/10.1016/J.IJPHA RM.2021.120437

Elmeshad, A. N., & El Hagrasy, A. S. (2011). Characterization and optimization of orodispersible mosapride film formulations. *AAPS PharmSciTech*, *12*(4), 1384–1392. https://doi.org/10.1208/s1224 9-011-9713-z

European Association of Hospital Pharmacists. (2020). *EAHP Position Paper on Pharmacy Preparations and Compounding*.

European Commission. (2020). *Conformity assessment procedures for 3D printing and 3D printed products to be used in a medical context for COVID-19* .

European Medicines Agency. (2014). *Guideline on the demonstration of palatability of veterinary medicinal products*.

European Medicines Agency. (2023a). *Final Programming Document 2023-2025* .

European Medicines Agency. (2023b). *Quality Innovation Group - Listen and Leard Focus Group (LLFG) meeting report*.

European Pharmacopoeia Commission. (2020a). 2.9.1. Disintegration of tablets and capsules. In *European Pharmacopoeia* (10.0, pp. 323–325). European Directorate for the Quality of Medicines (EDQM).

European Pharmacopoeia Commission. (2020b). 2.9.3. Dissolution test for solid dosage forms. In *European Pharmacopoeia* (10.0, pp. 326–333). European Directorate for the Quality of Medicines (EDQM).

European Pharmacopoeia Commission. (2020c). 2.9.6. Uniformity of content of single-dose preparations. In *European Pharmacopoeia* (10.0, p. 336).

European Directorate for the Quality of Medicines (EDQM).

European Pharmacopoeia Commission. (2020d). 2.9.40. Uniformity of Dosage Units. In *European Pharmacopoeia* (10.0, pp. 398–400). European Directorate for the Quality of Medicines (EDQM).

European Pharmacopoeia Commission. (2020e). Dosage forms. In *European Pharmacopoeia* (10.0, pp. 903–943). European Directorate for the Quality of Medicines (EDQM).

European Pharmacopoeia Commission. (2022a). Capsules. In *European Pharmacopoeia* (11th ed.). European Directorate for the Quality of Medicines & HealthCare (EDQM).

European Pharmacopoeia Commission. (2022b). Oromucosal Preparations. In *European Pharmacopoeia* (11th ed.). European Directorate for the Quality of Medicines & HealthCare (EDQM).

European Pharmacopoeia Commission. (2022c). Tablets. In *European Pharmacopoeia* (11th ed.). European Directorate for the Quality of Medicines & HealthCare (EDQM).

FabRx. (n.d.-a). *About FabRx*. Retrieved May 29, 2023, from https://www.fabrx.co.uk/about

FabRx. (n.d.-b). *FabRx Research*. Retrieved May 29, 2023, from

https://www.fabrx.co.uk/resear
ch

FabRx. (2020, April 6). *FabRx's pharmaceutical 3D printer for personalised medicines, M3DIMAKER™, is now available! [Press release].* https://www.fabrx.co.uk/2020/ 04/06/fabrxs-pharmaceutical-3d-printer-for-personalised-medicines-m3dimaker-is-now-available

FabRx. (2021, June 25). *FabRx And Gustave Roussy Enter Into An Agreement To Develop A Novel, Personalised, Multi-Drug Dosage Form For The Treatment Of Patients With Early-Stage Breast Cancer [Press release].* https://www.fabrx.co.uk/2021/ 06/25/fabrx-and-gustave-roussy-enter-into-an-agreement-to-develop-a-novel-personalised-multi-drug-dosage-form-for-the-treatment-of-patients-with-early-stage-breast-cancer

FabRx. (2023, February 5). *A new clinical study to begin in Spain for 3D printed personalised medicine [Press release].* https://www.fabrx.co.uk/2023/ 02/05/a-new-clinical-study-to-begin-in-spain-for-3d-printed-personalised-medicine

Falcone, G., Real, J. P., Palma, S. D., Aquino, R. P., Del Gaudio, P., Garofalo, E., & Russo, P. (2022). Floating Ricobendazole Delivery Systems: A 3D Printing Method by Co-Extrusion of Sodium Alginate and Calcium Chloride.

International Journal of Molecular Sciences, *23*(3), 1280. https://doi.org/10.3390/ijms23 031280

Falcone, G., Saviano, M., Aquino, R. P., Del Gaudio, P., & Russo, P. (2021). Coaxial semi-solid extrusion and ionotropic alginate gelation: A successful duo for personalized floating formulations via 3D printing. *Carbohydrate Polymers*, *260*, 117791. https://doi.org/10.1016/J.CARB POL.2021.117791

Fanous, M., Gold, S., Muller, S., Hirsch, S., Ogorka, J., & Imanidis, G. (2020). Simplification of fused deposition modeling 3D-printing paradigm: Feasibility of 1-step direct powder printing for immediate release dosage form production. *International Journal of Pharmaceutics*, *578*, 119124. https://doi.org/10.1016/J.IJPHA RM.2020.119124

Firth, J., Basit, A. W., & Gaisford, S. (2018). The Role of Semi-Solid Extrusion Printing in Clinical Practice. In J. Firth, A. W. Basit, & S. Gaisford (Eds.), *3D Printing of Pharmaceuticals* (pp. 133–151). Springer, Cham. https://doi.org/10.1007/978-3-319-90755-0

Foo, W. C., Khong, Y. M., Gokhale, R., & Chan, S. Y. (2018). A novel unit-dose approach for the pharmaceutical compounding of an orodispersible film. *International Journal of Pharmaceutics*, *539*(1–2), 165–

174. https://doi.org/10.1016/j.ijpharm.2018.01.047

Germini, G., & Peltonen, L. (2021). 3D Printing of Drug Nanocrystals for Film Formulations. *Molecules*, *26*(13), 3941. https://doi.org/10.3390/molecules26133941

Ghanizadeh Tabriz, A., Nandi, U., Hurt, A. P., Hui, H. W., Karki, S., Gong, Y., Kumar, S., & Douroumis, D. (2021). 3D printed bilayer tablet with dual controlled drug release for tuberculosis treatment. *International Journal of Pharmaceutics*, *593*. https://doi.org/10.1016/j.ijpharm.2020.120147

Gioumouxouzis, C. I., Karavasili, C., & Fatouros, D. G. (2019). Recent advances in pharmaceutical dosage forms and devices using additive manufacturing technologies. *Drug Discovery Today*, *24*(2), 636–643. https://doi.org/10.1016/j.drudis.2018.11.019

Goole, J., & Amighi, K. (2016). 3D printing in pharmaceutics : A new tool for designing customized drug delivery systems. *International Journal of Pharmaceutics*, *499*(1–2), 376–394. https://doi.org/10.1016/j.ijpharm.2015.12.071

Goyanes, A., Allahham, N., Trenfield, S. J., Stoyanov, E., Gaisford, S., & Basit, A. W. (2019). Direct powder extrusion 3D printing: Fabrication of drug products using a novel single-step process. *International Journal of Pharmaceutics*, *567*, 118471. https://doi.org/10.1016/j.ijpharm.2019.118471

Goyanes, A., Madla, C. M., Umerji, A., Duran Piñeiro, G., Giraldez Montero, J. M., Lamas Diaz, M. J., Gonzalez Barcia, M., Taherali, F., Sánchez-Pintos, P., Couce, M. L., Gaisford, S., & Basit, A. W. (2019). Automated therapy preparation of isoleucine formulations using 3D printing for the treatment of MSUD: First single-centre, prospective, crossover study in patients. *International Journal of Pharmaceutics*, *567*, 118497. https://doi.org/10.1016/J.IJPHARM.2019.118497

Goyanes, A., Scarpa, M., Kamlow, M., Gaisford, S., Basit, A. W., & Orlu, M. (2017). Patient acceptability of 3D printed medicines. *International Journal of Pharmaceutics*, *530*(1–2), 71–78. https://doi.org/10.1016/j.ijpharm.2017.07.064

Gudeman, J., Jozwiakowski, M., Chollet, J., & Randell, M. (2013). Potential Risks of Pharmacy Compounding. *Drugs in R&D*, *13*(1), 1–8. https://doi.org/10.1007/s40268-013-0005-9

Gueche, Y. A., Sanchez-Ballester, N. M., Bataille, B., Aubert, A., Leclercq, L., Rossi, J.-C., & Soulairol, I. (2021). Selective Laser Sintering of Solid Oral Dosage Forms with Copovidone

and Paracetamol Using a CO2 Laser. *Pharmaceutics*, *13*(2), 160. https://doi.org/10.3390/pharm aceutics13020160

Gupta, M. S., Kumar, T. P., Davidson, R., Kuppu, G. R., Pathak, K., & Gowda, D. V. (2021). Printing Methods in the Production of Orodispersible Films. *AAPS PharmSciTech*, *22*(3), 129. https://doi.org/10.1208/s1224 9-021-01990-3

Habib, W. A., Alanizi, A. S., Abdelhamid, M. M., & Alanizi, F. K. (2014). Accuracy of tablet splitting: Comparison study between hand splitting and tablet cutter. *Saudi Pharmaceutical Journal*, *22*(5), 454–459. https://doi.org/10.1016/j.jsps.2 013.12.014

Haring, A. P., Tong, Y., Halper, J., & Johnson, B. N. (2018). Programming of Multicomponent Temporal Release Profiles in 3D Printed Polypills via Core–Shell, Multilayer, and Gradient Concentration Profiles. *Advanced Healthcare Materials*, *7*(16), 1–10. https://doi.org/10.1002/adhm. 201800213

Helmy, S. A. (2015). Tablet Splitting: Is It Worthwhile? Analysis of Drug Content and Weight Uniformity for Half Tablets of 16 Commonly Used Medications in the Outpatient Setting. *Journal of Managed Care & Specialty Pharmacy*, *21*(1), 76–88.

https://doi.org/10.18553/jmcp. 2015.21.1.76

Herrada-Manchón, H., Rodríguez-González, D., Alejandro Fernández, M., Suñé-Pou, M., Pérez-Lozano, P., García-Montoya, E., & Aguilar, E. (2020). 3D printed gummies: Personalized drug dosage in a safe and appealing way. *International Journal of Pharmaceutics*, *587*, 119687. https://doi.org/10.1016/J.IJPHA RM.2020.119687

Hoffmann, E. M., Breitenbach, A., & Breitkreutz, J. (2011). Advances in orodispersible films for drug delivery. *Expert Opinion on Drug Delivery*, *8*(3), 299–316. https://doi.org/10.1517/17425 247.2011.553217

Holländer, J., Hakala, R., Suominen, J., Moritz, N., Yliruusi, J., & Sandler, N. (2018). 3D printed UV light cured polydimethylsiloxane devices for drug delivery. *International Journal of Pharmaceutics*, *544*(2), 433–442. https://doi.org/10.1016/J.IJPHA RM.2017.11.016

Hong, X., Han, X., Li, X., Li, J., Wang, Z., & Zheng, A. (2021). Binder Jet 3D Printing of Compound LEV-PN Dispersible Tablets: An Innovative Approach for Fabricating Drug Systems with Multicompartmental Structures. *Pharmaceutics*, *13*(11), 1780. https://doi.org/10.3390/pharm aceutics13111780

Hospodiuk, M., Moncal, K. K., Dey, M., & Ozbolat, I. T. (2018). Extrusion-Based Biofabrication in Tissue Engineering and Regenerative Medicine. In *3D Printing and Biofabrication* (pp. 255–281). Springer International Publishing. https://doi.org/10.1007/978-3-319-45444-3_10

Hu, J., Fitaihi, R., Abukhamees, S., & Abdelhakim, H. E. (2023). Formulation and Characterisation of Carbamazepine Orodispersible 3D-Printed Mini-Tablets for Paediatric Use. *Pharmaceutics*, *15*(1), 250. https://doi.org/10.3390/pharmaceutics15010250

International Organization for Standardization. (2015). Additive manufacturing — General principles — Terminology. In *ISO/ASTM 52900:2015(en)*.

Jamróz, W., Kurek, M., Łyszczarz, E., Szafraniec, J., Knapik-Kowalczuk, J., Syrek, K., Paluch, M., & Jachowicz, R. (2017). 3D printed orodispersible films with Aripiprazole. *International Journal of Pharmaceutics*, *533*(2), 413–420. https://doi.org/10.1016/j.ijpharm.2017.05.052

Januskaite, P., Xu, X., Ranmal, S. R., Gaisford, S., Basit, A. W., Tuleu, C., & Goyanes, A. (2020). I spy with my little eye: A paediatric visual preferences survey of 3d printed tablets. *Pharmaceutics*, *12*(11),

1–16. https://doi.org/10.3390/pharmaceutics12111100

Johannesson, J., Khan, J., Hubert, M., Teleki, A., & Bergström, C. A. S. (2021). 3D-printing of solid lipid tablets from emulsion gels. *International Journal of Pharmaceutics*, *597*, 120304. https://doi.org/10.1016/J.IJPHARM.2021.120304

Johannesson, J., Pathare, M. M., Johansson, M., Bergström, C. A. S., & Teleki, A. (2023). Synergistic stabilization of emulsion gel by nanoparticles and surfactant enables 3D printing of lipid-rich solid oral dosage forms. *Journal of Colloid and Interface Science*, *650*, 1253–1264. https://doi.org/10.1016/j.jcis.2023.07.055

Jovanović, M., Petrović, M., Cvijić, S., Tomić, N., Stojanović, D., Ibrić, S., & Uskoković, P. (2021). 3D Printed Buccal Films for Prolonged-Release of Propranolol Hydrochloride: Development, Characterization and Bioavailability Prediction. *Pharmaceutics*, *13*(12), 2143. https://doi.org/10.3390/pharmaceutics13122143

Karalia, D., Siamidi, A., Karalis, V., & Vlachou, M. (2021). 3D-Printed Oral Dosage Forms: Mechanical Properties, Computational Approaches and Applications. *Pharmaceutics*, *13*(9), 1401. https://doi.org/10.3390/pharmaceutics13091401

Karavasili, C., Gkaragkounis, A., Moschakis, T., Ritzoulis, C., & Fatouros, D. G. (2020). Pediatric-friendly chocolate-based dosage forms for the oral administration of both hydrophilic and lipophilic drugs fabricated with extrusion-based 3D printing. *European Journal of Pharmaceutical Sciences*, *147*, 105291. https://doi.org/10.1016/J.EJPS.2020.105291

Karavasili, C., Zgouro, P., Manousi, N., Lazaridou, A., Zacharis, C. K., Bouropoulos, N., Moschakis, T., & Fatouros, D. G. (2022). Cereal-Based 3D Printed Dosage Forms for Drug Administration During Breakfast in Pediatric Patients within a Hospital Setting. *Journal of Pharmaceutical Sciences*. https://doi.org/10.1016/j.xphs.2022.04.013

Karlsson, S. (2022, September 16). *3D-utskrivna läkemedel för barn ska testas i Uppsala*. Svensk Farmaci. https://www.svenskfarmaci.se/2022/09/16/3d-utskrivna-lakemedel-for-barn-ska-testas-i-uppsala/

Khairuzzaman, A. (2018). Regulatory Perspectives on 3D Printing in Pharmaceuticals. In A. Basit & S. Gaisford (Eds.), *3D Printing of Pharmaceuticals. AAPS Advances in the Pharmaceutical Sciences Series* (Vol. 31, pp. 215–236). Springer, Cham. https://doi.org/10.1007/978-3-319-90755-0_11

Khaled, S. A., Alexander, M. R., Wildman, R. D., Wallace, M. J., Sharpe, S., Yoo, J., & Roberts, C. J. (2018). 3D extrusion printing of high drug loading immediate release paracetamol tablets. *International Journal of Pharmaceutics*, *538*(1–2), 223–230. https://doi.org/10.1016/J.IJPHARM.2018.01.024

Khaled, S. A., Burley, J. C., Alexander, M. R., & Roberts, C. J. (2014). Desktop 3D printing of controlled release pharmaceutical bilayer tablets. *International Journal of Pharmaceutics*, *461*, 105–111. https://doi.org/10.1016/j.ijpharm.2013.11.021

Khaled, S. A., Burley, J. C., Alexander, M. R., Yang, J., & Roberts, C. J. (2015a). 3D printing of five-in-one dose combination polypill with defined immediate and sustained release profiles. *Journal of Controlled Release*, *217*, 308–314. https://doi.org/10.1016/j.jconrel.2015.09.028

Khaled, S. A., Burley, J. C., Alexander, M. R., Yang, J., & Roberts, C. J. (2015b). 3D printing of tablets containing multiple drugs with defined release profiles. *International Journal of Pharmaceutics*. https://doi.org/10.1016/j.ijpharm.2015.07.067

Khalil, S., & Sun, W. (2007). Biopolymer deposition for freeform fabrication of hydrogel

tissue constructs. *Materials Science and Engineering: C*, *27*(3), 469–478. https://doi.org/10.1016/J.MSEC.2006.05.023

Khamar, D., Pritchard, R. G., Bradshaw, I. J., Hutcheon, G. A., & Seton, L. (2011). Polymorphs of anhydrous theophylline: Stable form IV consists of dimer pairs and metastable form i consists of hydrogen-bonded chains. *Acta Crystallographica Section C: Crystal Structure Communications*, *67*(12). https://doi.org/10.1107/S010827011104786X

Klančar, U., Baumgartner, S., Legen, I., Smrdel, P., Kampuš, N. J., Krajcar, D., Markun, B., & Kočevar, K. (2015). Determining the Polymer Threshold Amount for Achieving Robust Drug Release from HPMC and HPC Matrix Tablets Containing a High-Dose BCS Class I Model Drug: In Vitro and In Vivo Studies. *AAPS PharmSciTech*, *16*(2), 398–406. https://doi.org/10.1208/s12249-014-0234-4

Kollamaram, G., Croker, D. M., Walker, G. M., Goyanes, A., Basit, A. W., & Gaisford, S. (2018). Low temperature fused deposition modeling (FDM) 3D printing of thermolabile drugs. *International Journal of Pharmaceutics*, *545*(1–2), 144–152. https://doi.org/10.1016/J.IJPHARM.2018.04.055

Krämer, J., Gajendran, J., Guillot, A., & Barakat, A. (2019). Chewable

Oral Drug Products. In N. Fotaki & S. Klein (Eds.), *In Vitro Drug Release Testing of Special Dosage Forms* (pp. 27–53). Wiley. https://doi.org/10.1002/9781118675748.ch2

Kreft, K., Lavrič, Z., Stanić, T., Perhavec, P., & Dreu, R. (2022). Influence of the Binder Jetting Process Parameters and Binder Liquid Composition on the Relevant Attributes of 3D-Printed Tablets. *Pharmaceutics*, *14*(8), 1568. https://doi.org/10.3390/pharmaceutics14081568

Lafeber, I., Tichem, J. M., Ouwerkerk, N., van Unen, A. D., van Uitert, J. J. D., Bijleveld-Olierook, H. C. M., Kweekel, D. M., Zaal, W. M., Le Brun, P. P. H., Guchelaar, H. J., & Schimmel, K. J. M. (2021). 3D printed furosemide and sildenafil tablets: Innovative production and quality control. *International Journal of Pharmaceutics*, *603*, 120694. https://doi.org/10.1016/J.IJPHARM.2021.120694

Li, P., Jia, H., Zhang, S., Yang, Y., Sun, H., Wang, H., Pan, W., Yin, F., & Yang, X. (2020). Thermal Extrusion 3D Printing for the Fabrication of Puerarin Immediate-Release Tablets. *AAPS PharmSciTech*, *21*(20). https://doi.org/10.1208/s12249-019-1538-1

Li, Q., Guan, X., Cui, M., Zhu, Z., Chen, K., Wen, H., Jia, D., Hou, J., Xu, W., Yang, X., & Pan, W. (2018). Preparation and investigation of

novel gastro-floating tablets with 3D extrusion-based printing. *International Journal of Pharmaceutics*, *535*(1–2), 325–332. https://doi.org/10.1016/J.IJPHARM.2017.10.037

Liew, K. Bin, Tan, Y. T. F., & Peh, K. K. (2014). Effect of polymer, plasticizer and filler on orally disintegrating film. *Drug Development and Industrial Pharmacy*, *40*(1), 110–119. https://doi.org/10.3109/03639045.2012.749889

Lin, S. Y., Hsu, C. H., & Ke, W. T. (2010). Solid-state transformation of different gabapentin polymorphs upon milling and co-milling. *International Journal of Pharmaceutics*, *396*(1–2), 83–90. https://doi.org/10.1016/j.ijpharm.2010.06.014

Lir, I., Haber, M., & Dodiuk-Kenig, H. (2007). Skin surface model material as a substrate for adhesion-to-skin testing. *Journal of Adhesion Science and Technology*, *21*(15), 1497–1512. https://doi.org/10.1163/156856107782844783

Liu, G., Hansen, T. B., Qu, H., Yang, M., Pajander, J. P., Rantanen, J., & Christensen, L. P. (2014). Crystallization of Piroxicam Solid Forms and the Effects of Additives. *Chemical Engineering and Technology*, *37*(8), 1297–1304. https://doi.org/10.1002/ceat.201400206

Liu, Z., & Zhang, M. (2019). 3D Food Printing Technologies and Factors Affecting Printing Precision. *Fundamentals of 3D Food Printing and Applications*, 19–40. https://doi.org/10.1016/B978-0-12-814564-7.00002-X

Lopez-Vidal, L., Real, J. P., Real, D. A., Camacho, N., Kogan, M. J., Paredes, A. J., & Palma, S. D. (2022). Nanocrystal-based 3D-printed tablets: Semi-solid extrusion using melting solidification printing process (MESO-PP) for oral administration of poorly soluble drugs. *International Journal of Pharmaceutics*, *611*, 121311. https://doi.org/10.1016/J.IJPHARM.2021.121311

Lyousoufi, M., Lafeber, I., Kweekel, D., de Winter, B. C. M., Swen, J. J., Le Brun, P. P. H., Bijleveld-Olierook, E. C. M., van Gelder, T., Guchelaar, H., Moes, D. J. A. R., & Schimmel, K. J. M. (2023). Development and Bioequivalence of 3D-Printed Medication at the Point-of-Care: Bridging the Gap Toward Personalized Medicine. *Clinical Pharmacology & Therapeutics*, *113*(5), 1125–1131. https://doi.org/10.1002/cpt.2870

Marriott, J. L., & Nation, R. L. (2002). Splitting tablets. *Australian Prescriber*, *25*(6), 133–135. https://doi.org/10.18773/austprescr.2002.131

Mathiyalagan, R., Sjöholm, E., Manandhar, S., Lakio, S., Rosenholm, J. M., Kaasalainen, M., Wang, X., & Sandler, N. (2023). Personalizing oral delivery of nanoformed piroxicam by semi-solid extrusion 3D printing. *European Journal of Pharmaceutical Sciences*, *188*, 106497. https://doi.org/10.1016/J.EJPS.2023.106497

MB Therapeutics. (n.d.). *MB Therapeutics*. Retrieved June 14, 2023, from https://mb-therapeutics.com/en/home/

McDevitt, J. T., Gurst, A. H., & Chen, Y. (1998). Accuracy of Tablet Splitting. *Pharmacotherapy*, *18*(1), 193–197. https://doi.org/10.1002/j.1875-9114.1998.tb03838.x

Melchels, F. P. W., Feijen, J., & Grijpma, D. W. (2010). A review on stereolithography and its applications in biomedical engineering. *Biomaterials*, *31*(24), 6121–6130. https://doi.org/10.1016/j.biomaterials.2010.04.050

Melocchi, A., Uboldi, M., Cerea, M., Foppoli, A., Maroni, A., Moutaharrik, S., Palugan, L., Zema, L., & Gazzaniga, A. (2020). A Graphical Review on the Escalation of Fused Deposition Modeling (FDM) 3D Printing in the Pharmaceutical Field. *Journal of Pharmaceutical Sciences*, *109*(10), 2943–2957. https://doi.org/10.1016/j.xphs.2020.07.011

Merck. (2022, July 27). *How Merck is using 3D printing to create innovative solutions*. https://www.merck.com/stories/how-merck-is-using-3d-printing-to-create-innovative-solutions/

Meulenbelt, M., & Betts, A. B. (2019). *Replacement Compounding: A Major Threat to the Marketing Authorization System*. Sidley. https://www.sidley.com/en/insights/publications/2019/12/replacement-compounding-a-major-threat-to-the-marketing-authorization-system

Mishra, R., & Amin, A. (2011). Manufacturing Techniques of Orally Dissolving Films. *Pharmaceutical Technology*, *35*(1).

Missouri Board of Pharmacy. (2023). *Annual Reports from 2006-2022.* https://pr.mo.gov/pharmacists-annual-reports.asp

Mohammed, N. N., Majumdar, S., Singh, A., Deng, W., Murthy, N. S., Pinto, E., Tewari, D., Durig, T., & Repka, M. A. (2012). Klucel™ EF and ELF polymers for immediate-release oral dosage forms prepared by melt extrusion technology. *AAPS PharmSciTech*, *13*(4), 1158–1169. https://doi.org/10.1208/s12249-012-9834-z

Mostafaei, A., Elliott, A. M., Barnes, J. E., Li, F., Tan, W., Cramer, C. L., Nandwana, P., & Chmielus, M. (2021). Binder jet 3D printing—

Process parameters, materials, properties, modeling, and challenges. *Progress in Materials Science*, *119*, 100707. https://doi.org/10.1016/J.PMATSCI.2020.100707

Musazzi, U. M., Khalid, G. M., Selmin, F., Minghetti, P., & Cilurzo, F. (2020). Trends in the production methods of orodispersible films. *International Journal of Pharmaceutics*, *576*, 118963. https://doi.org/https://doi.org/10.1016/j.ijpharm.2019.118963

Musazzi, U. M., Selmin, F., Ortenzi, M. A., Mohammed, G. K., Franzé, S., Minghetti, P., & Cilurzo, F. (2018). Personalized orodispersible films by hot melt ram extrusion 3D printing. *International Journal of Pharmaceutics*, *551*(1–2), 52–59. https://doi.org/10.1016/j.ijpharm.2018.09.013

Nair, A. B., Kumria, R., Harsha, S., Attimarad, M., Al-Dhubiab, B. E., & Alhaider, I. A. (2013). In vitro techniques to evaluate buccal films. *Journal of Controlled Release*, *166*(1), 10–21. https://doi.org/10.1016/j.jconrel.2012.11.019

Nguyen, M. N. U., Van Vo, T., Tran, P. H. L., & Tran, T. T. D. (2017). Zein-based solid dispersion for potential application in targeted delivery. *Journal of Pharmaceutical Investigation*, *47*(4), 357–364. https://doi.org/10.1007/s40005-017-0314-z

Nicoud, L., Owczarz, M., Arosio, P., & Morbidelli, M. (2015). A multiscale view of therapeutic protein aggregation: A colloid science perspective. In *Biotechnology Journal* (Vol. 10, Issue 3, pp. 367–378). Wiley-VCH Verlag. https://doi.org/10.1002/biot.201400858

Norman, J., Madurawe, R. D., Moore, C. M. V., Khan, M. A., & Khairuzzaman, A. (2017). A new chapter in pharmaceutical manufacturing: 3D-printed drug products. *Advanced Drug Delivery Reviews*, *108*, 39–50. https://doi.org/10.1016/J.ADDR.2016.03.001

Nyamweya, N. N., & Kimani, S. N. (2020). Chewable tablets: A review of formulation considerations. *Pharmaceutical Technology*, *44*(11), 38–44.

Nyamweya, N. N., Kimani, S. N., & Abuga, K. O. (2020). Chewable Antacid Tablets: Are Disintegration Tests Relevant? *AAPS PharmSciTech*, *21*(5). https://doi.org/10.1208/s12249-020-01696-y

Öblom, H., Cornett, C., Bøtker, J., Frokjaer, S., Hansen, H., Rades, T., Rantanen, J., & Genina, N. (2020). Data-enriched edible pharmaceuticals (DEEP) of medical cannabis by inkjet printing. *International Journal of Pharmaceutics*, *589*, 119866. https://doi.org/10.1016/J.IJPHARM.2020.119866

Öblom, H., Sjöholm, E., Rautamo, M., & Sandler, N. (2019). Towards printed pediatric medicines in hospital pharmacies: Comparison of 2d and 3d-printed orodispersible warfarin films with conventional oral powders in unit dose sachets. *Pharmaceutics*, *11*(7), 334. https://doi.org/10.3390/pharmaceutics11070334

Öblom, H., Zhang, J., Pimparade, M., Speer, I., Preis, M., Repka, M., & Sandler, N. (2019). 3D-Printed Isoniazid Tablets for the Treatment and Prevention of Tuberculosis—Personalized Dosing and Drug Release. *AAPS PharmSciTech*, *20*(2), 52. https://doi.org/10.1208/s12249-018-1233-7

2015/C 421/03 Council conclusions on personalised medicine for patients, EUR-Lex (2015). https://eur-lex.europa.eu/legal-content/EN/TXT/?uri=OJ%3AC%3A2015%3A421%3AFULL

Okwuosa, T. C., Pereira, B. C., Arafat, B., Cieszynska, M., Isreb, A., & Alhnan, M. A. (2017). Fabricating a Shell-Core Delayed Release Tablet Using Dual FDM 3D Printing for Patient-Centred Therapy. *Pharmaceutical Research*, *34*, 427–437. https://doi.org/10.1007/s11095-016-2073-3

Ong, J. J., Awad, A., Martorana, A., Gaisford, S., Stoyanov, E., Basit, A. W., & Goyanes, A. (2020). 3D printed opioid medicines with alcohol-resistant and abuse-deterrent properties. *International Journal of Pharmaceutics*, *579*, 119169. https://doi.org/10.1016/j.ijpharm.2020.119169

Ou, Y. H., Goh, W. J., & Lim, S. H. (2023). Form & formulation approaches for COntRollable Release in 3D printed Colonic Targeting (CORR3CT) budesonide tablet. *International Journal of Pharmaceutics*, *635*, 122680. https://doi.org/10.1016/J.IJPHARM.2023.122680

Palanisamy, M., & Khanam, J. (2011). Solid dispersion of prednisolone: Solid state characterization and improvement of dissolution profile. *Drug Development and Industrial Pharmacy*, *37*(4), 373–386. https://doi.org/10.3109/03639045.2010.513984

Panraksa, P., Udomsom, S., Rachtanapun, P., Chittasupho, C., Ruksiriwanich, W., & Jantrawut, P. (2020). Hydroxypropyl methylcellulose e15: A hydrophilic polymer for fabrication of orodispersible film using syringe extrusion 3d printer. *Polymers*, *12*(11), 2666. https://doi.org/10.3390/polym12112666

Parfenyuk, E. V., & Dolinina, E. S. (2017). Development of Novel Warfarin-Silica Composite for Controlled Drug Release. *Pharmaceutical Research*, *34*(4), 825–835.

https://doi.org/10.1007/s1109
5-017-2111-9

Park, B. J., Choi, H. J., Moon, S. J., Kim, S. J., Bajracharya, R., Min, J. Y., & Han, H. K. (2019). Pharmaceutical applications of 3D printing technology: current understanding and future perspectives. In *Journal of Pharmaceutical Investigation* (Vol. 49, Issue 6, pp. 575–585). Springer Netherlands. https://doi.org/10.1007/s4000 5-018-00414-y

Patel, V. M., Prajapati, B. G., Patel, J. K., & Patel, M. M. (2006). Physicochemical characterization and evaluation of buccal adhesive patches containing propranolol hydrochloride. *Current Drug Delivery*, *3*(3), 325–331. https://doi.org/10.2174/15672 0106777731082

Pechová, V., Gajdziok, J., Muselík, J., & Vetchý, D. (2018). *Development of Orodispersible Films Containing Benzydamine Hydrochloride Using a Modified Solvent Casting Method*. *19*(6). https://doi.org/10.1208/s1224 9-018-1088-y

Pflieger, T., Venkatesh, R., Dachtler, M., Eggenreich, K., Laufer, S., & Lunter, D. (2022). Novel Approach to Pharmaceutical 3D-Printing Omitting the Need for Filament—Investigation of Materials, Process, and Product Characteristics. *Pharmaceutics*, *14*(11), 2488.

https://doi.org/10.3390/pharm aceutics14112488

PubChem. (n.d.-a). *Compound Summary; Gabapentin*. Retrieved May 5, 2022, from https://pubchem.ncbi.nlm.nih.g ov/compound/gabapentin

PubChem. (n.d.-b). *Compound Summary; Theophylline*. Retrieved May 5, 2022, from https://pubchem.ncbi.nlm.nih.g ov/compound/theophylline

Qian, H., Chen, D., Xu, X., Li, R., Yan, G., & Fan, T. (2022). FDM 3D-Printed Sustained-Release Gastric-Floating Verapamil Hydrochloride Formulations with Cylinder, Capsule and Hemisphere Shapes, and Low Infill Percentage. *Pharmaceutics*, *14*(2). https://doi.org/10.3390/pharm aceutics14020281

Quodbach, J., Bogdahn, M., Breitkreutz, J., Chamberlain, R., Eggenreich, K., Elia, A. G., Gottschalk, N., Gunkel-Grabole, G., Hoffmann, L., Kapote, D., Kipping, T., Klinken, S., Loose, F., Marquetant, T., Windolf, H., Geißler, S., & Spitz, T. (2022). Quality of FDM 3D Printed Medicines for Pediatrics: Considerations for Formulation Development, Filament Extrusion, Printing Process and Printer Design. *Therapeutic Innovation & Regulatory Science*, *56*(6), 910–928. https://doi.org/10.1007/s4344 1-021-00354-0

R. Sheth, A., W. Lubach, J., J. Munson, E., X. Muller, F., & J. W. Grant, D. (2005). Mechanochromism of Piroxicam Accompanied by Intermolecular Proton Transfer Probed by Spectroscopic Methods and Solid-Phase Changes. *Journal of the American Chemical Society*, *127*(18), 6641–6651. https://doi.org/10.1021/ja045823t

Ranjous, Y., & Hsian, J. (2013). Improvement in the physical and chemical stability of gabapentin by using different excipients. *International Journal of Pharmaceutical Sciences Review and Research*, *23*(1), 81–86.

Rautamo, M., Kvarnström, K., Sivén, M., Airaksinen, M., Lahdenne, P., & Sandler, N. (2020). Benefits and Prerequisites Associated with the Adoption of Oral 3D-Printed Medicines for Pediatric Patients: A Focus Group Study among Healthcare Professionals. *Pharmaceutics*, *12*(3), 229. https://doi.org/10.3390/pharmaceutics12030229

Ravasi, E., Melocchi, A., Arrigoni, A., Chiappa, A., Gennari, C. G. M., Uboldi, M., Bertarelli, C., Zema, L., & Briatico Vangosa, F. (2023). Electrospinning of pullulan-based orodispersible films containing sildenafil. *International Journal of Pharmaceutics*, *643*, 123258. https://doi.org/10.1016/j.ijpharm.2023.123258

Real, J. P., Barberis, M. E., Camacho, N. M., Sánchez Bruni, S., & Palma, S. D. (2020). Design of novel oral ricobendazole formulation applying melting solidification printing process (MESO-PP): An innovative solvent-free alternative method for 3D printing using a simplified concept and low temperature. *International Journal of Pharmaceutics*, *587*, 119653. https://doi.org/10.1016/J.IJPHARM.2020.119653

Real, J. P., Real, D. A., Lopez-Vidal, L., Barrientos, B. A., Bolaños, K., Tinti, M. G., Litterio, N. J., Kogan, M. J., & Palma, S. D. (2023). 3D-Printed Gastroretentive Tablets Loaded with Niclosamide Nanocrystals by the Melting Solidification Printing Process (MESO-PP). *Pharmaceutics*, *15*(5), 1387. https://doi.org/10.3390/pharmaceutics15051387

Redenti, E., Zanol, M., Ventura, P., Fronza, G., Comotti, A., Taddei, P., & Bertoluzza, A. (1999). Raman and Solid State 13 C-NMR Investigation of the Structure of the 1 : 1 Amorphous Piroxicam :- Cyclodextrin Inclusion Compound. *Biospectroscopy*, *5*, 243–251.

Rizvi, S. A. A., & Saleh, A. M. (2018). Applications of nanoparticle systems in drug delivery technology. In *Saudi Pharmaceutical Journal* (Vol. 26, Issue 1). https://doi.org/10.1016/j.jsps.2017.10.012

Roche, A., Sanchez-Ballester, N. M., Aubert, A., Rossi, J.-C., Begu, S., & Soulairol, I. (2023). Preliminary Study on the Development of Caffeine Oral Solid Form 3D Printed by Semi-Solid Extrusion for Application in Neonates. *AAPS PharmSciTech*, *24*(5), 122. https://doi.org/10.1208/s12249-023-02582-z

Roulon, S., Soulairol, I., Lavastre, V., Payre, N., Cazes, M., Delbreilh, L., & Alié, J. (2021). Production of Reproducible Filament Batches for the Fabrication of 3D Printed Oral Forms. *Pharmaceutics*, *13*(4), 472. https://doi.org/10.3390/pharmaceutics13040472

Rycerz, K., Stepien, K. A., Czapiewska, M., Arafat, B. T., Habashy, R., Isreb, A., Peak, M., & Alhnan, M. A. (2019). Embedded 3D printing of novel bespoke soft dosage form concept for pediatrics. *Pharmaceutics*, *11*(12), 630. https://doi.org/10.3390/pharmaceutics11120630

Salawi, A. (2022). An Insight into Preparatory Methods and Characterization of Orodispersible Film—A Review. *Pharmaceuticals*, *15*(7), 844. https://doi.org/10.3390/ph15070844

Sandler, N., & Preis, M. (2016). Printed Drug-Delivery Systems for Improved Patient Treatment. *Trends in Pharmacological Sciences*, *37*(12), 1070–1080.

https://doi.org/10.1016/j.tips.2016.10.002

Scoutaris, N., Ross, S. A., & Douroumis, D. (2018). 3D Printed "Starmix" Drug Loaded Dosage Forms for Paediatric Applications. *Pharmaceutical Research*, *2*(35), 34. https://doi.org/10.1007/s11095-017-2284-2

Scoutaris, N., Ross, S., & Douroumis, D. (2016). Current Trends on Medical and Pharmaceutical Applications of Inkjet Printing Technology. *Pharmaceutical Research*, *33*(8), 1799–1816. https://doi.org/10.1007/s11095-016-1931-3

Sen, K., Mehta, T., Sansare, S., Sharifi, L., Ma, A. W. K., & Chaudhuri, B. (2021). Pharmaceutical applications of powder-based binder jet 3D printing process – A review. *Advanced Drug Delivery Reviews*, *177*, 113943. https://doi.org/10.1016/j.addr.2021.113943

Seoane-Viaño, I, Januskaite, P., Alvarez-Lorenzo, C., Basit, A. W., & Goyanes, A. (2021). Semi-solid extrusion 3D printing in drug delivery and biomedicine: Personalised solutions for healthcare challenges. *Journal of Controlled Release*, *332*, 367–389. https://doi.org/10.1016/J.JCONREL.2021.02.027

Seoane-Viaño, I., Ong, J. J., Luzardo-Álvarez, A., González-Barcia, M., Basit, A. W., Otero-Espinar, F. J., & Goyanes, A. (2021). 3D printed

tacrolimus suppositories for the treatment of ulcerative colitis. *Asian Journal of Pharmaceutical Sciences*, *16*(1), 110–119. https://doi.org/10.1016/J.AJPS. 2020.06.003

Shukla, A. J., & Price, J. C. (1989). Effect of Drug (Core) Particle Size on the Dissolution of Theophylline from Microspheres Made from Low Molecular Weight Cellulose Acetate Propionate. *Pharmaceutical Reserach*, *6*(5), 418–421. https://doi.org/https://doi.org/ 10.1023/A:1015939600866

Singh, A., Worku, Z. A., & Van den Mooter, G. (2011). Oral formulation strategies to improve solubility of poorly water-soluble drugs. *Expert Opinion on Drug Delivery*, *8*(10), 1361–1378. https://doi.org/10.1517/17425 247.2011.606808

Singhvi, G., Patil, S., Girdhar, V., Chellappan, D. K., Gupta, G., & Dua, K. (2018). 3D-printing: an emerging and a revolutionary technology in pharmaceuticals. *Panminerva Medica*, *60*(4). https://doi.org/10.23736/S003 1-0808.18.03467-5

Siyawamwaya, M., du Toit, L. C., Kumar, P., Choonara, Y. E., Kondiah, P. P. P. D., & Pillay, V. (2019). 3D printed, controlled release, tritherapeutic tablet matrix for advanced anti-HIV-1 drug delivery. *European Journal of Pharmaceutics and Biopharmaceutics*, *138*, 99–110.

https://doi.org/10.1016/J.EJPB. 2018.04.007

Sjöholm, E., Mathiyalagan, R., Lindfors, L., Wang, X., Ojala, S., & Sandler, N. (2022). Semi-solid extrusion 3D printing of tailored ChewTs for veterinary use - A focus on spectrophotometric quantification of gabapentin. *European Journal of Pharmaceutical Sciences*, *174*, 106190. https://doi.org/10.1016/J.EJPS. 2022.106190

Sjöholm, E., Mathiyalagan, R., Prakash, D. R., Lindfors, L., Wang, Q., Wang, X., Ojala, S., & Sandler, N. (2020). 3D-Printed Veterinary Dosage Forms - A Comparative Study of Three Semi-Solid Extrusion 3D Printers. *Pharmaceutics*, *12*, 1239. https://doi.org/10.3390/pharm aceutics12121239

Sjöholm, E., Mathiyalagan, R., Wang, X., & Sandler, N. (2022). *Compounding Tailored Veterinary Chewable Tablets Close to the Point-of-Care by Means of 3D Printing*. https://doi.org/10.3390/pharm aceutics14071339

Sjöholm, E., & Sandler, N. (2019). Additive manufacturing of personalized orodispersible warfarin films. *International Journal of Pharmaceutics*, *564*, 117–123. https://doi.org/10.1016/j.ijphar m.2019.04.018

Sohail Arshad, M., Zafar, S., Yousef, B., Alyassin, Y., Ali, R., AlAsiri, A., Chang, M. W., Ahmad, Z., Ali Elkordy, A., Faheem, A., & Pitt, K. (2021). A review of emerging technologies enabling improved solid oral dosage form manufacturing and processing. *Advanced Drug Delivery Reviews*, *178*, 113840. https://doi.org/10.1016/J.ADDR .2021.113840

Steiner, D., Finke, J. H., & Kwade, A. (2016). Efficient production of nanoparticle-loaded orodispersible films by process integration in a stirred media mill. *International Journal of Pharmaceutics*, *511*(2), 804–813. https://doi.org/10.1016/j.ijphar m.2016.07.058

Suárez-González, J., Magariños-Triviño, M., Díaz-Torres, E., Cáceres-Pérez, A. R., Santoveña-Estévez, A., & Fariña, J. B. (2021). Individualized orodispersible pediatric dosage forms obtained by molding and semi-solid extrusion by 3D printing: A comparative study for hydrochlorothiazide. *Journal of Drug Delivery Science and Technology*, *66*, 102884. https://doi.org/10.1016/J.JDDS T.2021.102884

Sydney Gladman, A., Matsumoto, E. A., Nuzzo, R. G., Mahadevan, L., & Lewis, J. A. (2016). Biomimetic 4D printing. *Nature Materials*, *15*(4), 413–418. https://doi.org/10.1038/nmat4 544

Szakonyi, G., & Zelkó, R. (2012). The effect of water on the solid state characteristics of pharmaceutical excipients : Molecular mechanisms , measurement techniques , and quality aspects of final dosage form. *International Journal of Pharmaceutical Investigation*, *2*(1), 18–25. https://doi.org/10.4103/2230-973X.96922

Tabriz, A. G., Fullbrook, D. H. G., Vilain, L., Derrar, Y., Nandi, U., Grau, C., Morales, A., Hooper, G., Hiezl, Z., & Douroumis, D. (2021). Personalised tasted masked chewable 3d printed fruit-chews for paediatric patients. *Pharmaceutics*, *13*(8), 1301. https://doi.org/10.3390/pharm aceutics13081301

Taddei, P., Torreggiani, A., & Simoni, R. (2000). Influence of Environment on Piroxicam Polymorphism: Vibrational Spectroscopic Study. *Biopolymers*, *62*, 68–78.

Tagami, T., Ando, M., Nagata, N., Goto, E., Yoshimura, N., Takeuchi, T., Noda, T., & Ozeki, T. (2019). Fabrication of Naftopidil-Loaded Tablets Using a Semisolid Extrusion-Type 3D Printer and the Characteristics of the Printed Hydrogel and Resulting Tablets. *Journal of Pharmaceutical Sciences*, *108*(2), 907–913. https://doi.org/10.1016/J.XPHS. 2018.08.026

Tagami, T., Ito, E., Kida, R., Hirose, K., Noda, T., & Ozeki, T. (2021). 3D

printing of gummy drug formulations composed of gelatin and an HPMC-based hydrogel for pediatric use. *International Journal of Pharmaceutics*, *594*, 120118. https://doi.org/10.1016/J.IJPHA RM.2020.120118

Tagami, T., Okamura, M., Ogawa, K., & Ozeki, T. (2022). Fabrication of Mucoadhesive Films Containing Pharmaceutical Ionic Liquid and Eudragit Polymer Using Pressure-Assisted Microsyringe-Type 3D Printer for Treating Oral Mucositis. *Pharmaceutics*, *14*(9), 1930. https://doi.org/10.3390/pharm aceutics14091930

Takashima, H., Tagami, T., Kato, S., Pae, H., Ozeki, T., & Shibuya, Y. (2022). Three-Dimensional Printing of an Apigenin-Loaded Mucoadhesive Film for Tailored Therapy to Oral Leukoplakia and the Chemopreventive Effect on a Rat Model of Oral Carcinogenesis. *Pharmaceutics*, *14*(8), 1575. https://doi.org/10.3390/pharm aceutics14081575

Thabet, Y., Lunter, D., & Breitkreutz, J. (2018). Continuous manufacturing and analytical characterization of fixed-dose, multilayer orodispersible films. *European Journal of Pharmaceutical Sciences*, *117*(2017), 236–244. https://doi.org/10.1016/j.ejps.2 018.02.030

Tiboni, M., Campana, R., Frangipani, E., & Casettari, L. (2021). 3D

printed clotrimazole intravaginal ring for the treatment of recurrent vaginal candidiasis. *International Journal of Pharmaceutics*, *596*. https://doi.org/10.1016/j.ijphar m.2021.120290

Tomar, M., Ajay Kumar, S., & Amit Raj, S. (2017). Effect of Moisture Content of Exicipient (Microcrystalline Cellulose) on Direct Compressible Solid Dosage Forms. *International Journal of Pharmaceutical Sciences and Research*, *8*(1), 282–288. https://doi.org/10.13040/IJPSR. 0975-8232.8(1).282-88

Trenfield, S. J., Madla, C. M., Basit, A. W., & Gaisford, S. (2018). *Binder Jet Printing in Pharmaceutical Manufacturing* (pp. 41–54). https://doi.org/10.1007/978-3-319-90755-0_3

Triastek. (n.d.). *About Triastek*. Retrieved May 27, 2023, from https://www.triastek.com/

Triastek. (2022a). *Triastek and Siemens announce strategic collaboration to accelerate digital transformation of the pharmaceutical industry [Press release]*. https://www.triastek.com/detai l/24.html

Triastek. (2022b). *Triastek announces research collaboration with Lilly to explore the application of 3D printing technology in oral delivery of drugs [Press release]*.

https://www.triastek.com/detail/33.html

Triastek. (2023). *Triastek Announces Collaboration with Boehringer Ingelheim to Advance and Accelerate Research and Development of Innovative Pharmaceutical Products with MED® 3D Printing Technology [Press release].* https://www.triastek.com/detail/44.html

United States Pharmacopeial Convention. (2017). Pharmaceutical Dosage Forms. In *United States Pharmacopeia*.

U.S. Food & Drug Administration. (2018, September 27). *Precision Medicine*. https://www.fda.gov/medical-devices/in-vitro-diagnostics/precision-medicine

U.S. Food and Drug Administration. (2015). *SPRITAM - levetiracetam approval document*. https://www.accessdata.fda.gov/drugsatfda_docs/lab

U.S. Food and Drug Administration. (2017). *Technical Considerations for Additive Manufactured Medical Devices - Guidance for Industry and Food and Drug Administration Staff Preface Public Comment*. http://www.regulations.gov

U.S. Food and Drug Administration. (2018). *Quality Attribute Considerations for Chewable Tablets Guidance for Industry*.

U.S. Food and Drug Administration. (2020). *Compounding Laws and Policies*. https://www.fda.gov/drugs/human-drug-compounding/compounding-laws-and-policies

U.S. Food and Drug Association. (2015). *Compounding Animal Drugs From Bulk Drug Substances; Draft Guidance for Industry; Availability; Withdrawal of Compliance Policy Guide; Section 608.400 Compounding of Drugs for Use in Animals*. https://www.federalregister.gov/documents/2015/05/19/2015-11982/compounding-animal-drugs-from-bulk-drug-substances-draft-guidance-for-industry-availability

Vakili, H., Wickström, H., Desai, D., Preis, M., & Sandler, N. (2017). Application of a handheld NIR spectrometer in prediction of drug content in inkjet printed orodispersible formulations containing prednisolone and levothyroxine. *International Journal of Pharmaceutics*, *524*(1–2), 414–423. https://doi.org/10.1016/j.ijpharm.2017.04.014

Vaz, V. M., & Kumar, L. (2021). 3D Printing as a Promising Tool in Personalized Medicine. *AAPS PharmSciTech*, *22*(1), 49. https://doi.org/10.1208/s12249-020-01905-8

Viridén, A., Wittgren, B., Andersson, T., & Larsson, A. (2009). The

effect of chemical heterogeneity of HPMC on polymer release from matrix tablets. *European Journal of Pharmaceutical Sciences*, *36*(4–5), 392–400. https://doi.org/10.1016/J.EJPS.2008.11.003

Visser, J. C., Woerdenbag, H. J., Crediet, S., Gerrits, E., Lesschen, M. A., Hinrichs, W. L. J., Breitkreutz, J., & Frijlink, H. W. (2015). Orodispersible films in individualized pharmacotherapy: The development of a formulation for pharmacy preparations. *International Journal of Pharmaceutics*, *478*(1), 155–163. https://doi.org/10.1016/j.ijpharm.2014.11.013

Vitae Industries. (n.d.). *Vitae Industries*. Retrieved May 29, 2023, from https://www.vitaeindustries.com/

Vithani, K., Goyanes, A., Jannin, V., Basit, A. W., Gaisford, S., & Boyd, B. J. (2019a). A Proof of Concept for 3D Printing of Solid Lipid-Based Formulations of Poorly Water-Soluble Drugs to Control Formulation Dispersion Kinetics. *Pharmaceutical Research*, *36*(7), 102. https://doi.org/10.1007/s11095-019-2639-y

Vithani, K., Goyanes, A., Jannin, V., Basit, A. W., Gaisford, S., & Boyd, B. J. (2019b). An Overview of 3D Printing Technologies for Soft Materials and Potential Opportunities for Lipid-based

Drug Delivery Systems. *Pharmaceutical Research*, *36*(1), 4. https://doi.org/10.1007/s11095-018-2531-1

Vuddanda, P. R., Alomari, M., Dodoo, C. C., Trenfield, S. J., Velaga, S., Basit, A. W., & Gaisford, S. (2018). Personalisation of warfarin therapy using thermal ink-jet printing. *European Journal of Pharmaceutical Sciences*, *117*(February), 80–87. https://doi.org/10.1016/j.ejps.2018.02.002

Wang, C.-C., Tejwani (Motwani), M. R., Roach, W. J., Kay, J. L., Yoo, J., Surprenant, H. L., Monkhouse, D. C., & Pryor, T. J. (2006). Development of Near Zero-Order Release Dosage Forms Using Three-Dimensional Printing (3-DP™) Technology. *Drug Development and Industrial Pharmacy*, *32*(3), 367–376. https://doi.org/10.1080/03639040500519300

Wang, F., Li, L., Zhu, X., Chen, F., & Han, X. (2023). Development of pH-Responsive Polypills via Semi-Solid Extrusion 3D Printing. *Bioengineering*, *10*(4), 402. https://doi.org/10.3390/bioengineering10040402

Wang, J., Goyanes, A., Gaisford, S., & Basit, A. W. (2016). Stereolithographic (SLA) 3D printing of oral modified-release dosage forms. *International Journal of Pharmaceutics*.

https://doi.org/10.1016/j.ijpharm.2016.03.016

Wang, P., Zou, B., Xiao, H., Ding, S., & Huang, C. (2019). Effects of printing parameters of fused deposition modeling on mechanical properties, surface quality, and microstructure of PEEK. *Journal of Materials Processing Technology*, *271*, 62–74. https://doi.org/10.1016/J.JMATPROTEC.2019.03.016

Wang, Z., Li, J., Hong, X., Han, X., Liu, B., Li, X., Zhang, H., Gao, J., Liu, N., Gao, X., & Zheng, A. (2021). Taste Masking Study Based on an Electronic Tongue: the Formulation Design of 3D Printed Levetiracetam Instant-Dissolving Tablets. *Pharmaceutical Research*, *38*(5), 831–842. https://doi.org/10.1007/s11095-021-03041-9

Watson, C. J., Whitledge, J. D., Siani, A. M., & Burns, M. M. (2021). Pharmaceutical Compounding: a History, Regulatory Overview, and Systematic Review of Compounding Errors. *Journal of Medical Toxicology*, *17*(2), 197–217. https://doi.org/10.1007/s13181-020-00814-3

Woertz, C., Preis, M., Breitkreutz, J., & Kleinebudde, P. (2013). Assessment of test methods evaluating mucoadhesive polymers and dosage forms: An overview. *European Journal of Pharmaceutics and Biopharmaceutics*, *85*(3 PART B), 843–853. https://doi.org/10.1016/j.ejpb.2013.06.023

Wu, M., Zhang, Y., Huang, H., Li, J., Liu, H., Guo, Z., Xue, L., Liu, S., & Lei, Y. (2020). Assisted 3D printing of microneedle patches for minimally invasive glucose control in diabetes. *Materials Science and Engineering: C*, *117*, 111299. https://doi.org/10.1016/J.MSEC.2020.111299

Yan, T.-T., Lv, Z.-F., Tian, P., Lin, M.-M., Lin, W., Huang, S.-Y., & Chen, Y.-Z. (2020). Semi-solid extrusion 3D printing ODFs: an individual drug delivery system for small scale pharmacy. *Drug Development and Industrial Pharmacy*, *46*(4), 531–538. https://doi.org/10.1080/03639045.2020.1734018

Yang, H. S., & Kim, D. W. (2023). Fabrication of Gastro-Floating Famotidine Tablets: Hydroxypropyl Methylcellulose-Based Semisolid Extrusion 3D Printing. *Pharmaceutics*, *15*(2), 316. https://doi.org/10.3390/pharmaceutics15020316

Yang, M. L., & Song, Y. M. (2015). Synthesis and investigation of water-soluble anticoagulant warfarin/ferulic acid grafted rare earth oxide nanoparticle materials. *RSC Advances*, *5*(23), 17824–17833. https://doi.org/10.1039/c4ra14633f

Yang, Y., Bi, V., & Dürig, T. (2016). *The Impact of Hydroxypropyl Methylcellulose and Methylcellulose Molecular Weight and Degree of Substitution on Crystallization Inhibition of Felodipine in Aqueous Media*. http://www.drugbank.ca/drugs/DB01023

Yang, Y., Wang, X., Lin, X., Xie, L., Ivone, R., Shen, J., & Yang, G. (2020). A tunable extruded 3D printing platform using thermo-sensitive pastes. *International Journal of Pharmaceutics*, *583*, 119360. https://doi.org/10.1016/J.IJPHARM.2020.119360

Yang, Y., Xu, Y., Wei, S., & Shan, W. (2021). Oral preparations with tunable dissolution behavior based on selective laser sintering technique. *International Journal of Pharmaceutics*, *593*, 120127. https://doi.org/10.1016/J.IJPHARM.2020.120127

Yi, S., Xie, J., Chen, L., & Xu, F. (2023). Preparation of Loratadine Orally Disintegrating Tablets by Semi-solid Extrusion 3D Printing. *Current Drug Delivery*, *20*(6), 818–829. https://doi.org/10.2174/1567201819666221011094913

Yu, D.-G., Shen, X.-X., Branford-White, C., Zhu, L.-M., White, K., & Yang, X. L. (2009). Novel oral fast-disintegrating drug delivery devices with predefined inner structure fabricated by Three-Dimensional Printing. *Journal of Pharmacy and Pharmacology*, *61*(3), 323–329. https://doi.org/10.1211/jpp/61.03.0006

Zema, L., Melocchi, A., Maroni, A., & Gazzaniga, A. (2017). Three-Dimensional Printing of Medicinal Products and the Challenge of Personalized Therapy. *Journal of Pharmaceutical Sciences*, *106*(7), 1697–1705. https://doi.org/10.1016/j.xphs.2017.03.021

Zhang, B., Teoh, X. Y., Yan, J., Gleadall, A., Belton, P., Bibb, R., & Qi, S. (2022). Development of combi-pills using the coupling of semi-solid syringe extrusion 3D printing with fused deposition modelling. *International Journal of Pharmaceutics*, *625*, 122140. https://doi.org/10.1016/J.IJPHARM.2022.122140

Zheng, Z., Lv, J., Yang, W., Pi, X., Lin, W., Lin, Z., Zhang, W., Pang, J., Zeng, Y., Lv, Z., Lao, H., Chen, Y., & Yang, F. (2020). Preparation and application of subdivided tablets using 3D printing for precise hospital dispensing. *European Journal of Pharmaceutical Sciences*, *149*, 105293. https://doi.org/10.1016/J.EJPS.2020.105293

Zhu, M., Wang, Y., Li, F., Bao, Y., Huang, X., Shi, H., & Hao, H. (2019). Theoretical model and experimental investigations on solution-mediated polymorphic transformation of theophylline: From polymorph I to polymorph II. *Crystals*, *9*(5), 260.

https://doi.org/10.3390/cryst9
050260

Zidan, A., Alayoubi, A., Coburn, J., Asfari, S., Ghammraoui, B., Cruz, C. N., & Ashraf, M. (2019). Extrudability analysis of drug loaded pastes for 3D printing of modified release tablets. *International Journal of Pharmaceutics*, *554*, 292–301. https://doi.org/10.1016/J.IJPHA RM.2018.11.025

Appendix: Original publications